Colloid facilitated transport of radionuclides

Stepan Kalmykov

f Element Production in Thermal Neutron Fission of Uranium

Reactor Charge:
967kg ^{238}U, **33kg** ^{235}U, **0.26kg** ^{234}U irradiated for 33,000 MWd/t U burnup at a power density of 30MW/t U and neutron flux of 2.92×10^{13} Ncm^{-2}s^{-1}
(Choppin & Rydberg, Nuclear Chemistry)

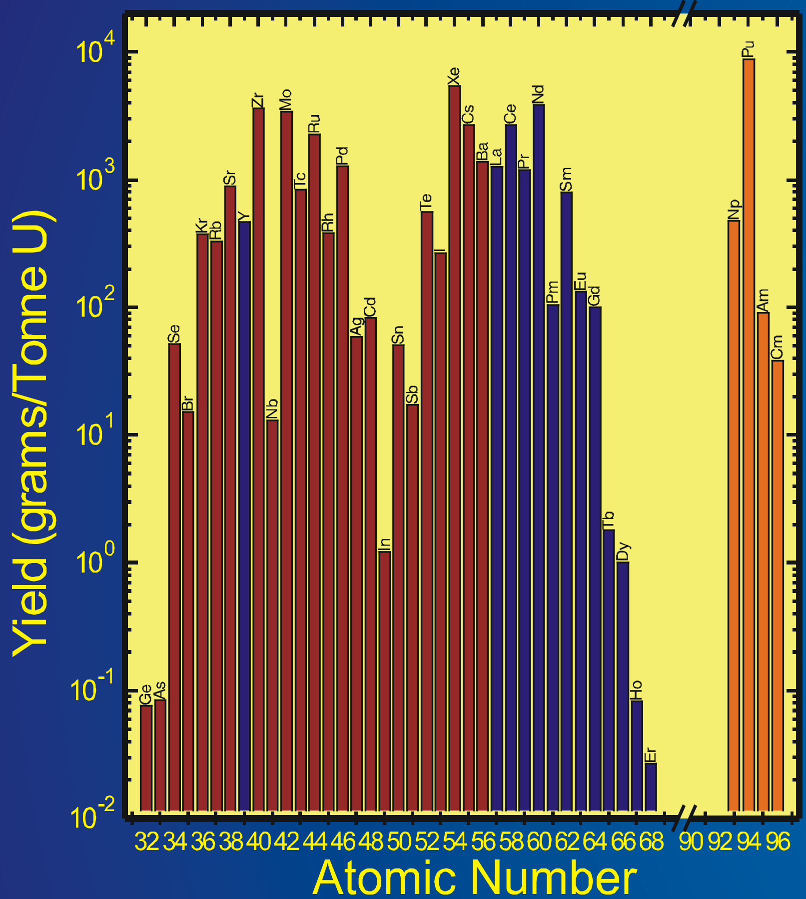

50 kg $^{235, 238}$U consumed (950 kg remain)

14 kg ^{236}U and transuranics produced

36 kg of fission products (10 kg Ln)

Actinides:
^{238}U(**942kg**), ^{236}U(**4.5kg**), ^{235}U(**8kg**), ^{234}U(120g), ^{237}Np(482g), ^{238}Pu(168g), ^{239}Pu(5,260g), ^{240}Pu(2,160g), ^{241}Pu(1,008g), ^{242}Pu(352g), ^{241}Am(44.1g), ^{242m}Am(0.4g), ^{243}Am(91.2g), ^{242}Cm(5.82g), ^{243}Cm(0.12g), ^{244}Cm(31.1g), ^{245}Cm(1.76g)

Radiation Dose and Decay

14,410,000 Ci/tonne @ discharge
1,497,000 Ci @ 1 year
394,000 Ci @ 10 years
39,800 Ci @ 100 years
1590 Ci @ 1000 years
820 Ci @ 1000 years if U/Pu removed
18 Ci @ 1000 years if An transmuted
2 Ci in 1 tonne of uranium ore

Radiotoxicity as Ingestion Hazard

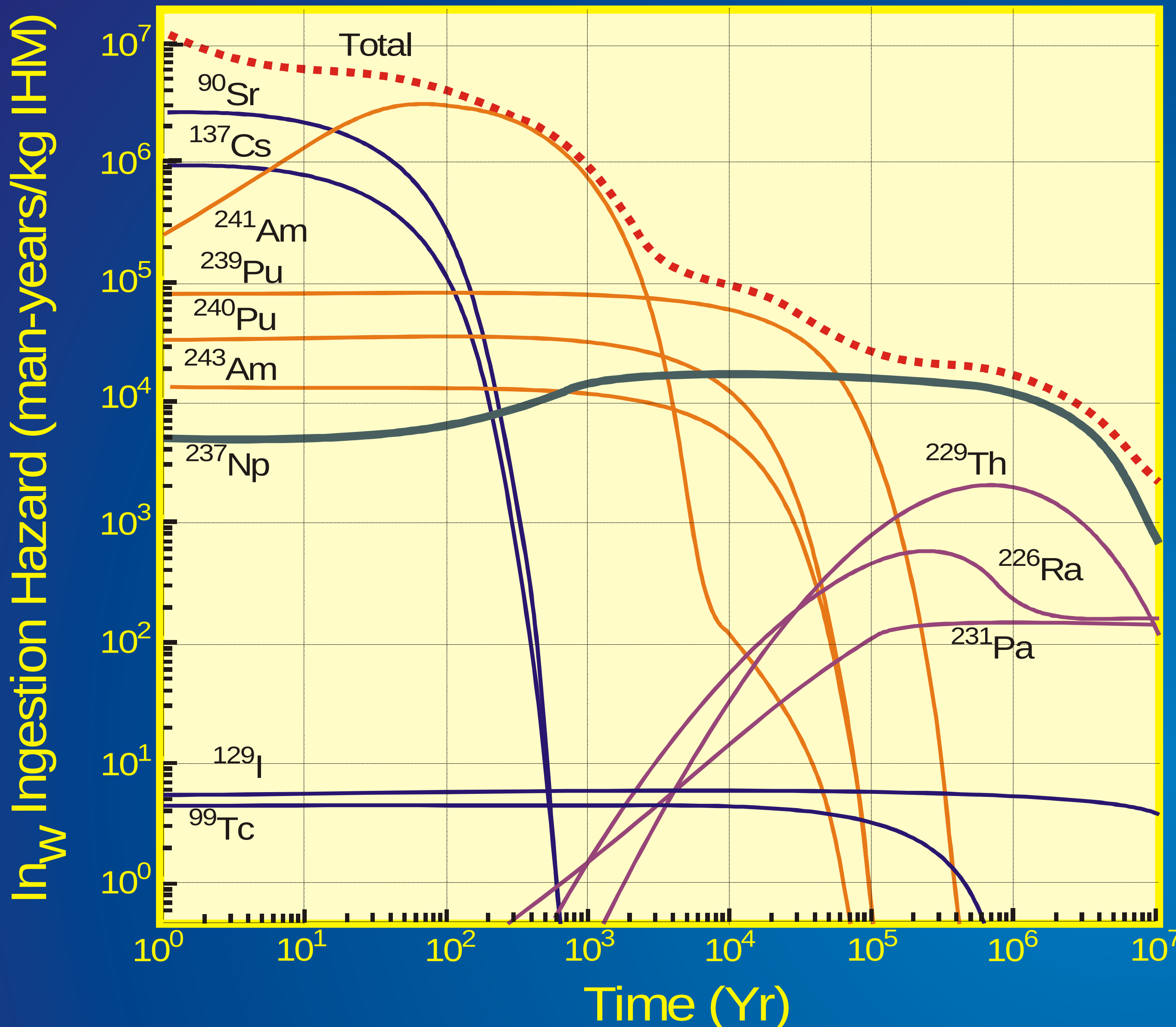

In_w = A/ALI (man-years/kg spent fuel)
where A is activity in Bq and ALI is the Annual Limit for Ingestion)

Why do we need speciation ?

Clean-up the legacy sites

Successive stories:
Radionuclide speciation / partitioning needs:

Rocky Flats

In 1995, DOE estimated that the cleanup for Rocky Flats would cost in excess of $37 billion and take 70 years to complete. By 1996, DOE and Kaiser-Hill initiated a massive accelerated closure effort that resulted in a plan to reach closure by December 31, 2006, at a contracted cost of $7 billion.

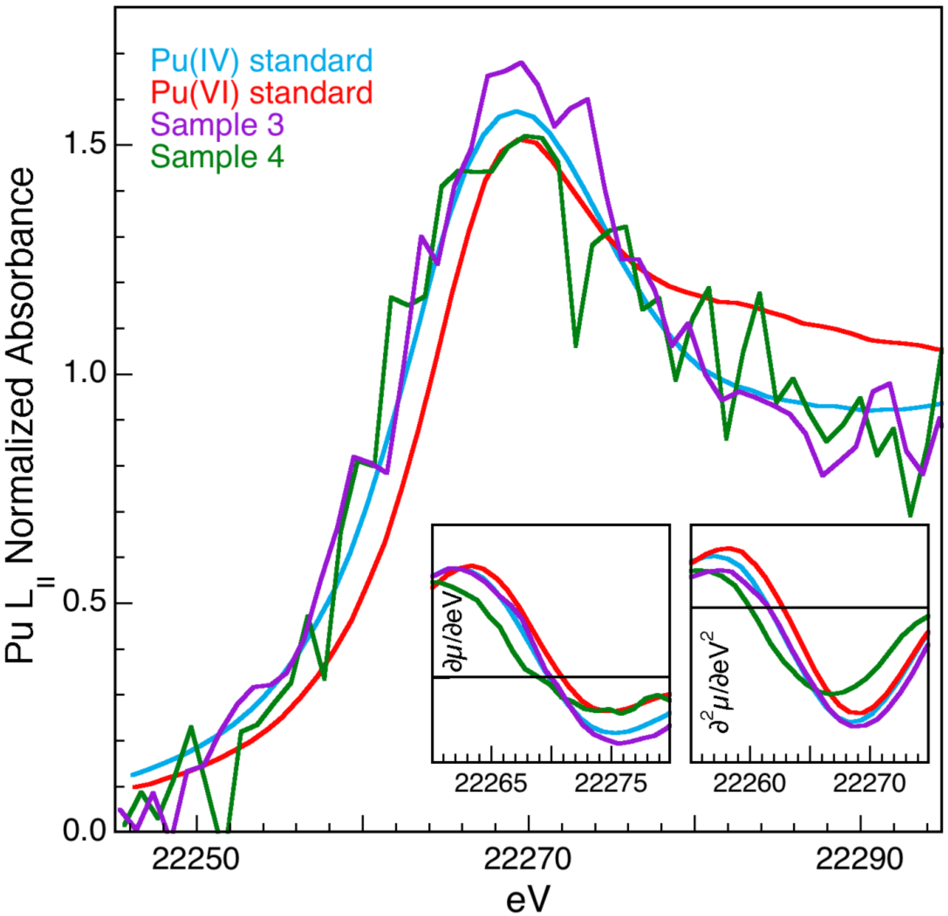

XAFS was used to determine the speciation and the remediation strategy was based on these data

Nuclear legacy

Liquid nuclear wastes –
105 sites
500 Mm^3
total α activity is 1.9×10^{16} Bq
total β activity is 7.3×10^{11} Bq

Solid nuclear wastes –
274 sites
180 Mtonns
total α activity is 6.0×10^{15} Bq
total β activity is 8.1×10^{18} Bq

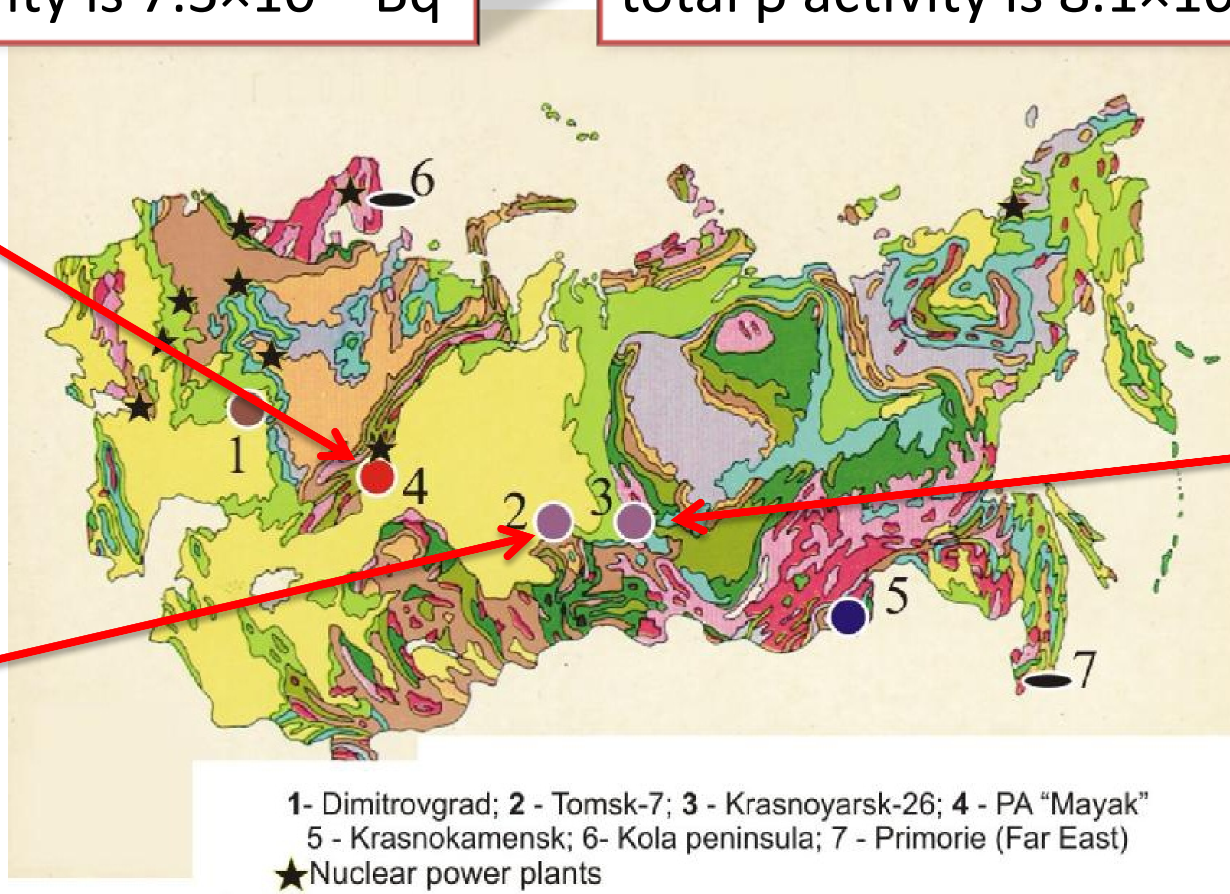

“Mayak” site

Sources of radioactive contamination of South Ural

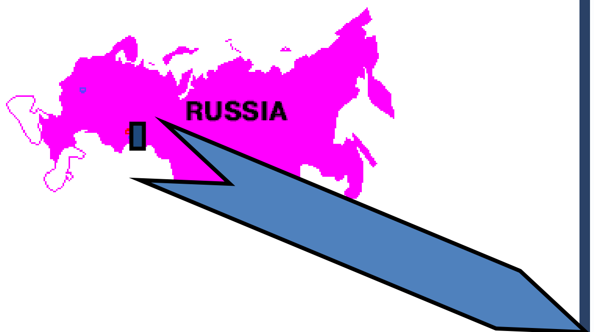

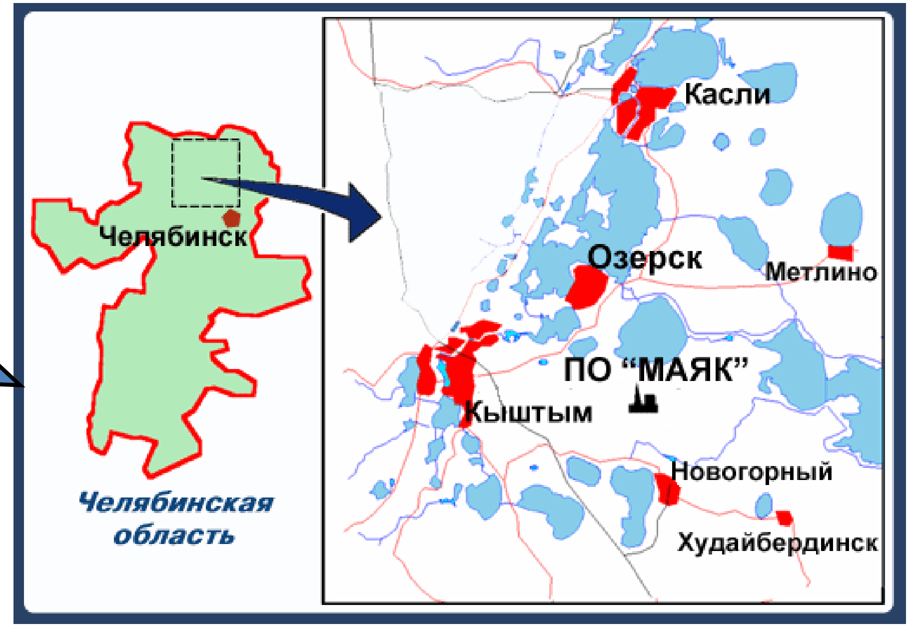

Dec. 22, 1948 – the plant to separate weapon grade Pu from irradiated uranium was launched

Production capacity was around 1 ton of U blocks per day

about 10^5 Ci of wastes

Year before the plant was launched, complex "C" was constructed that is the assembly of tanks for HLW. The capacity was estimated around 15000 m^3 per year. However the real volume of wastes was 200 m^3 per day.

All tanks were filled with HLW before 1950 (about a year after the plant was launched).
The construction of new tanks for HLW was too expensive.

From 1949 till 1951 wastes were disposed to Techa river. During this period c.a. 76 Mm^3 of waste solutions were disposed equal to 2.8 MCi.

Industrial reservoirs at PA “Mayak”

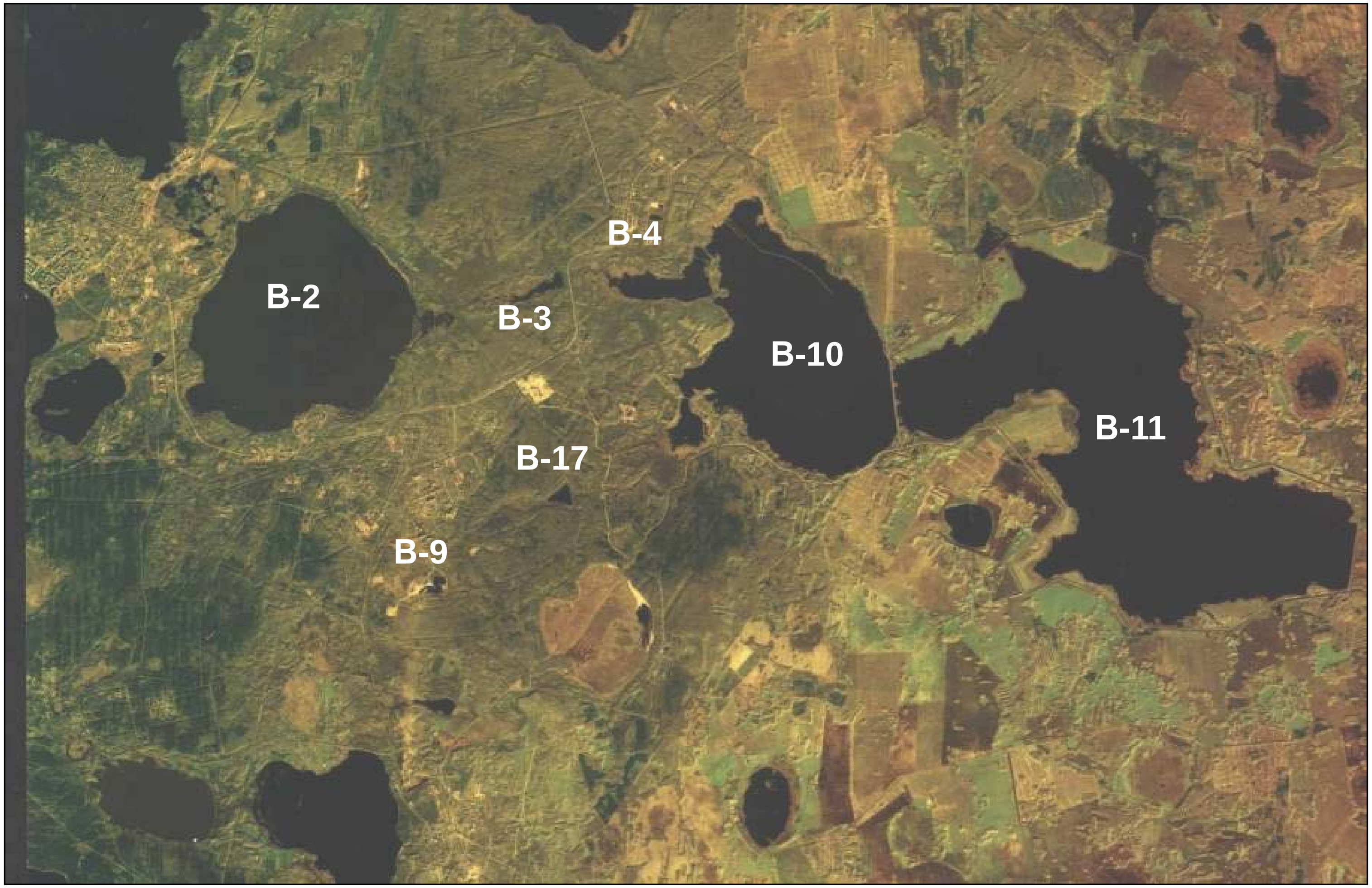

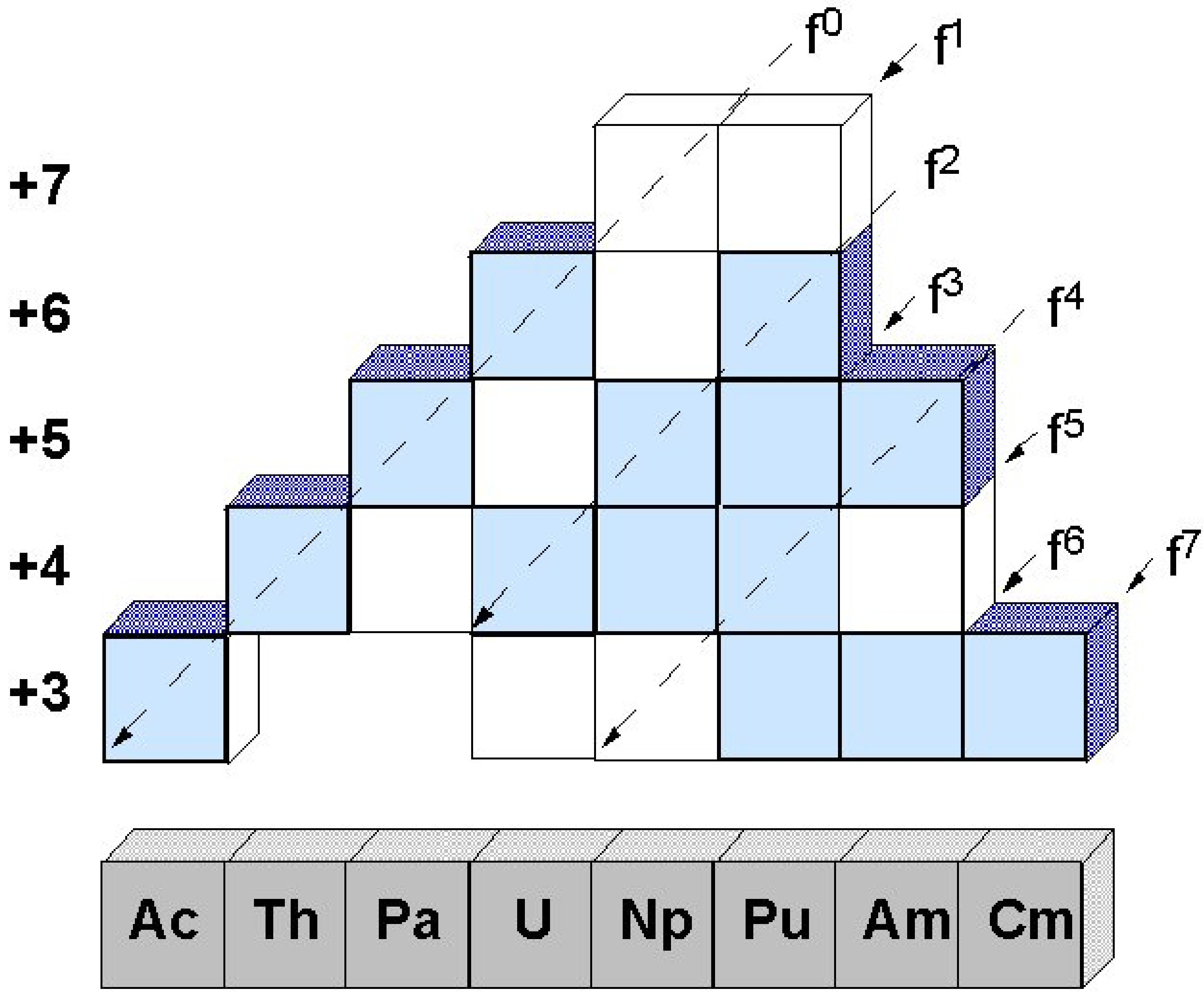

f0
f1
f2
f3
f4
f5
f6
f7
+7
+6
+5
+4
+3
Ac
Th
Pa
U
Np
Pu
Am
Cm

Plutonium behavior in environment

Plutonium – the element of surprise

Gregory Choppin

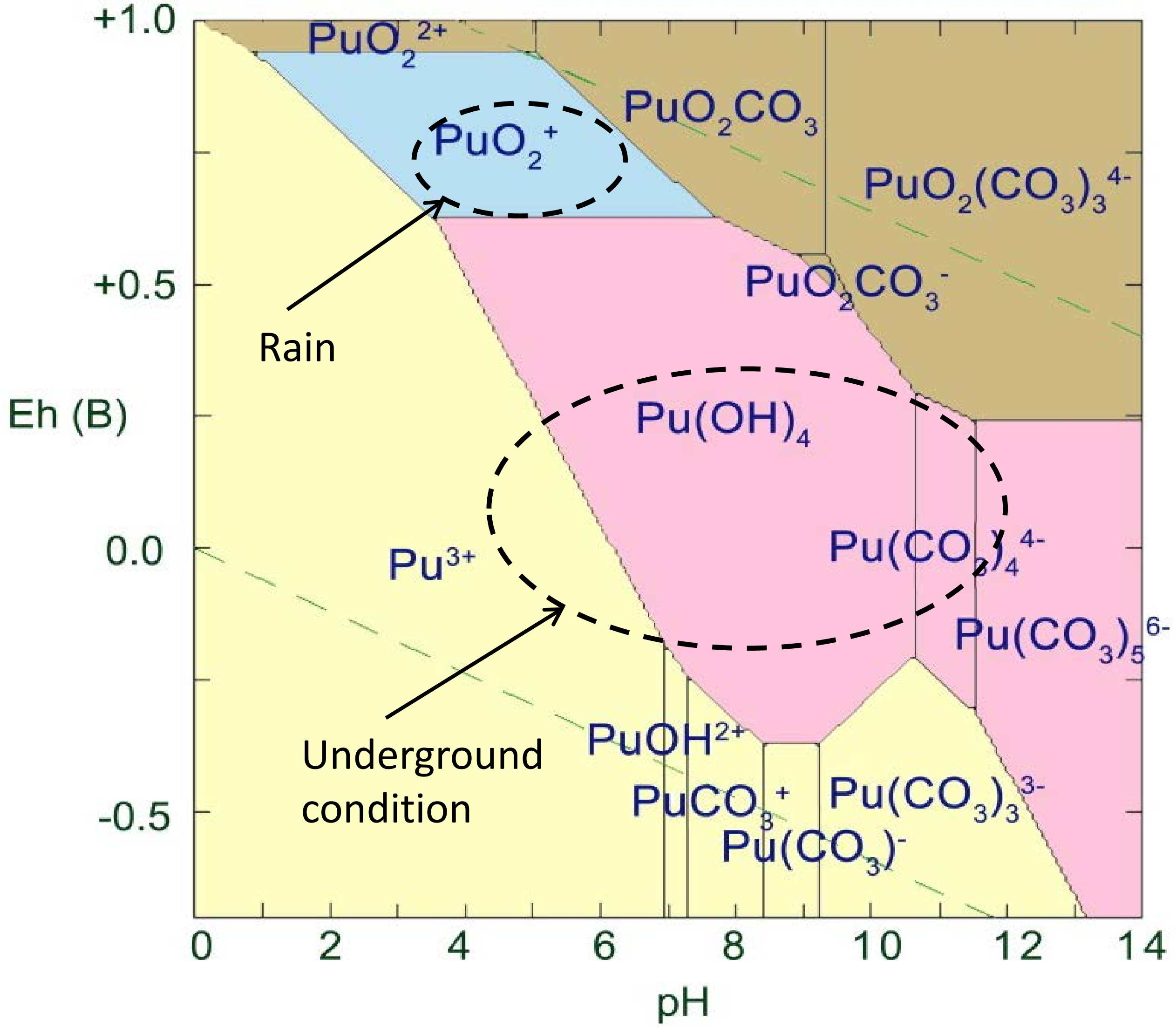

The ability to easily change the oxidation state

Plutonium behavior in the environment

Solubility of Pu(III, IV, V и VI)

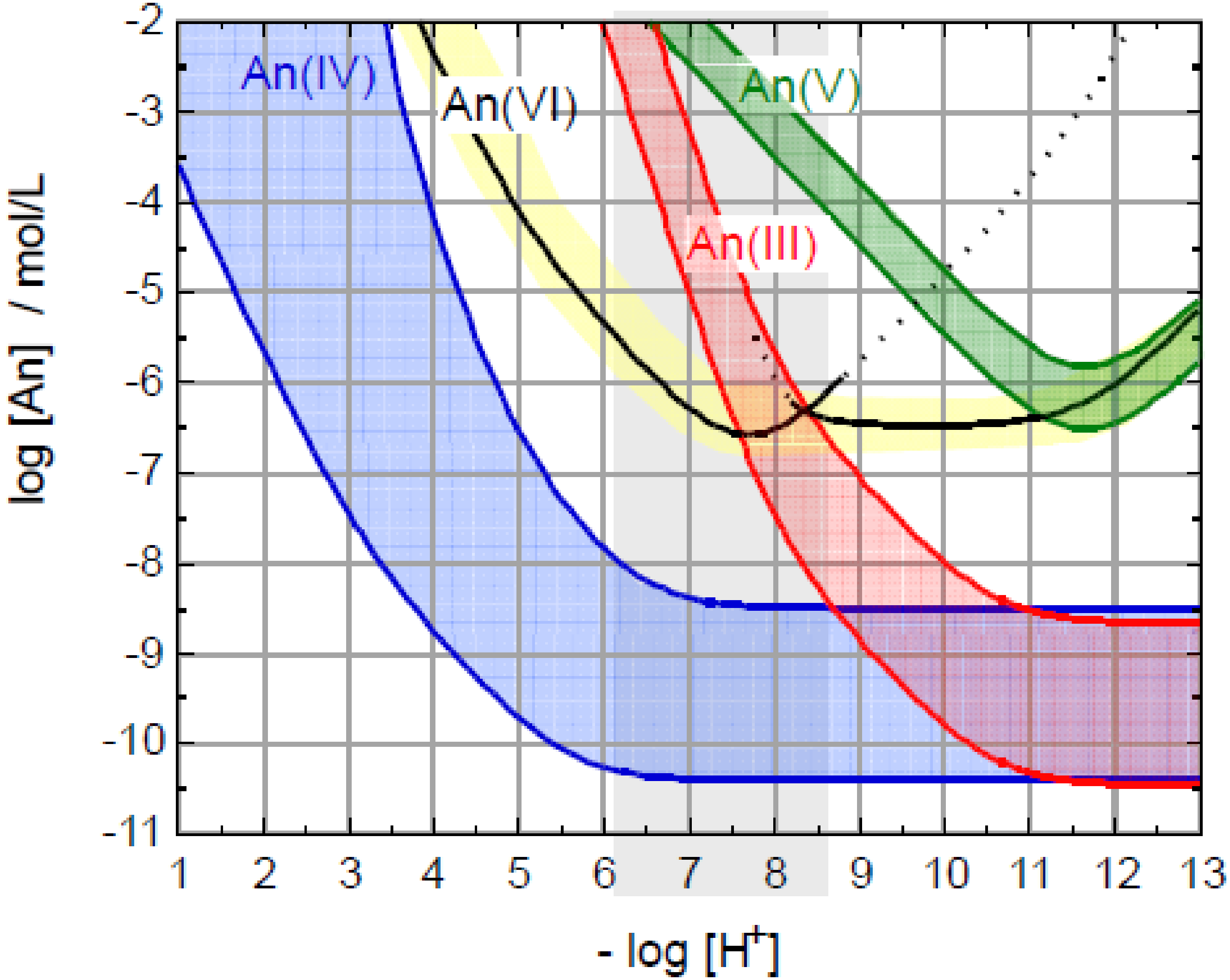

Extremely low solubility of Pu(IV) in aqueous solutions

Plutonium behavior in the environment

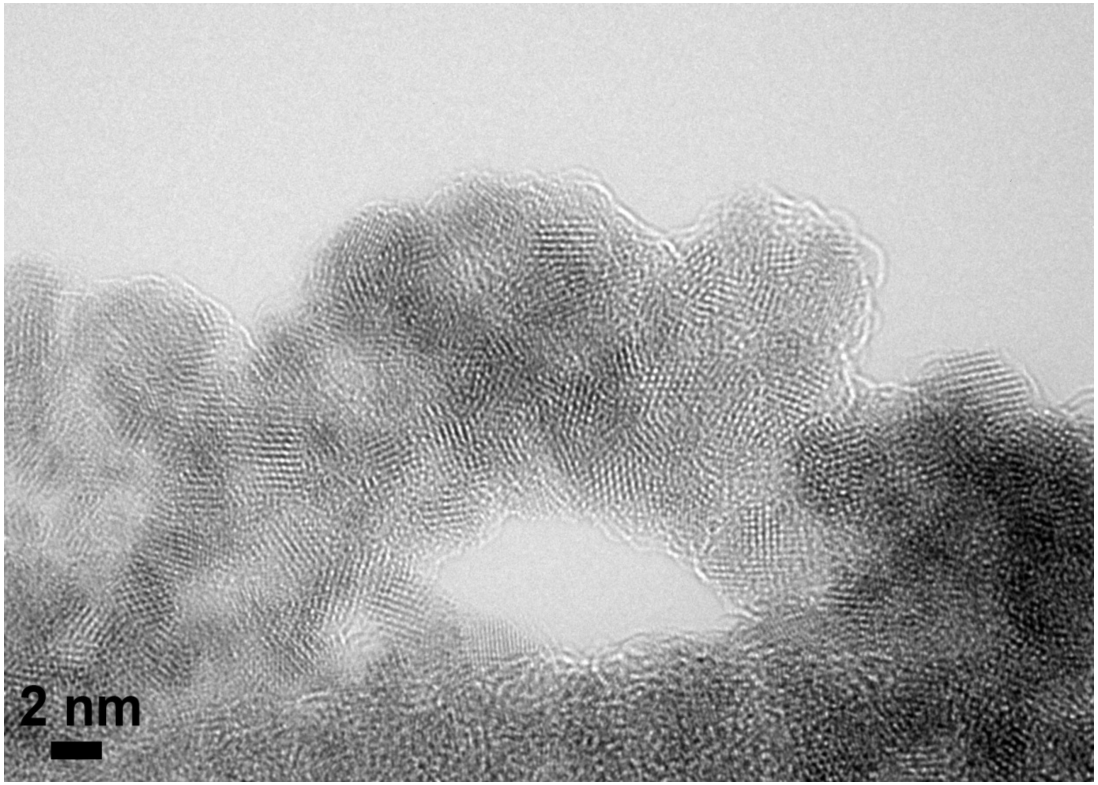

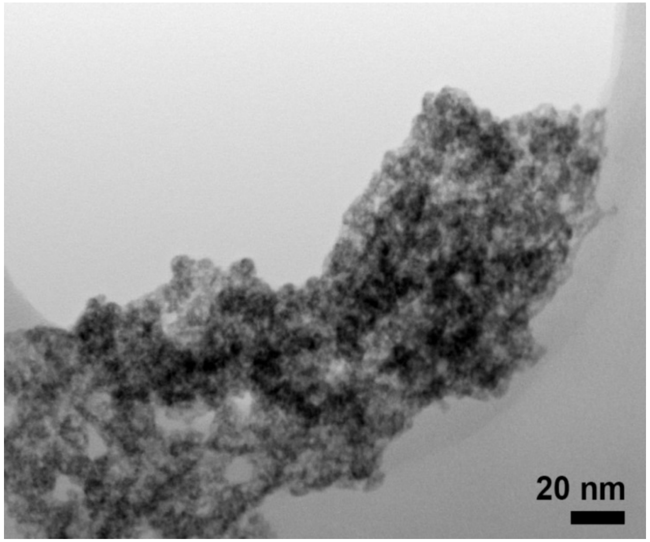

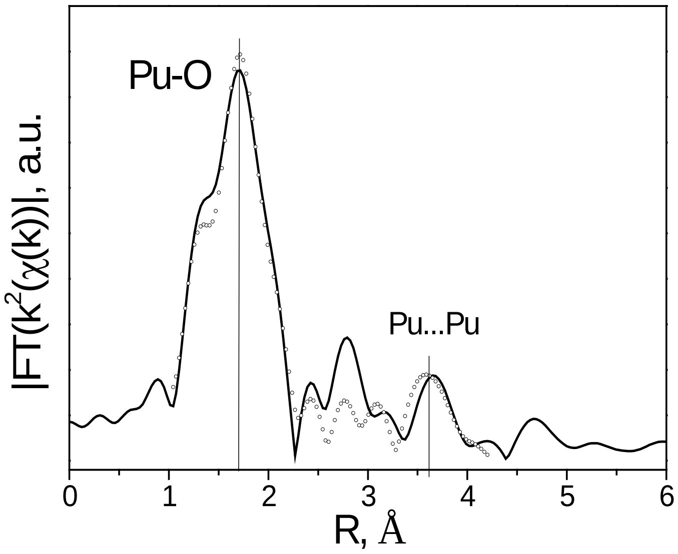

Pu(IV) forms intrinsic colloids – $PuO_{2+x}\cdot nH_2O$ nanoparticles

Reactions that control actinides behavior in the environment

- Sorption
- Redox
- Solubility
- Complexation

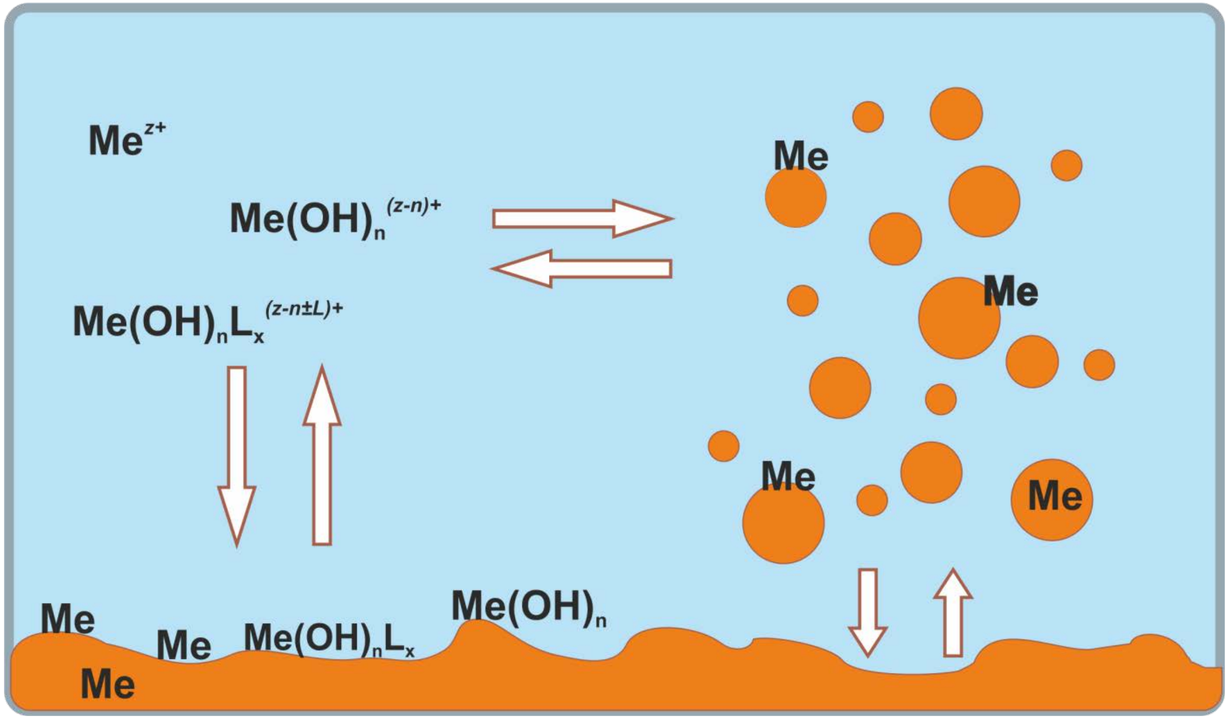

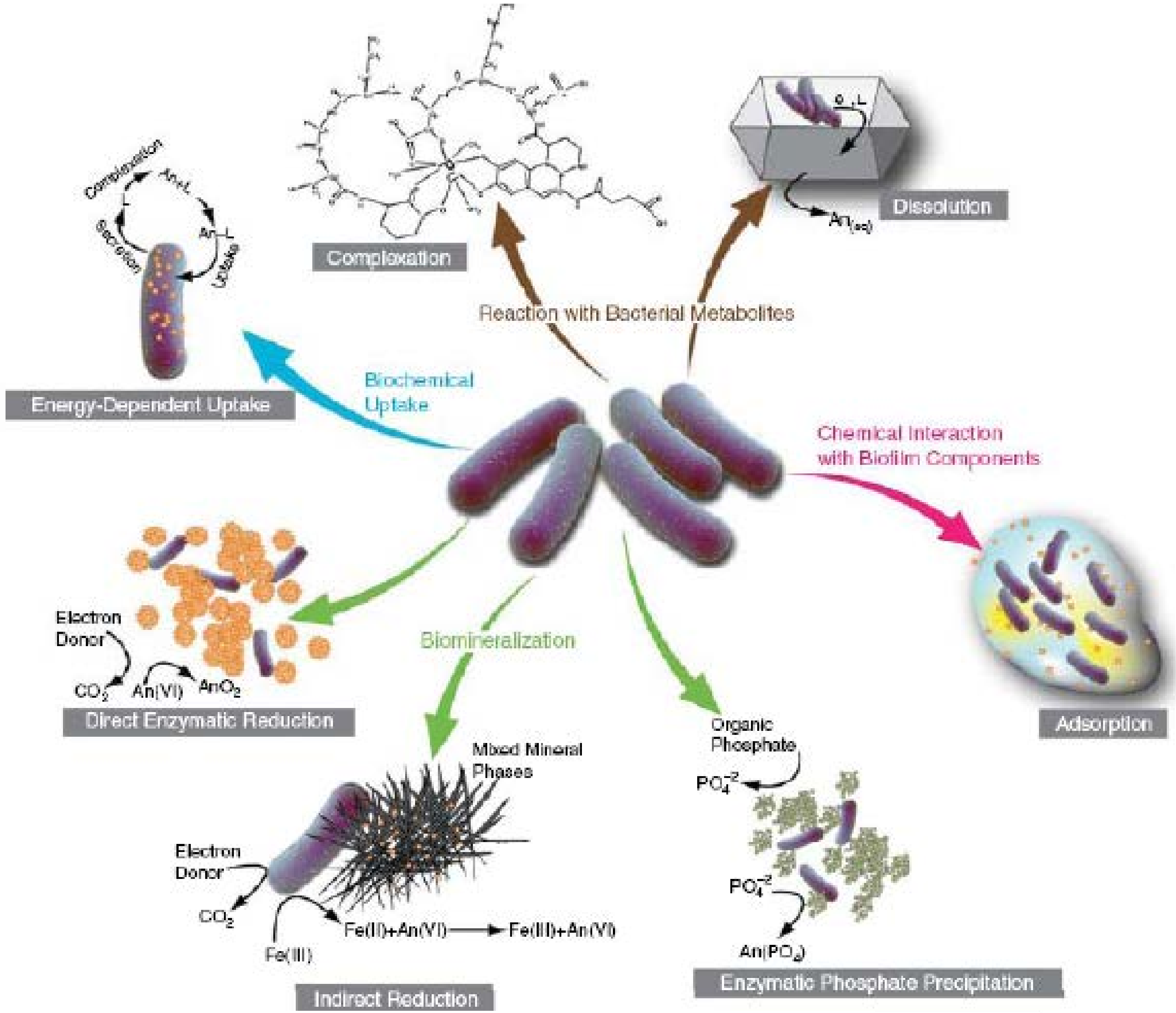

M. Neu et al., MRS Bulletin, 35, 2010

Reduced species, An(III), An(IV) have low solubility and strong sorption affinity

Their migration in geologic conditions is defined by PARTICLES:

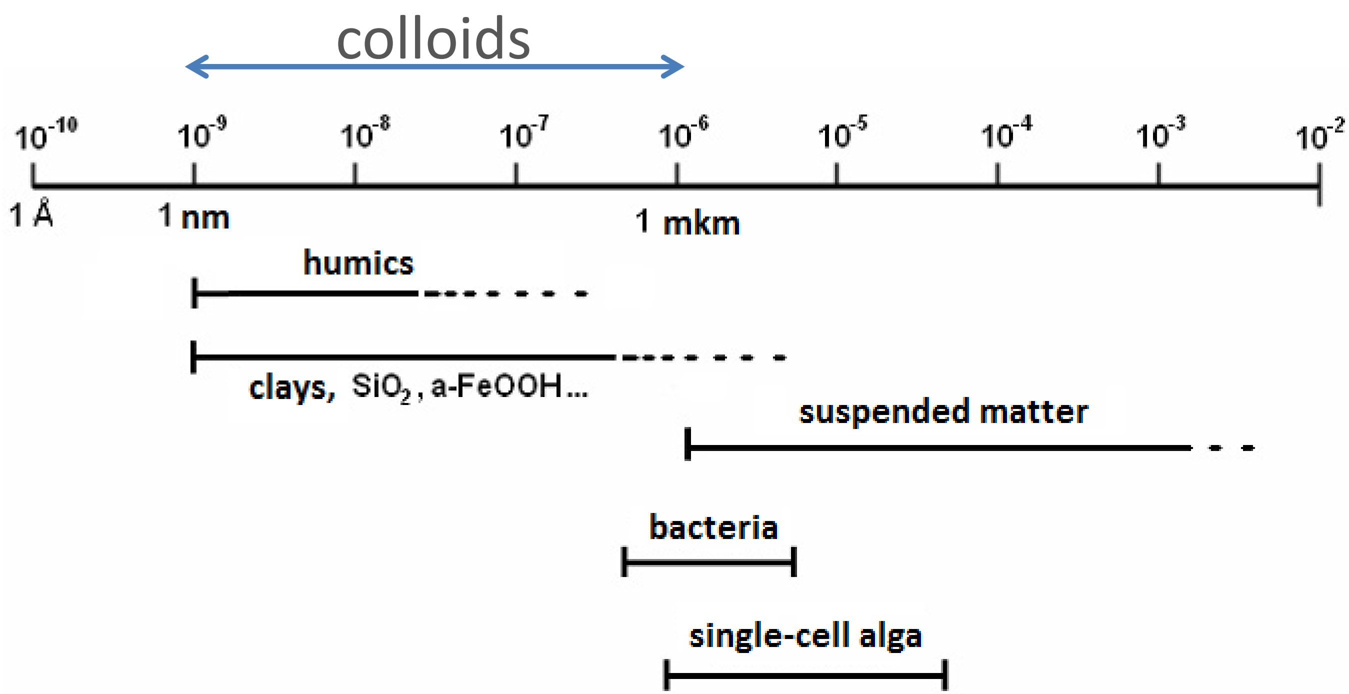

Nanoparticles – particles with the size in the order of 10^{-9} m for which size effects are observed (difference in properties with larger size particles)

Colloids – Radionuclide Migration

H. Geckeis

- Mineral particles (Ironoxides, Clay etc.)

Colloidal Particles in a granitic groundwater (Grimsel, Switzerland)

[Degueldre et al., Appl. Geochem, (1996)]

- Humic substances, bacteria, viruses

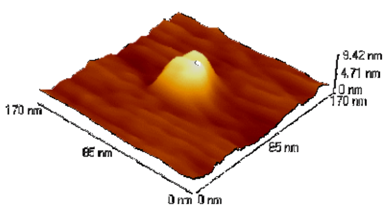

Humic colloids in a sandy aquifer
(Gorleben, Germany)
[M. Plaschke et al, Environ. Sci. Technol. (2002)]

- Radionuclide-Oxidhydrates (e.g. $PuO(OH)_2$)

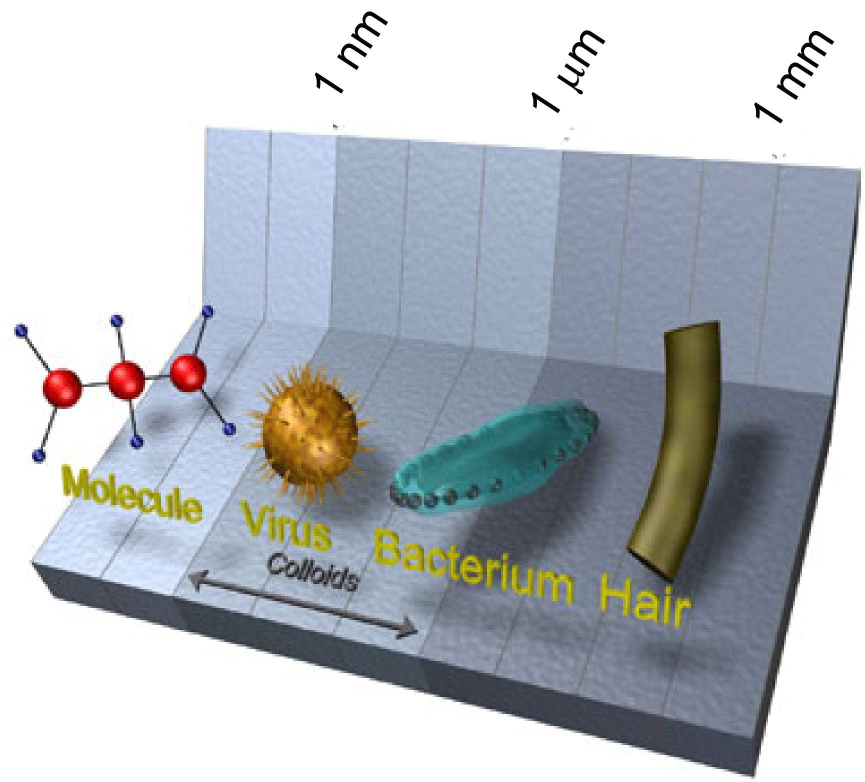

Colloids can contribute to radionuclide transport

Nevada test site

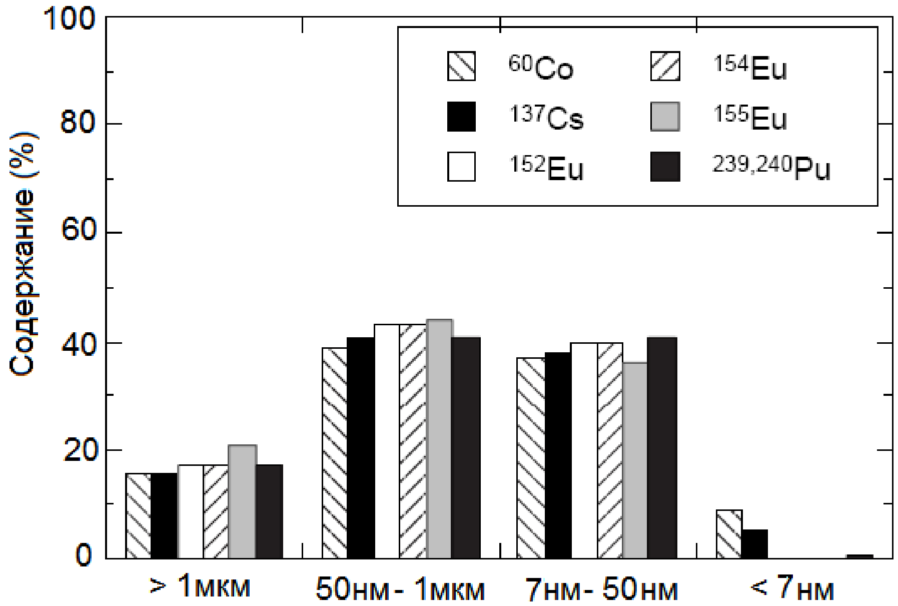

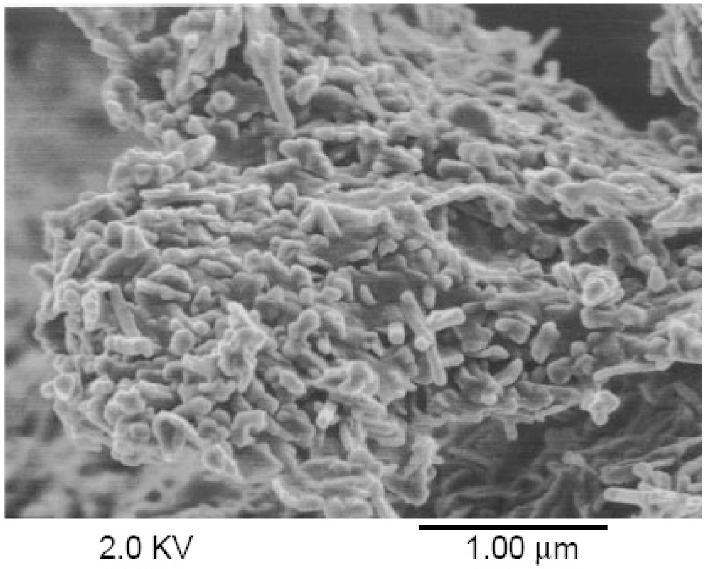

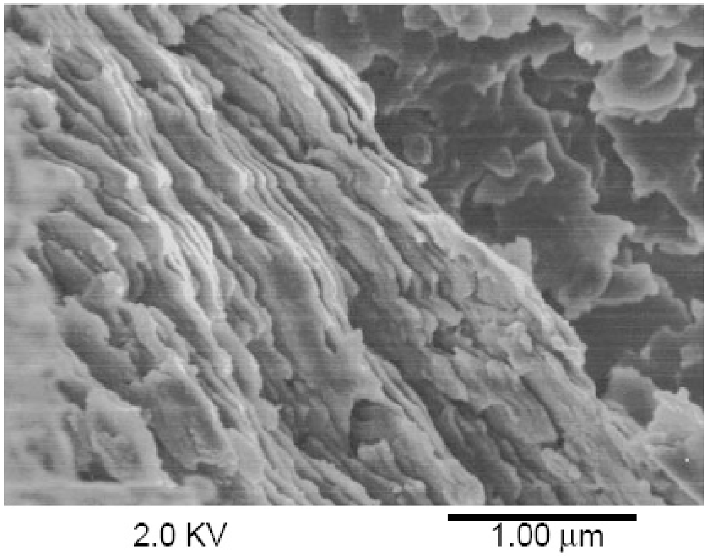

Kersting A.B., Efurd D.W., Finnegan D.L., Rokop D.J., Smith D.K., Thompson J.L., Migration of plutonium in groundwater at the Nevada Test Site. Nature 1999, v. 397, p. 56-59

Colloid Transport of Plutonium in the Far-Field of the Mayak Production Association, Russia

Alexander P. Novikov,[1] Stepan N. Kalmykov,[1,2] Satoshi Utsunomiya,[3] Rodney C. Ewing,[3*] François Horreard,[4] Alex Merkulov,[4] Sue B. Clark,[5] Vladimir V. Tkachev,[1] Boris F. Myasoedov[1]

Sorption of actinides, particularly plutonium, onto submicrometer-sized colloids increases their mobility, but these plutonium colloids are difficult to detect in the far-field. We identified actinides on colloids in the groundwater from the Mayak Production Association, Urals, Russia; at the source, the plutonium activity is ~1000 becquerels per liter. Plutonium activities are still 0.16 becquerels per liter at a distance of 3 kilometers, where 70 to 90 mole percent of the plutonium is sorbed onto colloids, confirming that colloids are responsible for the long-distance transport of plutonium. Nano–secondary ion mass spectrometry elemental maps reveal that amorphous iron oxide colloids adsorb Pu(IV) hydroxides or carbonates along with uranium carbonates.

Submicrometer-sized colloids, consisting of inorganic and/or organic compounds, occur at up to 10^{17} particles per liter in groundwater and provide an important means of transporting elements with low solubilities, including the actinides (*1–3*). The stability of these colloids is a function of the composition of groundwater and the hydrologic conditions (*4*).

The formation of actinide pseudo-colloids, in which the actinide sorbs onto aquatic colloids, can stabilize actinides in natural waters and increase their concentrations by many orders of magnitude over the values expected from solubility calculations (*2*, *5*). The association of Pu with colloids 25 to 450 nm in size has been observed 3.4 km from a source at Los Alamos National Laboratory (*6*). This migration distance is greater than modeled estimates (*7*). Similar transport has also been seen at the Savannah River Site (*8*). At Nevada Test Site, Pu has migrated 1.3 km in 30 years in groundwater by means of colloids with sizes of 7 nm to 1 μm (*9*). Model results imply that colloid-facilitated transport of actinides at Yucca Mountain could lead to as much as a 60-fold increase in the total effective dose equivalent to an exposed population (*10*).

Colloid-facilitated transport is likely the means for actinides' long-distance transport in groundwater. Many previous studies have experimentally demonstrated adsorption of Pu onto a variety of minerals and mineral assemblage (*11–13*). However, little is known of the speciation of the actinides or the type of colloids with which they are associated, particularly during the transport in the far-field where there are many competing processes, such as desorption from the colloids and resorption onto minerals.

To understand the colloid-associated actinides and their long-distance transport in groundwater, we investigated Pu migration in the natural groundwater system at one of the most contaminated nuclear sites in the world: Mayak, Russia. Mayak is a nuclear waste reprocessing plant near Kyshtym, in the Southern Urals, Russia (*14*) (Fig. 1). Waste effluents containing ^{90}Sr, ^{137}Cs, ^{241}Am, and ^{239}Pu were discharged into Lake Karachai (*15*, *16*); these were weakly alkaline $NaNO_3$ brine solutions with a pH of 7.9 to 9.3 and a salt concentration of 16 to 145 g/liter. The major dissolved ionic species were NO_3^- (11 to 78 g/liter), CH_3COO^- (0.6 to 20 g/liter), $C_2O_4^{2-}$ (0.9 to 14 g/liter), SO_4^{2-} (0.12 to 1.3 g/liter), Na^+ (6 to 32 g/liter), Cl^- (20 to 350 mg/liter), U(VI) (13 to 196 mg/liter), Ca^{2+} (8 to 80 mg/liter), and

[1]Vernadsky Institute of Geochemistry and Analytical Chemistry, Russian Academy of Sciences, Moscow 119991, Russia. [2]Radiochemistry Division, Chemistry Department, Lomonosov Moscow State University, Moscow 119992, Russia. [3]Department of Geological Sciences, University of Michigan, Ann Arbor, MI 48109–1005, USA. [4]Cameca, 92622 Gennevilliers Cedex, 92403, France. [5]Department of Chemistry and Nuclear Radiation Center, Washington State University, Pullman, WA 99164–4630, USA.

*To whom correspondence should be addressed. E-mail: rodewing@umich.edu

SCIENTIFIC AMERICAN

SEARCH

• Log In or
• Log In to

Energy & Sustainability Evolution Health Mind & Brain Space

Home » News »

News | More Science

Colloids in Russia: Have Plutonium, Will Travel

By David Biello | October 26, 2006 | 2

Share Email Print

The Future of Nuclear Power
The U.S.--and the world--is gearing up to build a potentially massive fleet of new nuclear reactors, in part to fight climate change. But can nuclear power handle the load? »
January 26, 2009

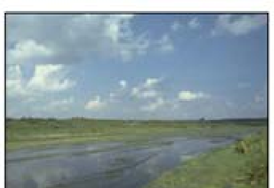

Among the list of environmental disasters created by Soviet central planning, Mayak must rank high. Commissioned as a plant in southern Russia to manufacture plutonium for bombs in 1948, it soon segued into a long life as a reprocessing center for nuclear

Follow Scientific American

Scientific American Newsletter

Get weekly coverage delivered to your inbox.

Sign Up Now

Various mineral particles have different properties (pHiep, ξ-potential, ΔG of "XO-Cat" bond formation, …) the distribution of radionuclides is very heterogeneous.

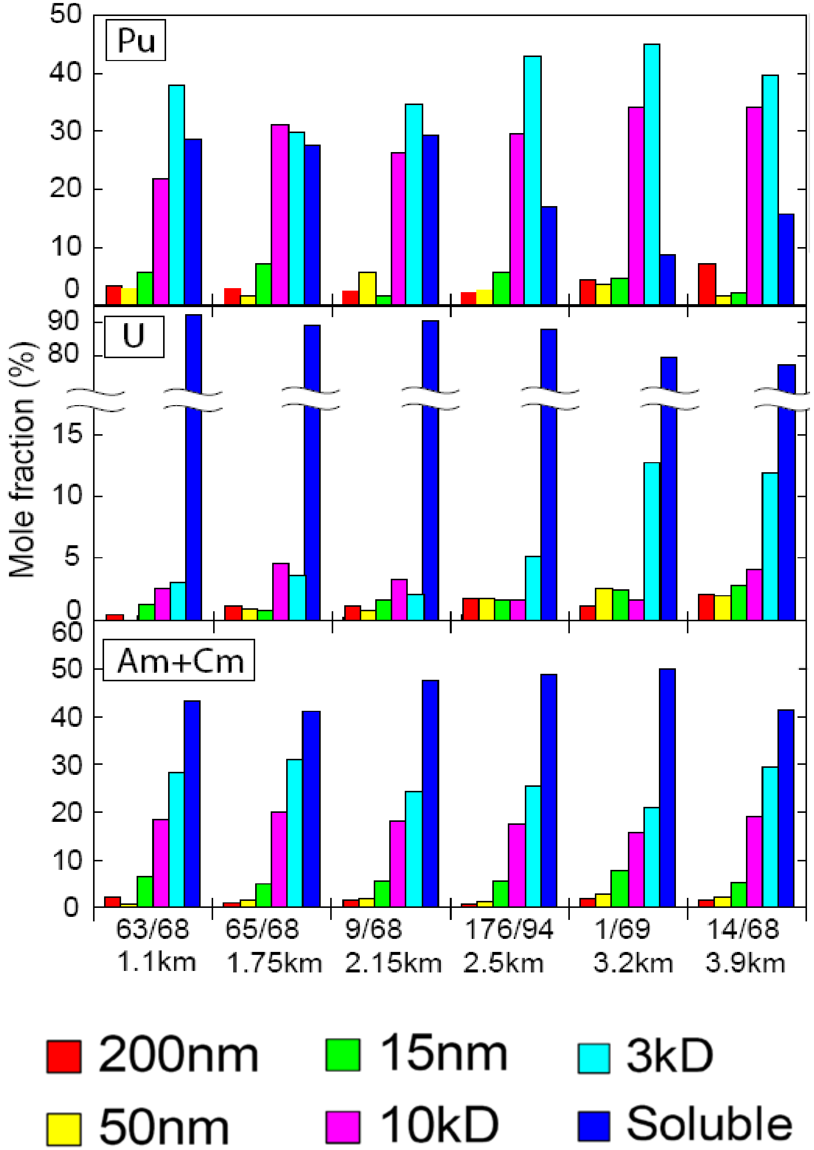

Novikov A.P., Kalmykov St.N., Utsunomiya S., Ewing R.C., Horreard F., Merkulov A., Clark S.B., Tkachev V.V., Myasoedov B.F. Colloid Transport of Plutonium in the Far-field of the Mayak Production Association, Russia. // Science, Vol. 314, 2006, p. 638-641

nano-SIMS elemental maps

Kalmykov et al.

Ferrihydrite

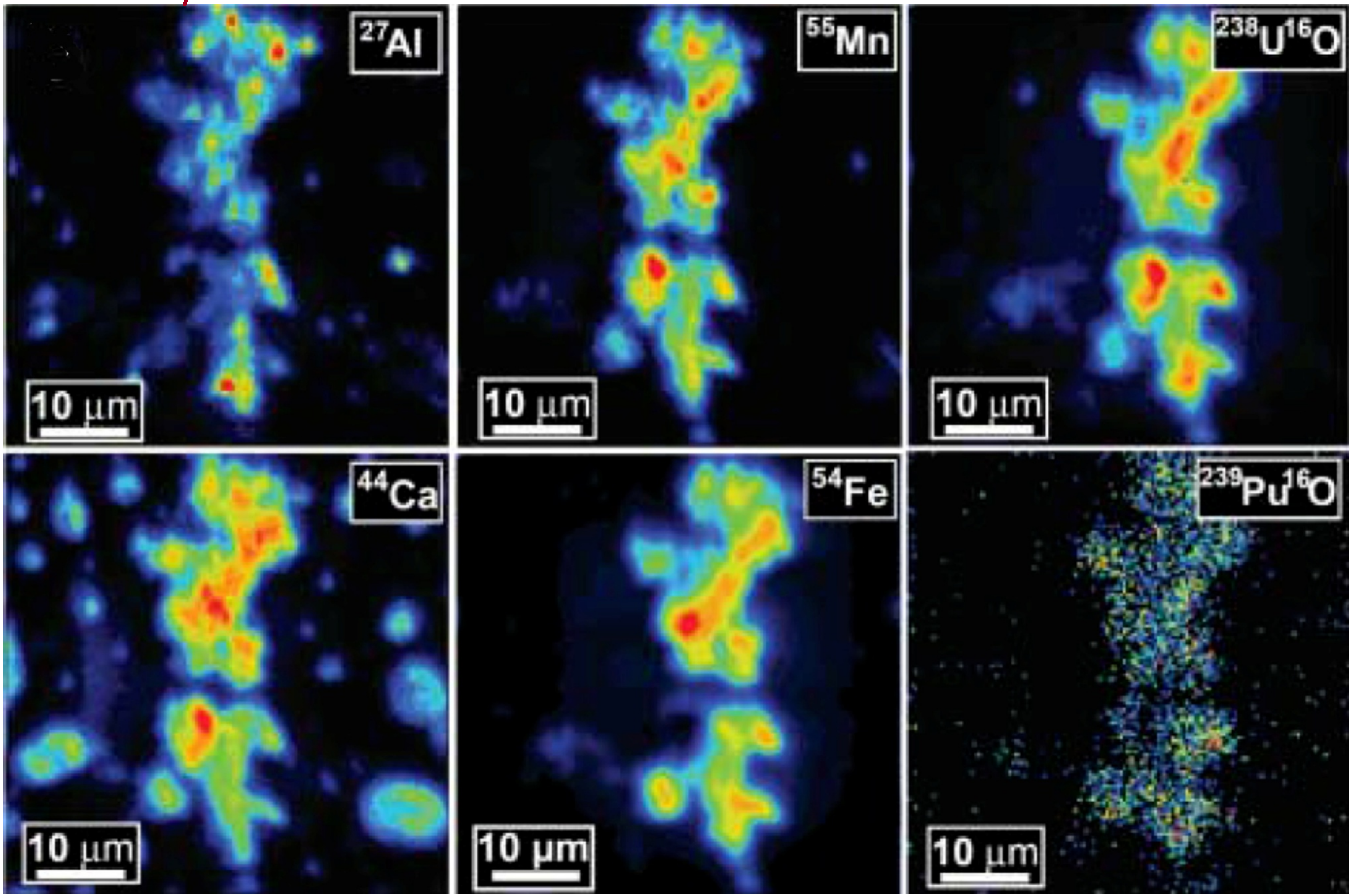

Novikov A.P., Kalmykov S.N., Utsunomiya S., Ewing R.C., Horreard F., Merkulov A., Clark S.B., Tkachev V.V., Myasoedov B.F., Colloid transport of plutonium in the far-field of the Mayak Production Association, Russia, Science 2006, v. 314, p. 638-641

Подземная лаборатория в Швейцарских Альпах

Система: трещиноватые граниты / глины

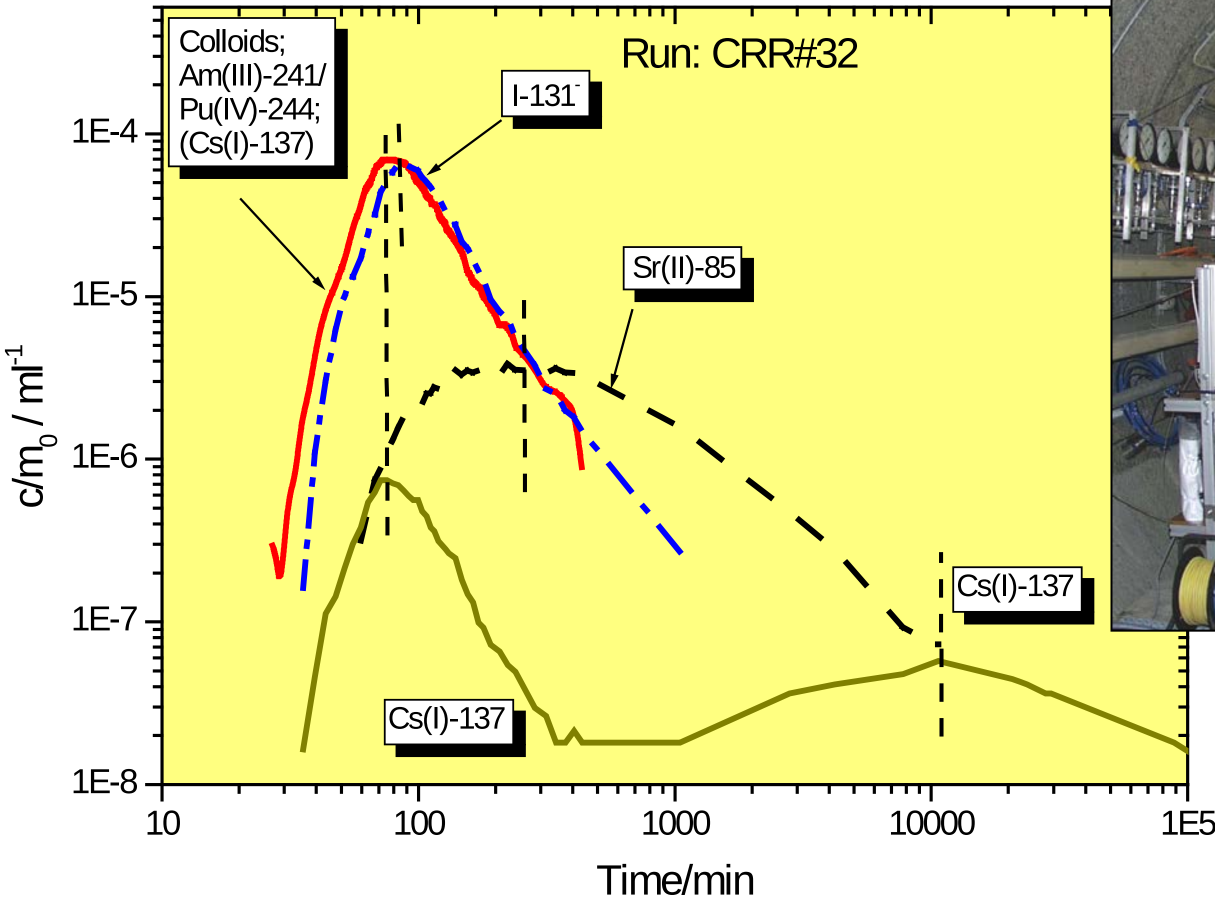

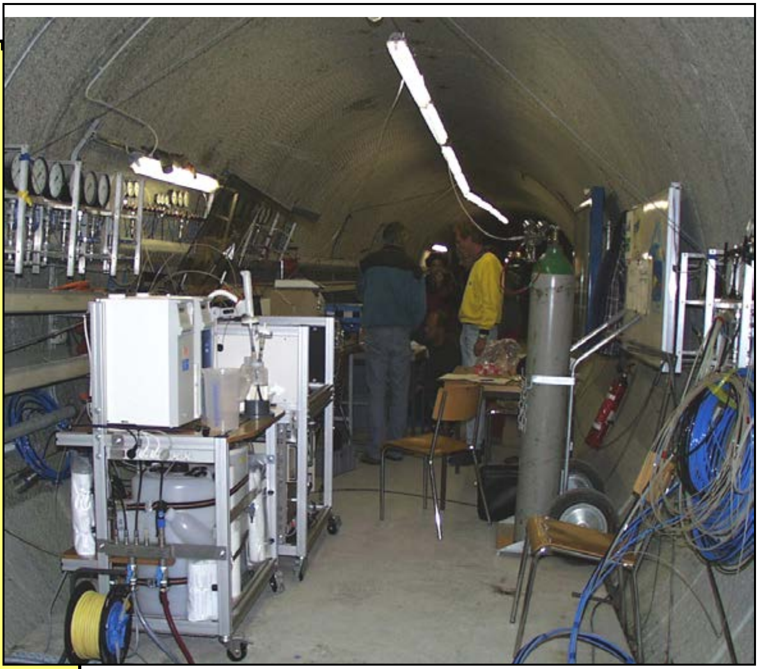

Am(III), Pu(IV) и частично Cs(I) связаны с коллоидными частицами глин, Коллоидные формы радионуклидов мигрируют быстрее, чем ионные формы.

A. Möri et al.,Coll.Surf. 217 (2003),
H. Geckeis et al., Radiochim. Acta, 92 (2004)

Criteria for colloid facilitated transport

(1)colloids must be generated ;

(2) contaminants must associate with the colloids;

(3) colloids must be transported through the groundwater.

Colloid stability

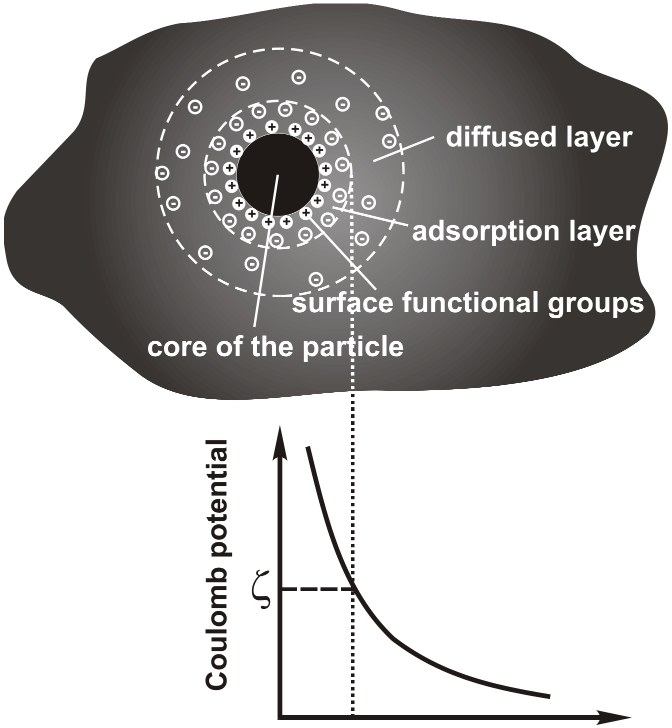

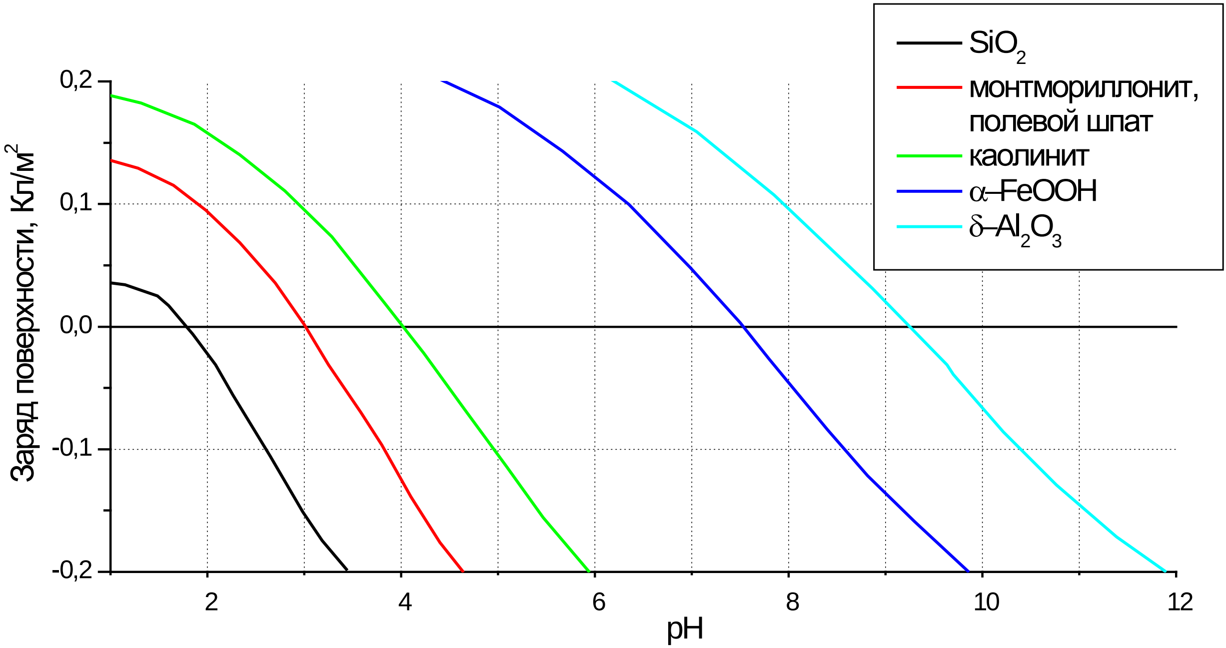

	pHтнз
α-Al_2O_3	9.1
α-$Al(OH)_3$	5.0
Fe_3O_4	6.5
$Fe(OH)_3$ am	8.5
σ-MnO_2	2.8
SiO_2	2.0
kaolinite	4.6

Colloid interaction with rock surfaces – fluorescence microcopy

1. Enhanced colloid sorption at surface defects

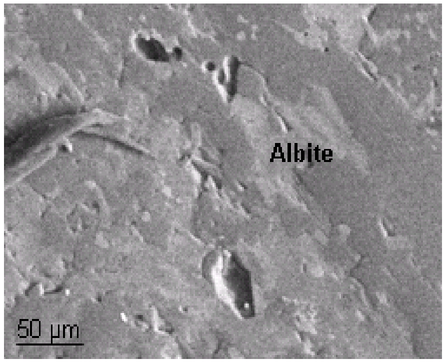

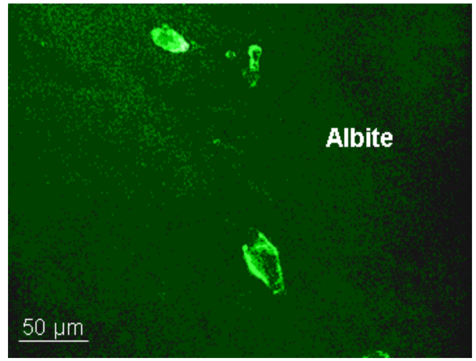

pH = 4; I = 0.01 M NaCl;
$c_{colloids}$ = 0.05 g/l

2. Enhanced colloid sorption at mineral edges

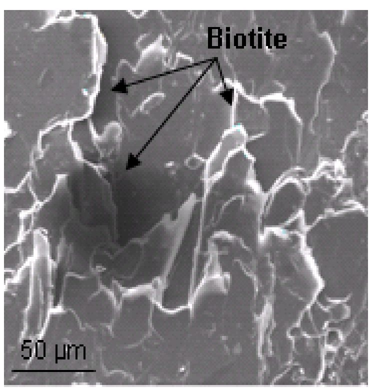

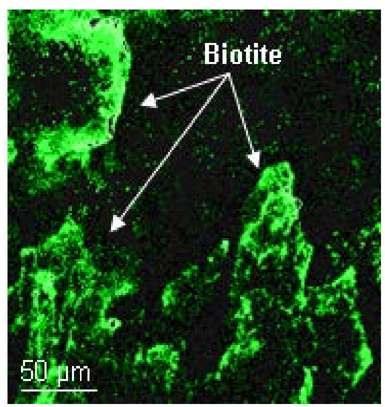

A. Filby, M. Plaschke, 2008

The effect of sorbed species on colloid stability

ξ-potential of SiO_2

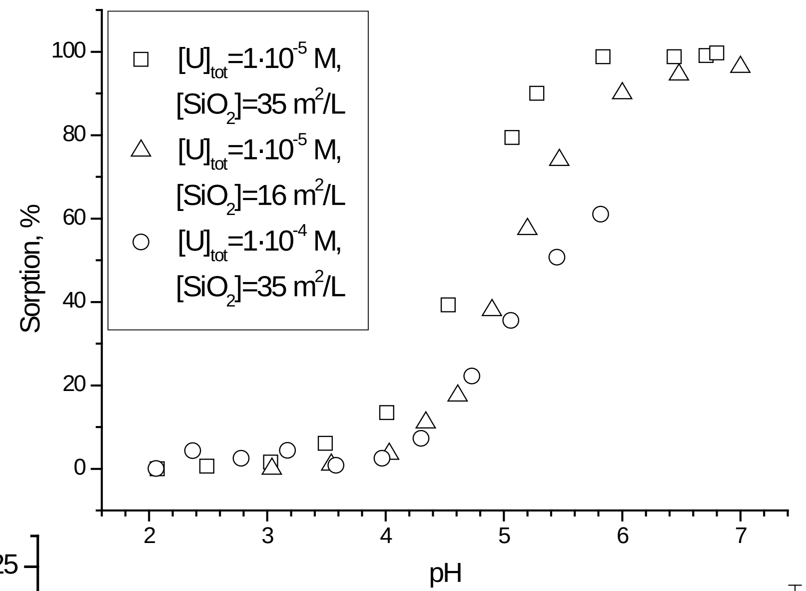

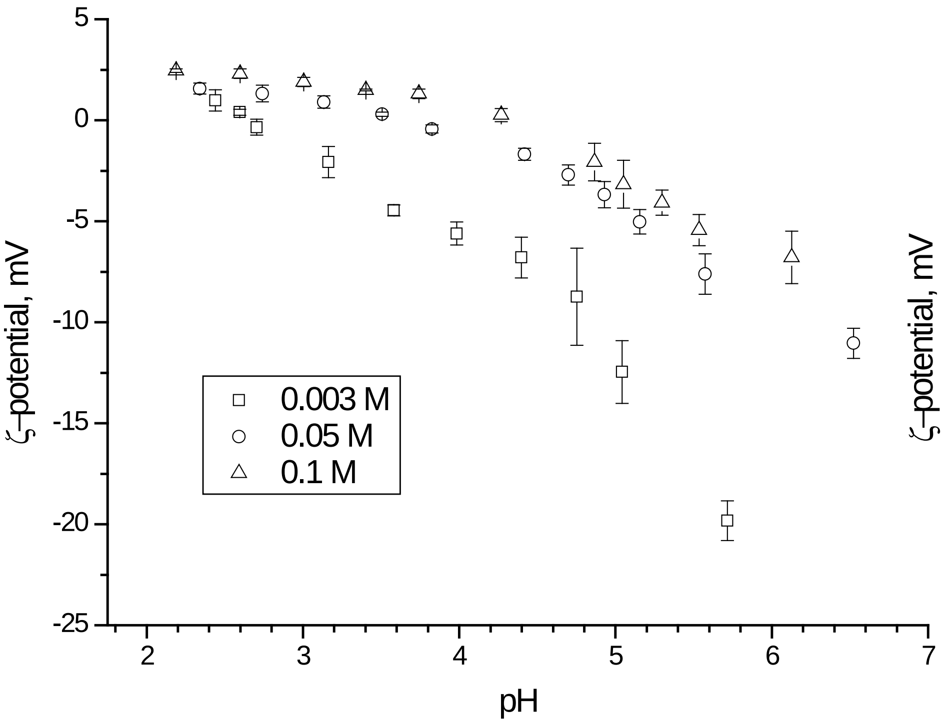

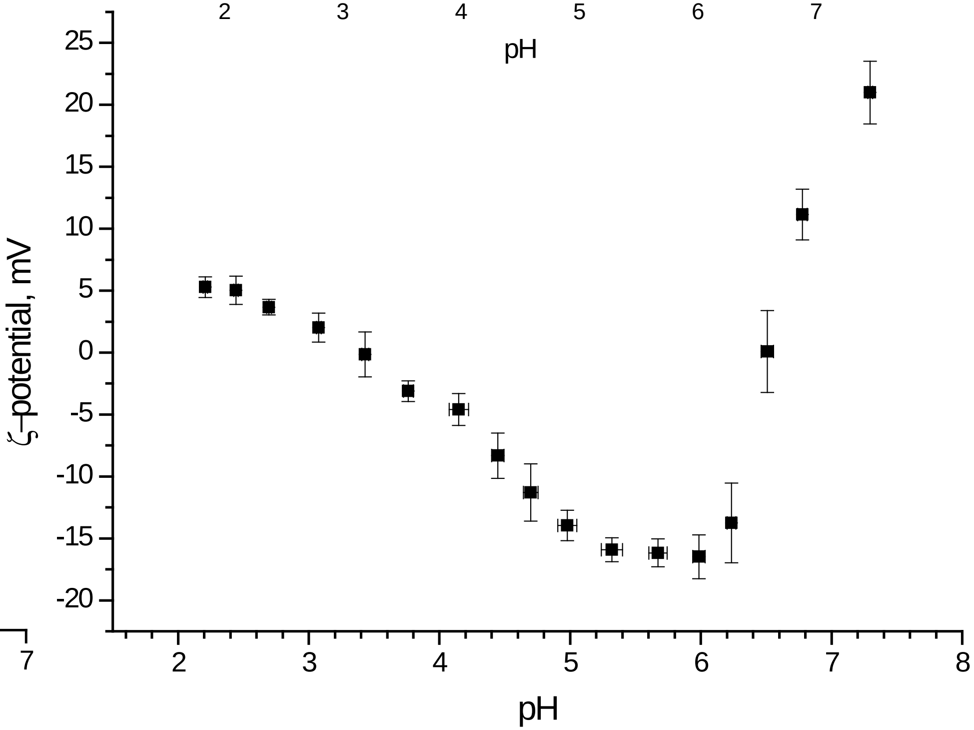

Stability of colloid suspensions

Ionic strength effect

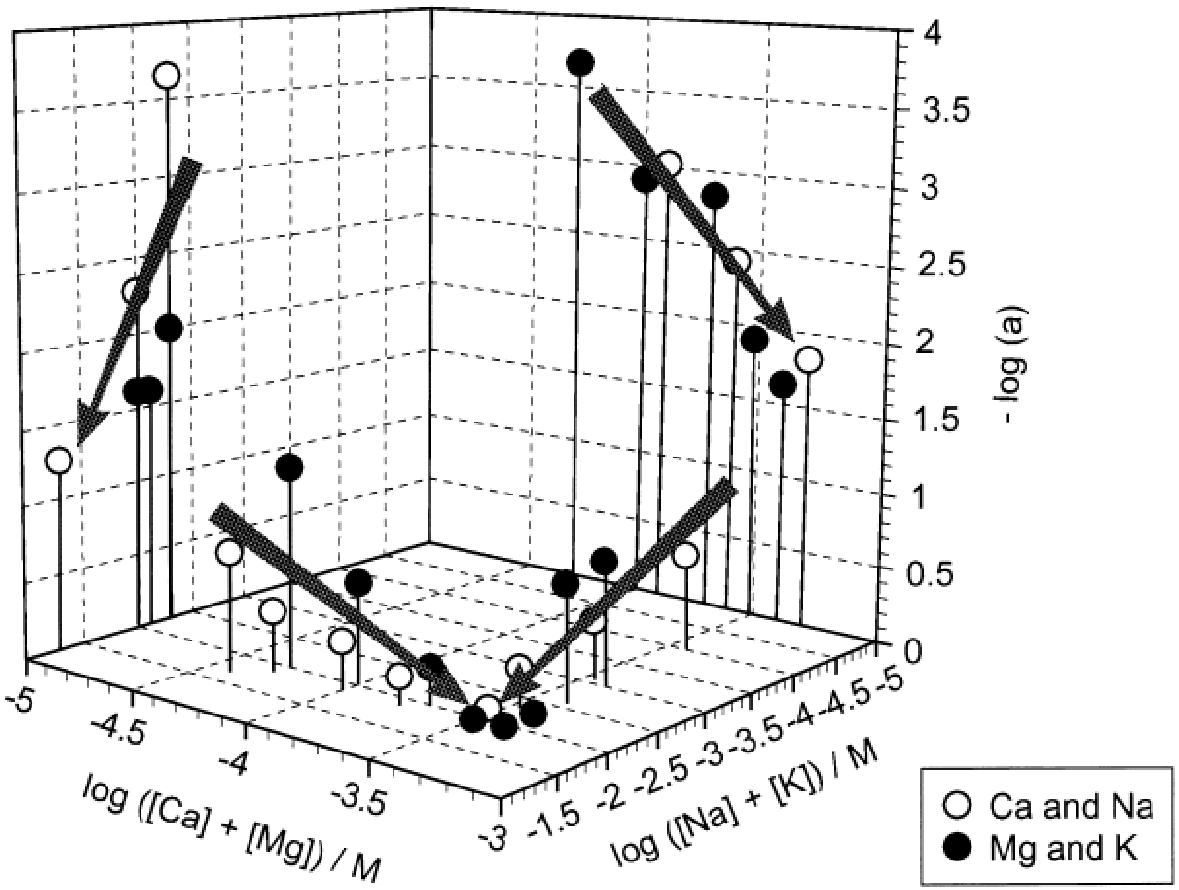

Stability
IA group cations less than
<u>$1 \cdot 10^{-2}$ M</u>,
IIA group cations less than
<u>$1 \cdot 10^{-4}$ M</u>

McCarthy J. et al. 1993

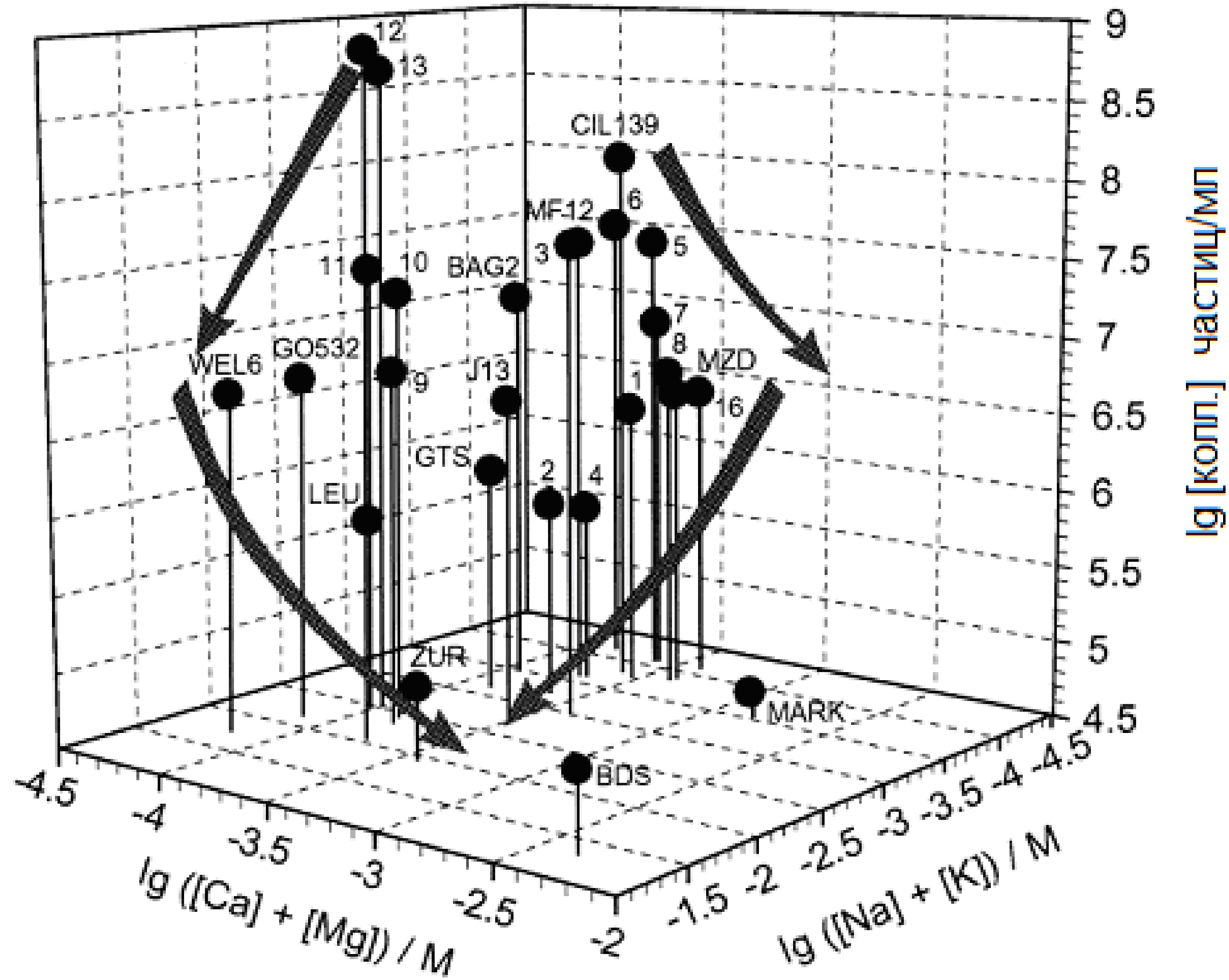
12
13
CIL139
6
MF12
3
5
11
10
BAG2
7
8
MZD
WEL6
GO532
9
J13
1
16
GTS
2
4
LEU
ZUR
MARK
BDS
9
8.5
8
7.5
7
6.5
6
5.5
5
4.5
lg [колл.] частиц/мл
-4.5
-4
-3.5
-3
-2.5
-2
lg ([Ca] + [Mg]) / M
-1.5
-2
-2.5
-3
-3.5
-4
-4.5
lg ([Na] + [K]) / M

The effect of surface films on colloid stability

	Distance, m	Depth	Colloid concentration, g/L	Colloid mean radius, nm
63/68	1000	30	0.02975	603.9 ± 5.3
		80	0.43218	373.4 ± 4.7
64/68	1250	20	0.05066	608.7 ± 30.1
		80	0.20611	399.2 ± 4.7
50/79	3000	20	0.02955	903.7 ± 16.8
		50	0.09565	650.1 ± 9.1
160/70	1000	20	0.00500	496.5 ± 16.4
		100	0.01393	393.7 ± 43.4

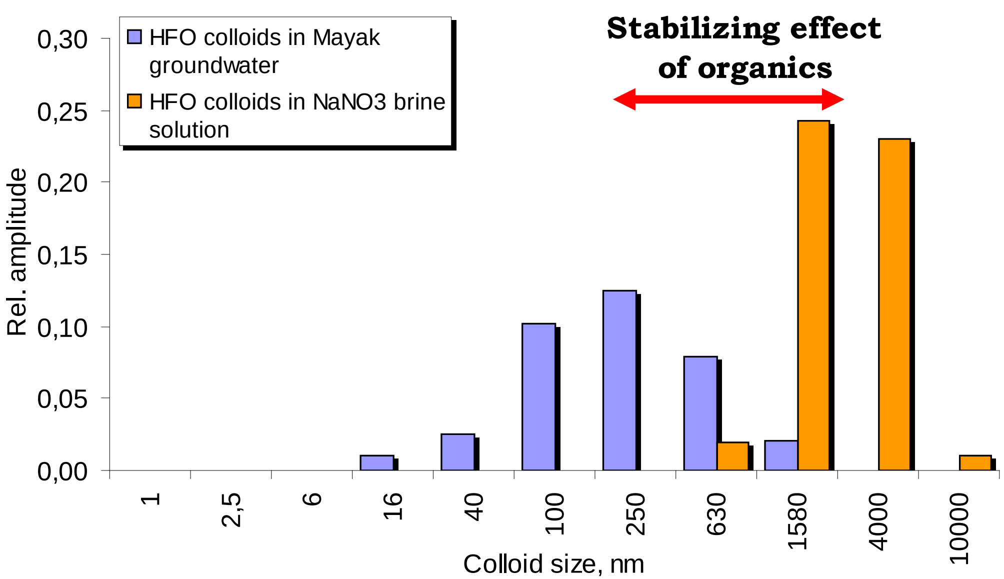

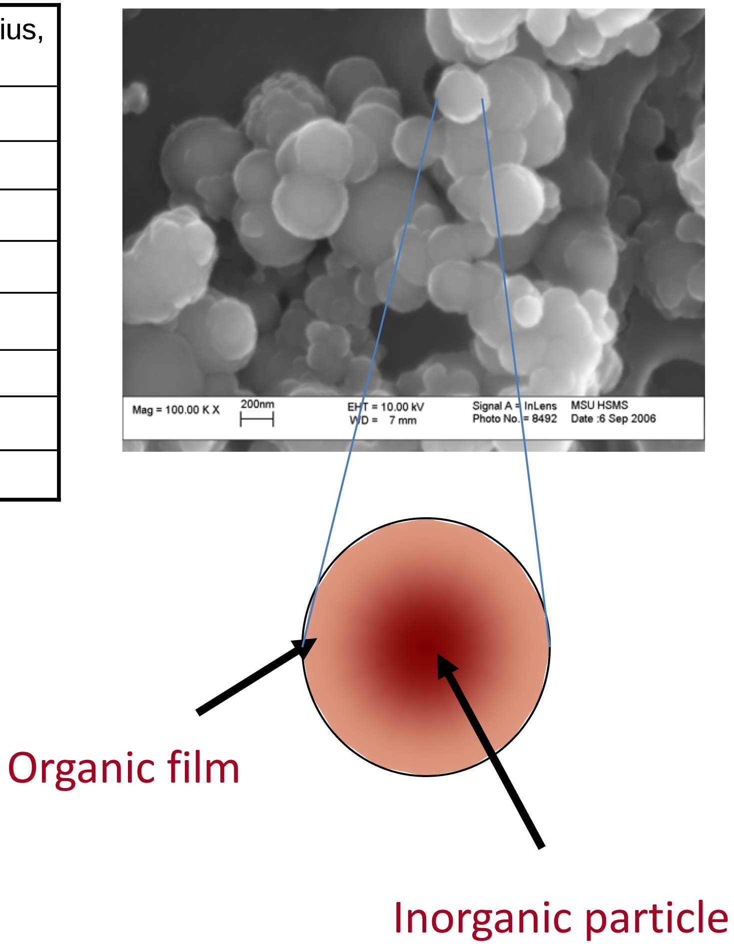

The effect of surface films on colloid stability

	Distance, m	Depth	Colloid concentration, g/L	Colloid mean radius, nm
63/68	1000	30	0.02975	603.9 ± 5.3
		80	0.43218	373.4 ± 4.7
64/68	1250	20	0.05066	608.7 ± 30.1
		80	0.20611	399.2 ± 4.7
50/79	3000	20	0.02955	903.7 ± 16.8
		50	0.09565	650.1 ± 9.1
160/70	1000	20	0.00500	496.5 ± 16.4
		100	0.01393	

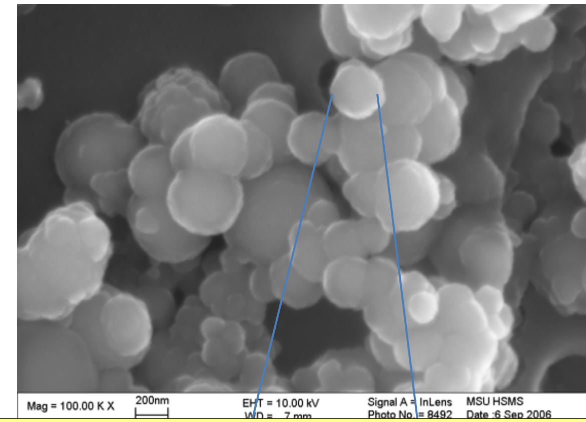

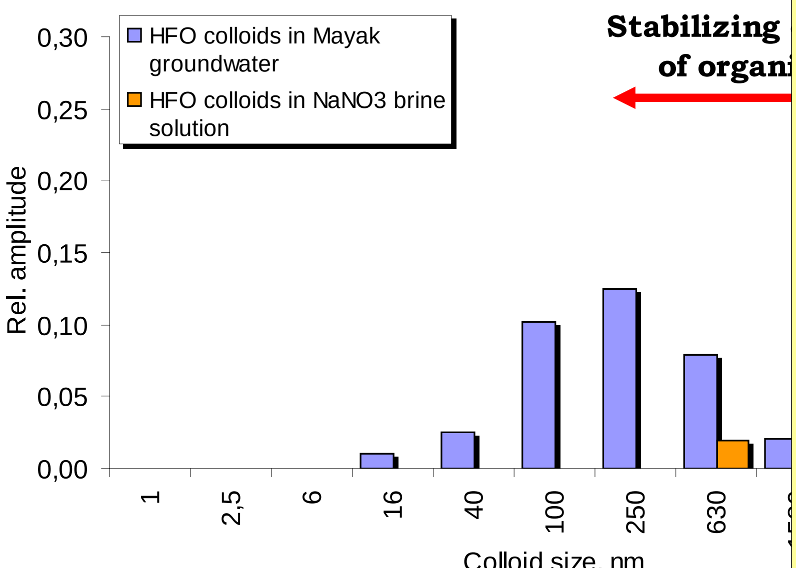

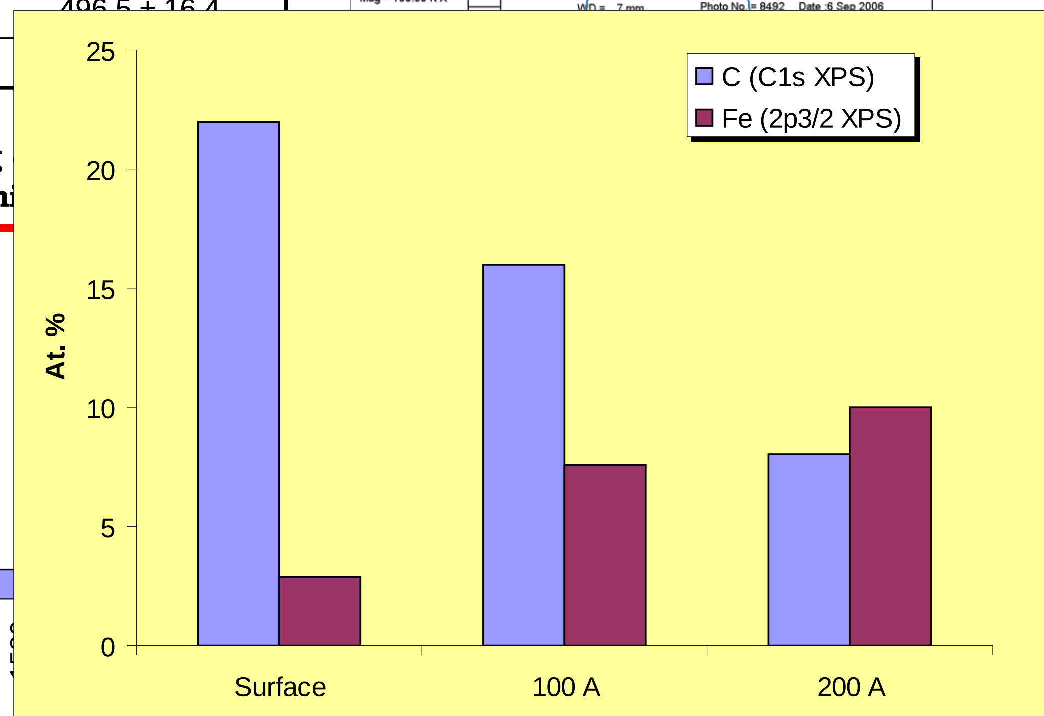

Radionuclide interaction with colloids

Radionuclide transport with particles

Sorption mechanisms:

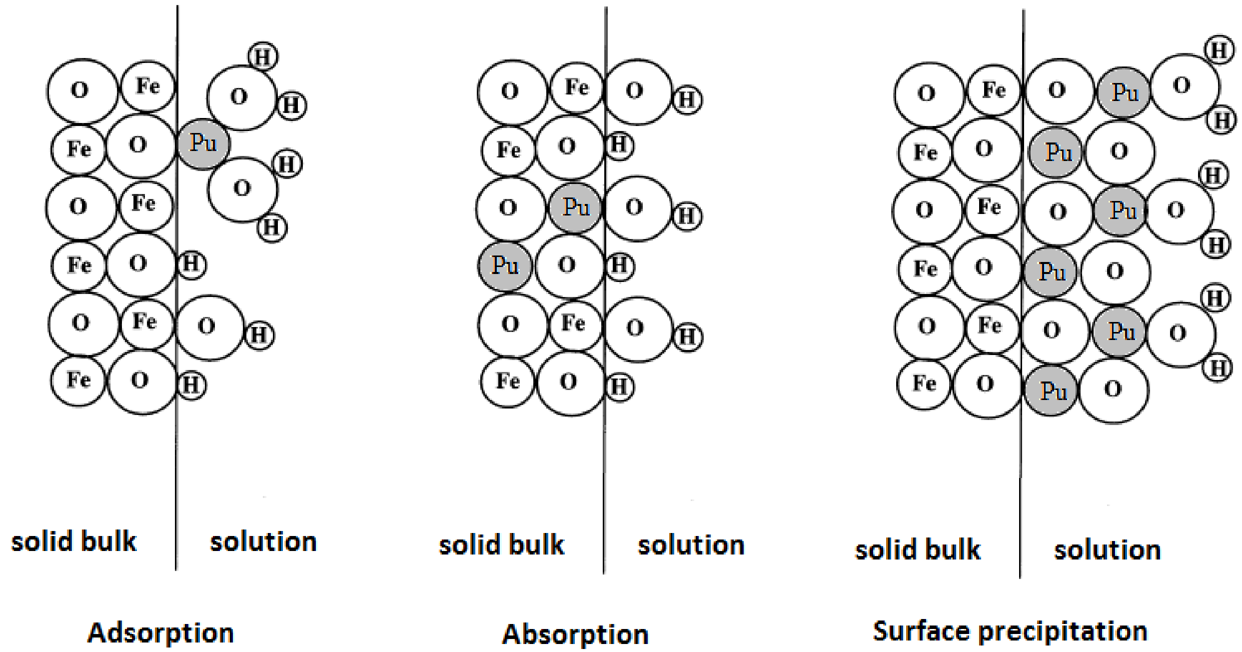

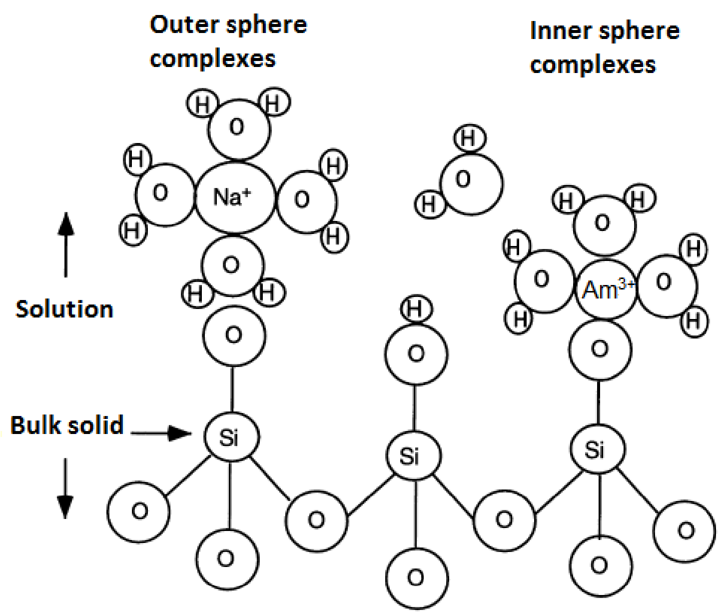

Surface complexation vs. ion exchange

Cs(I) sorption onto bentonite

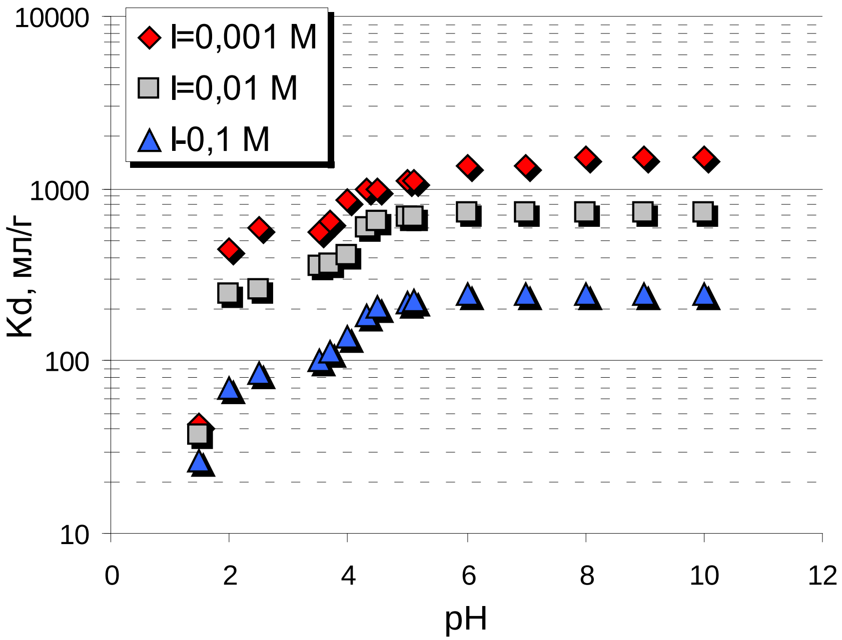

Np(V) sorption onto bentonite

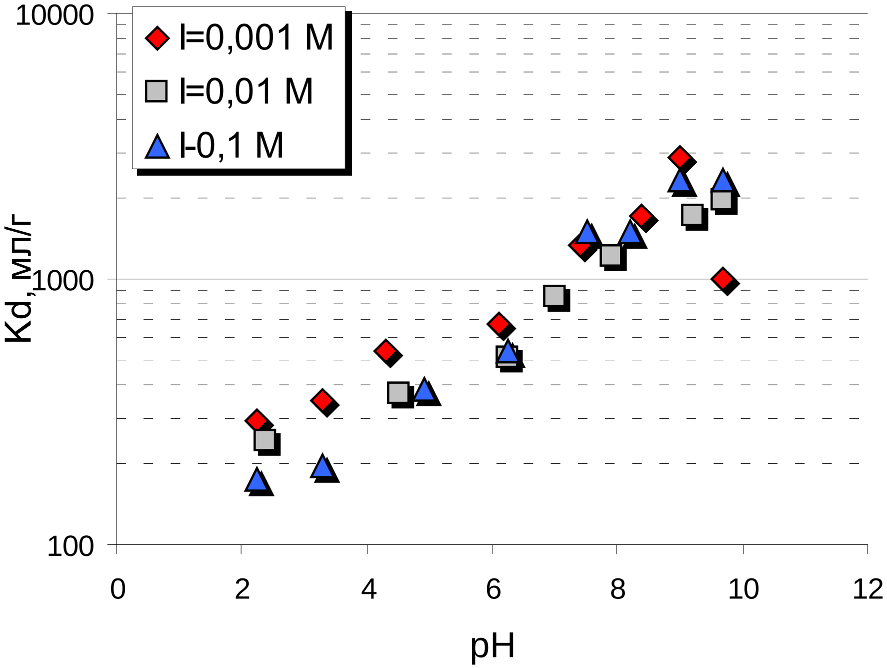

Ln(III)/An(III) sorption onto hematite – literature Kd values recalculated in L/m²

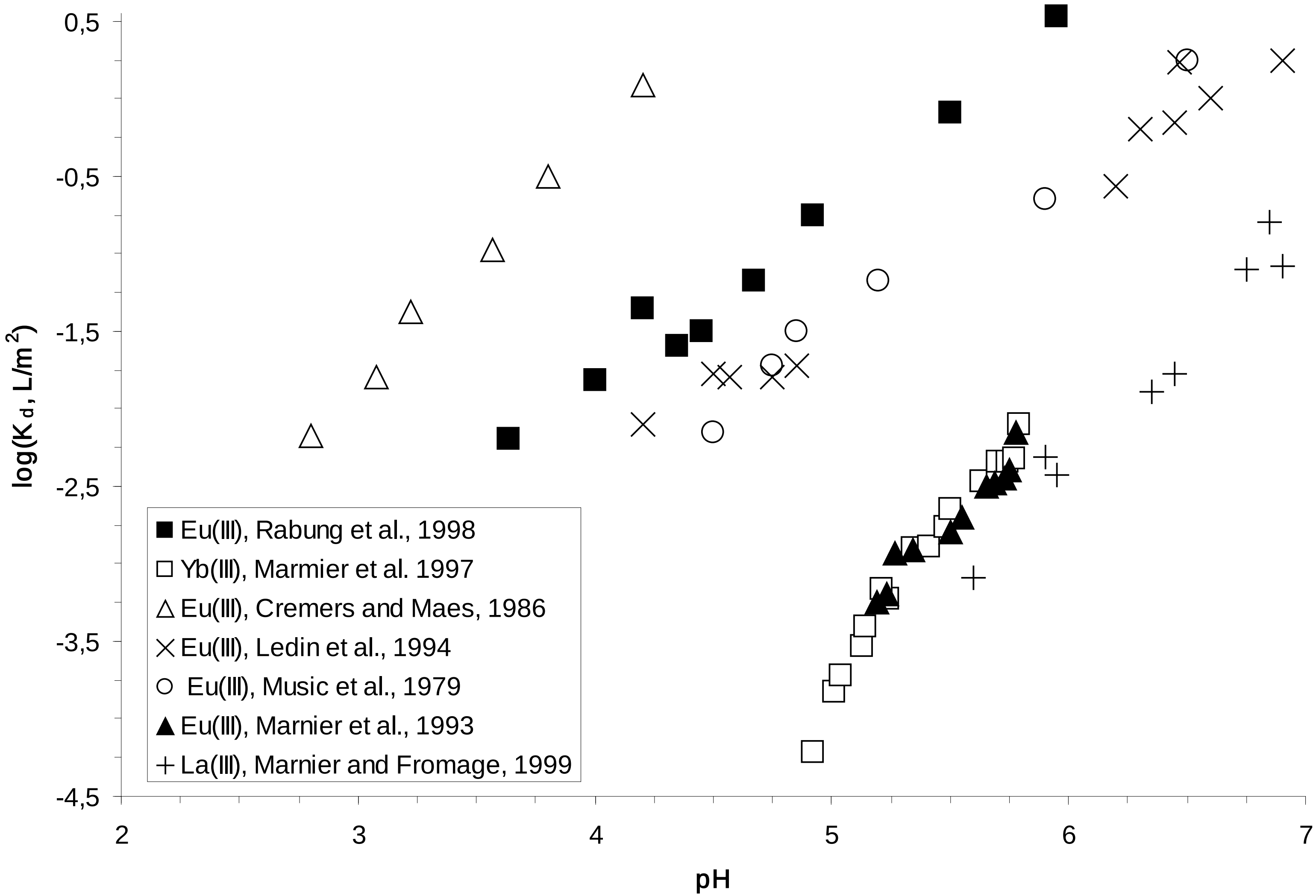

Oxide surface reactions

Acid-base equilibrium:

$$XOH + H^{+} \leftrightarrow \equiv XOH_2^{+}$$

$$K_{a1} = \frac{[\equiv XOH_2^{+}]}{[\equiv XOH][H^{+}]}\exp(-F\Psi / RT)$$

$$XOH \leftrightarrow \equiv XO^{-} + H^{+}$$

$$K_{a2} = \frac{[\equiv XO^{-}][H^{+}]}{[\equiv XOH]}\exp(-F\Psi / RT)$$

Monodentate surface complex formation:

$$Met^{3+} + \equiv XOH \longleftrightarrow \equiv XOMet^{2+} + H^{+}$$

$$\beta_1 = \frac{[\equiv XOMet^{2+}][H^{+}]}{[Met^{3+}][\equiv XOH]}\exp(-F\Psi / RT)$$

$$MetOH^{2+} + \equiv XOH \longleftrightarrow \equiv XOMetOH^{+} + H^{+}$$

$$\beta_2 = \frac{[\equiv XOMetOH^{+}][H^{+}]}{[MetOH^{2+}][\equiv XOH]}\exp(-F\Psi / RT)$$

$$Met(OH)_2^{+} + \equiv XOH \longleftrightarrow \equiv XOMet(OH)_2 + H^{+}$$

$$\beta_3 = \frac{[\equiv XOMet(OH)_2][H^{+}]}{[Met(OH)_2^{+}][\equiv XOH]}\exp(-F\Psi / RT)$$

Reactions in solutions

Hydrolysis (as an example):

$$Met^{3+} + OH^{-} \longleftrightarrow MetOH^{2+}$$

$$\beta_4 = \frac{[MetOH^{2+}]}{[Met^{3+}][OH^{-}]}$$

$$Met^{3+} + 2OH^{-} \longleftrightarrow Met(OH)_2^{+}$$

$$\beta_5 = \frac{[Met(OH)_2^{+}]}{[Met^{3+}][OH^{-}]^2}$$

$$Met^{3+} + 3OH^{-} \longleftrightarrow Met(OH)_3$$

$$\beta_6 = \frac{[Met(OH)_3]}{[Met^{3+}][OH^{-}]^3}$$

$$\boxed{K_d = \frac{[\equiv X - OH]\{\beta_1 + \beta_2\beta_4[OH^{-}] + \beta_3\beta_5[OH^{-}]^2\}}{[H^{+}]\{1 + \beta_4[OH^{-}] + \beta_5[OH^{-}]^2 + \beta_6[OH^{-}]^3\}}}$$

Surface complexation modeling for actinide/colloid interaction

Model experiments under well-defined laboratory conditions

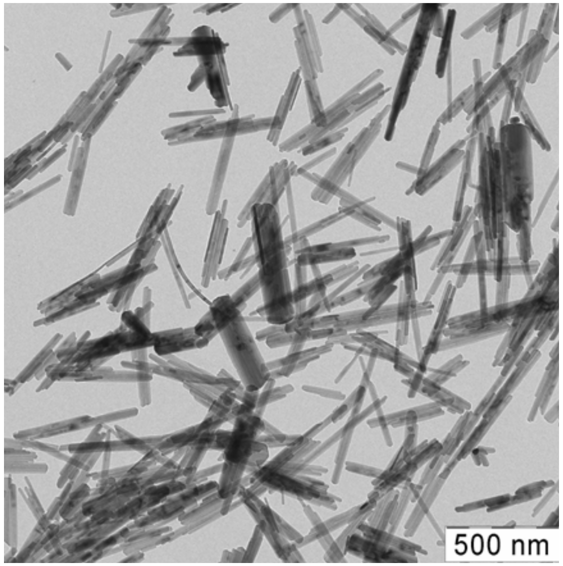

Goethite, α-FeOOH

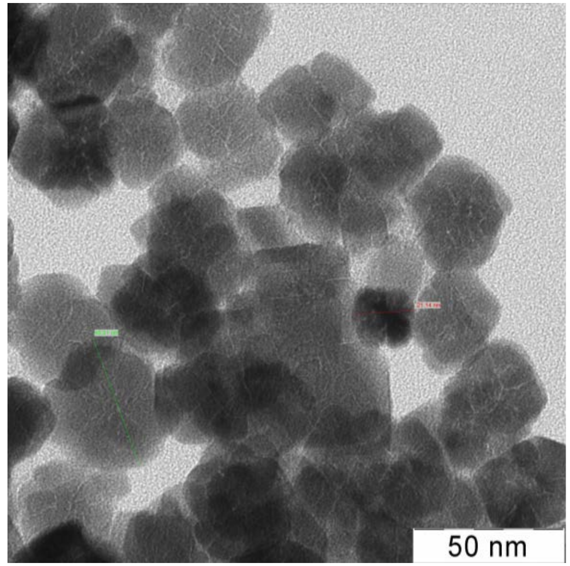

Hematite, α-Fe_2O_3

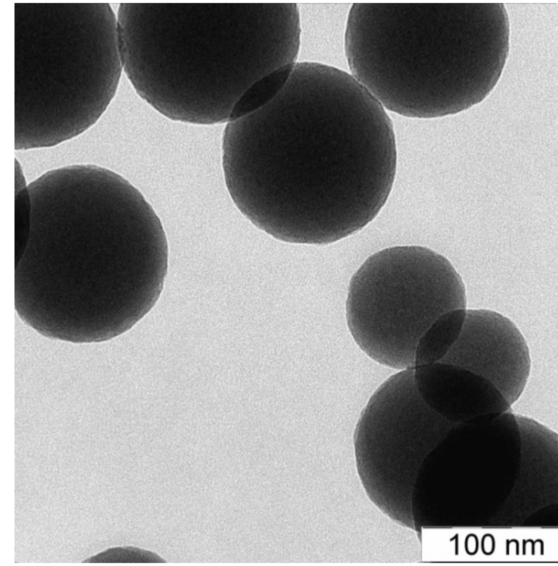

Amorphous SiO_2 microspheres

Sorption pH edges at different total actinide concentrations, various Eh and ionic strangths

Spectroscopic characterization of surface species (XAFS, XPS, TRLIF for U(VI), Eu(III))

Surface complexation modeling

Molecular-level understanding of the surface reactions and fundamental thermodynamic data for migration modeling

Example: actinide sorption onto silica colloids

Time-resolved laser induced fluorescence (TRLIF for U(VI) speciation on the surface

U(VI) sorption pH edge onto SiO_2

TRLIF (2,5 µsec), delay 1 µsec

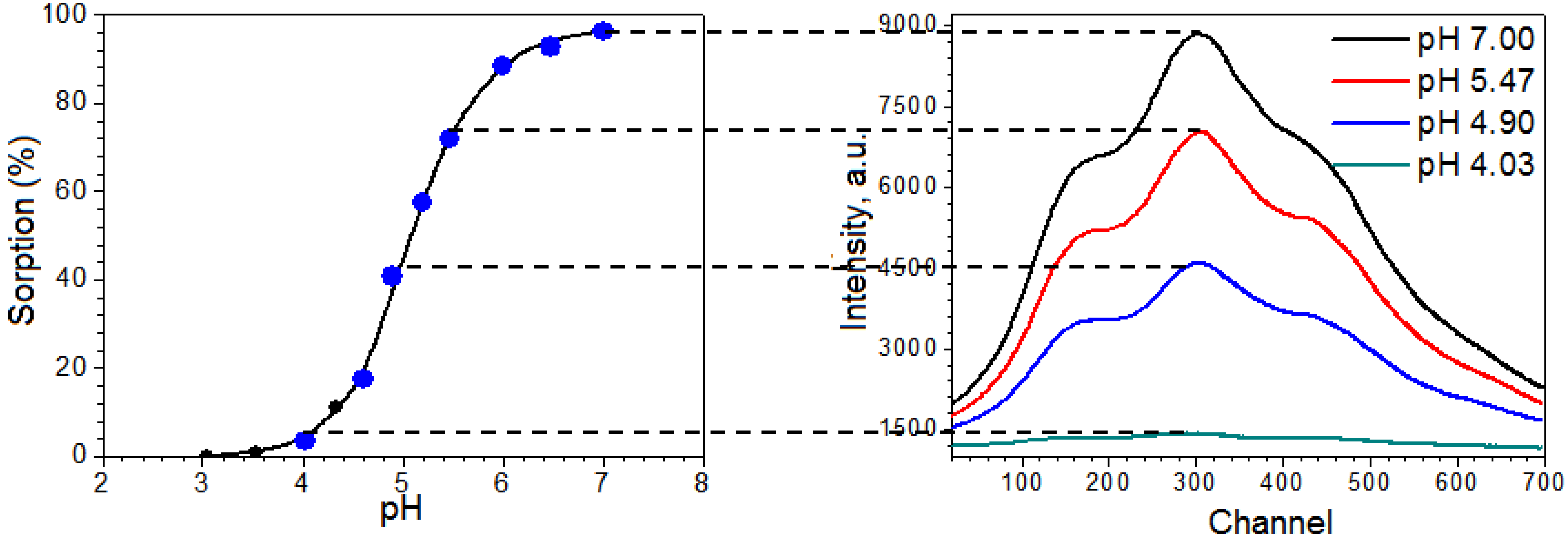

The fluorescence intensity is increase upon interaction with the SiO_2 surface

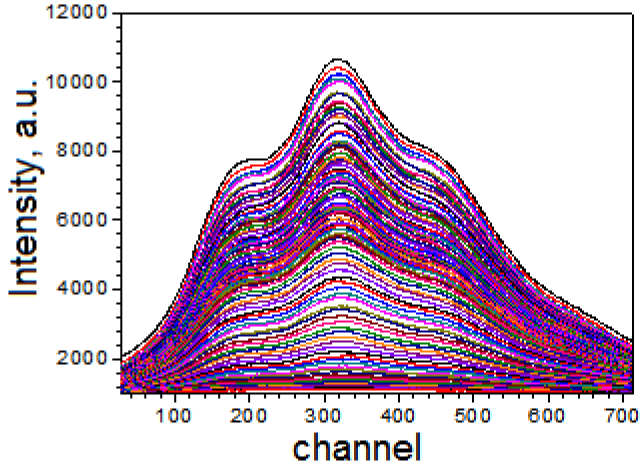

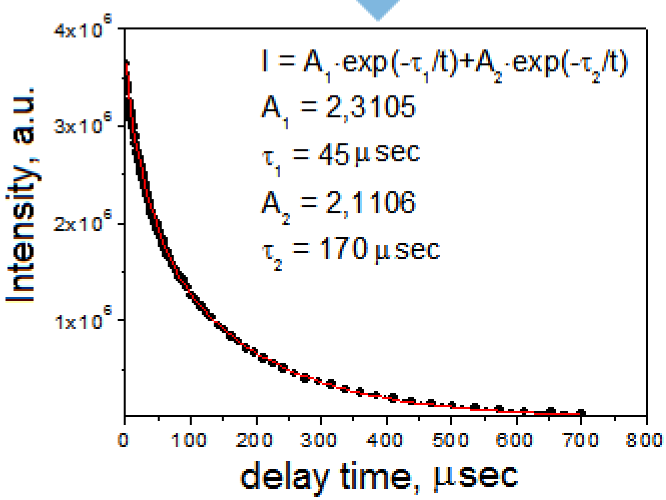

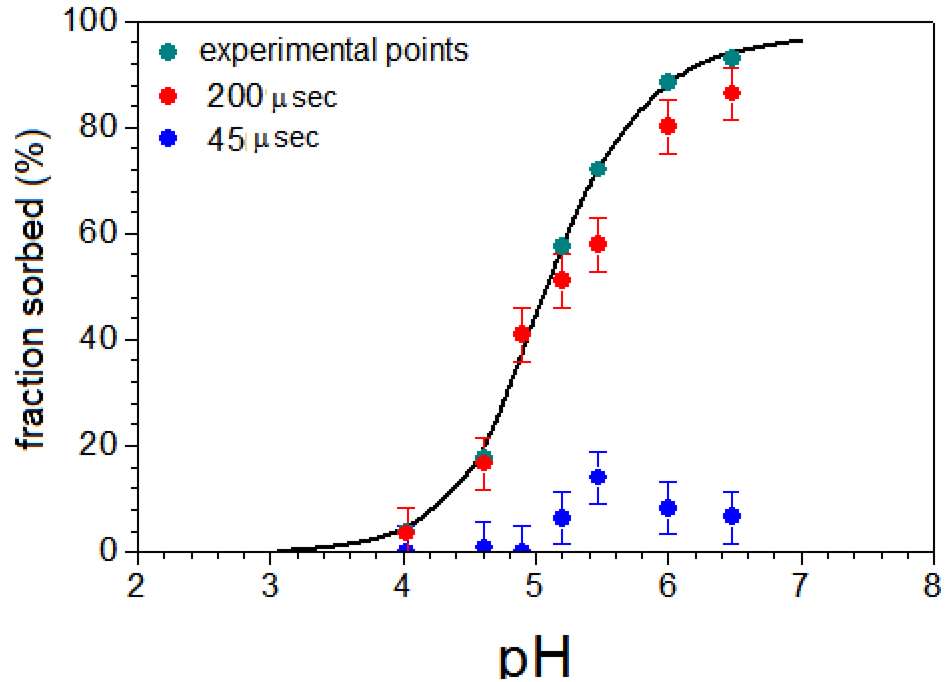

The fluorescence decay is characterized by two contributions with τ1 = 50 μsec τ2 = 200 μsec

The sorption of U(VI) proceed through the formation of two surface species

What is their stoichiometry and structure?

EXAFS for U(VI) speciation on the surface

Structural models used of U(VI) surface complexes used in EXAFS fitting

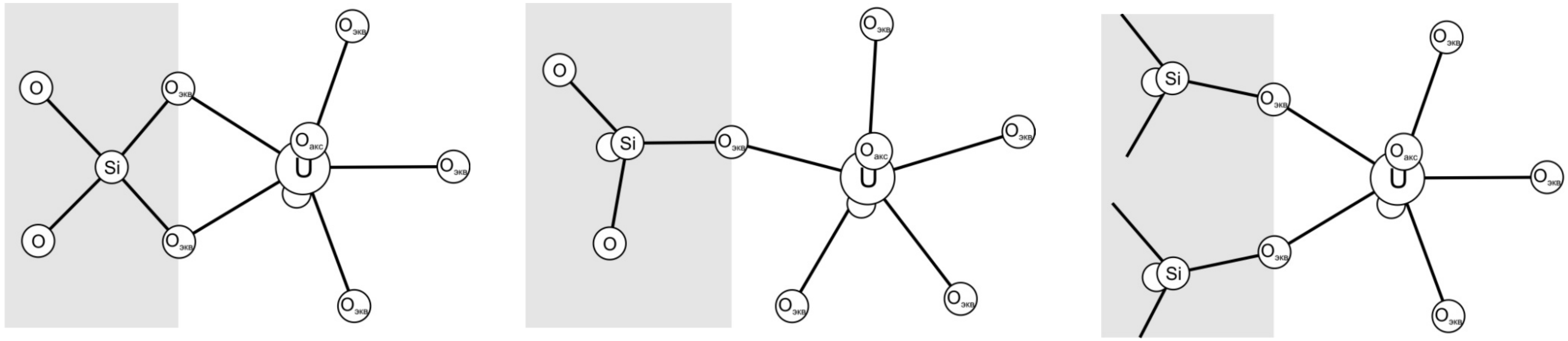

- bi- vs. monodentate complexation,
- number of Si atoms in the complex,
- plynuclear complex formation or surface precipoitation (U-U interaction in EXAFS spectra)

U(VI) silicates:

U-(O_2)-U 3.84-3.85 Å

U-O-Si 3.85-3.90 Å

U-(O_2)-Si 3.06-3.15 Å

EXAFS for U(VI) speciation on the surface

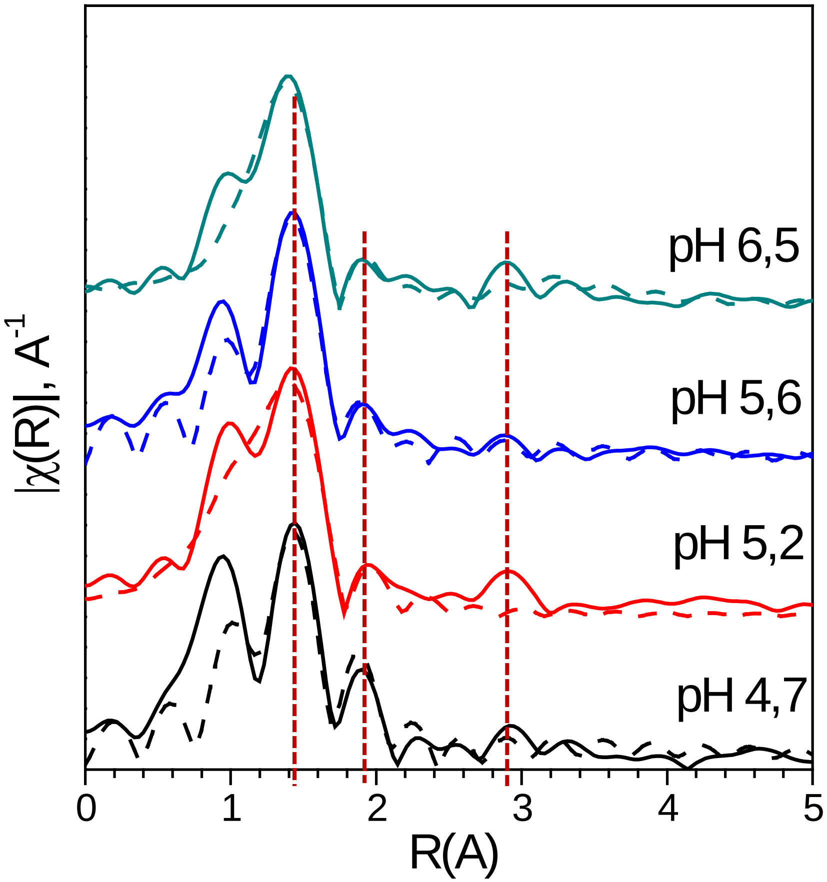

Sample	Coord sphere	R, Å	N	σ^2, Å^2	ΔE_0, eV
pH 4,7	$U\text{-}O_{ax}$	1,79	2	0,002	-10
	$U\text{-}O_{eq}1$	2,23	2,3(±0,5)	0,009	
	$U\text{-}O_{eq}2$	2,41	4,5(±2,0)	0,009	
pH 5,2	$U\text{-}O_{ax}$	1,80	2	0,002	-13
	$U\text{-}O_{eq}1$	2,24	1,7(±0,6)	0,009	
	$U\text{-}O_{eq}2$	2,43	3,6(±2,4)	0,009	
pH 5,6	$U\text{-}O_{ax}$	1,79	2	0,002	-8
	$U\text{-}O_{eq}1$	2,23	1,5(±0,8)	0,009	
	$U\text{-}O_{eq}2$	2,43	2,8(±2,2)	0,009	
pH 6,5	$U\text{-}O_{ax}$	1,76	2	0,002	-11
	$U\text{-}O_{eq}1$	2,21	2,2(±0,3)	0,009	
	$U\text{-}O_{eq}2$	2,40	2,5(±1,4)	0,009	

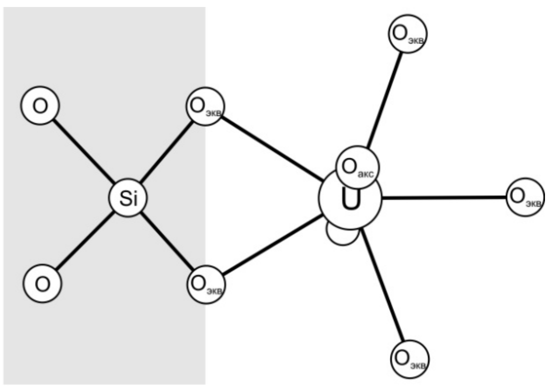

U(VI) forms bidentate complexes with the surface hydroxyl groups, considering TRLIF data we proposed two surface species:

$>SiO_2UO_2(H_2O)_3$ $>SiO_2UO_2(OH)(H_2O)_2^-$

Small angle X-ray scattering for nano-scale structural characterization

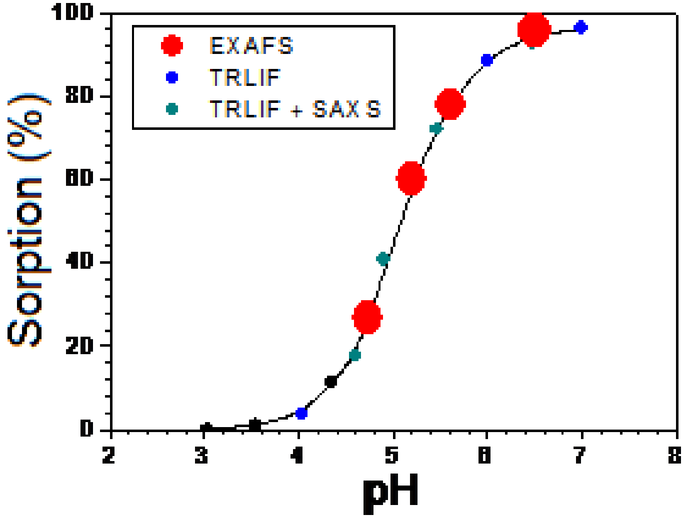

The distribution of the scattering centers in SiO_2 microspheres with and without U(VI)

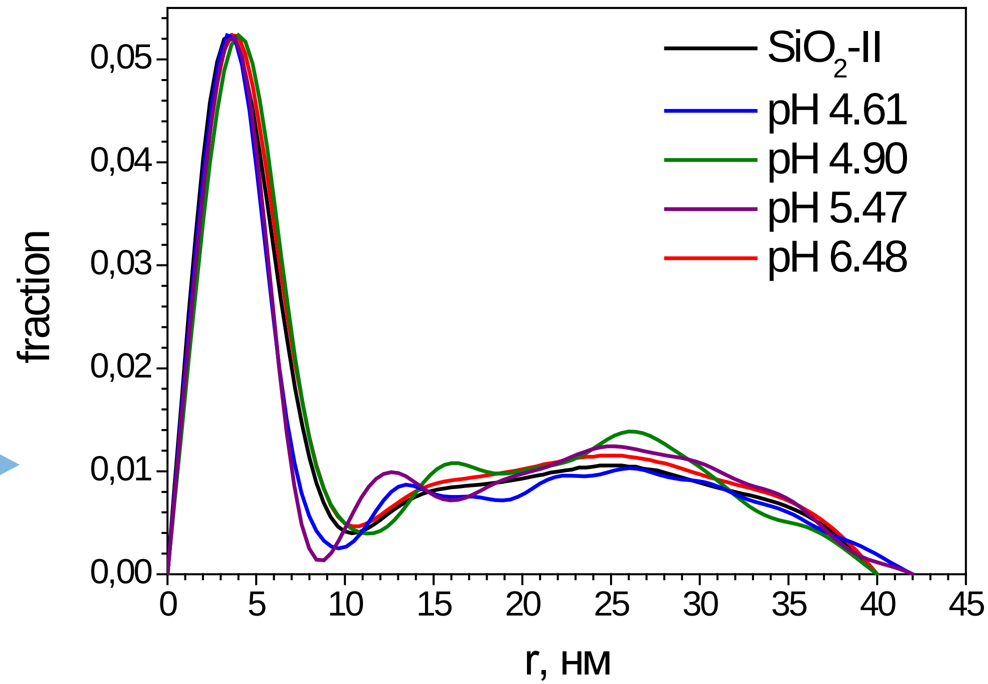

The distribution does not depend on U presence -
U(VI) uniformly covers the particles and no U surface precipitates take place

Surface complexation modeling

Based on the TRLIF and EXAFS two reactions were modelled:

$$>Si(OH)_2 + UO_2^{2+} \leftrightarrow >SiO_2UO_2 + 2H^+ \quad (1)$$

$$>Si(OH)_2 + UO_2^{2+} + H_2O \leftrightarrow >SiO_2UO_2OH^{-}+3H^+ \quad (2)$$

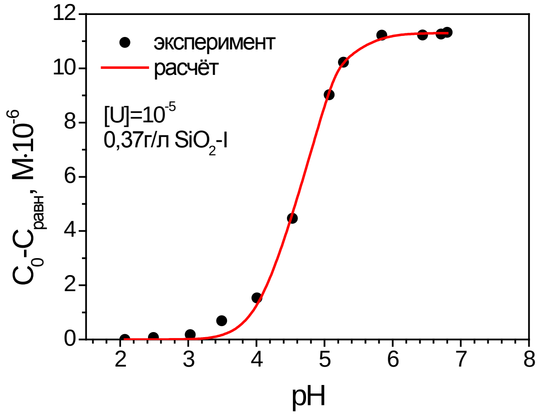

SiO_2-I
[U] 10^{-5}M
lgK_1 = -2,0
lgK_2 = -6,2

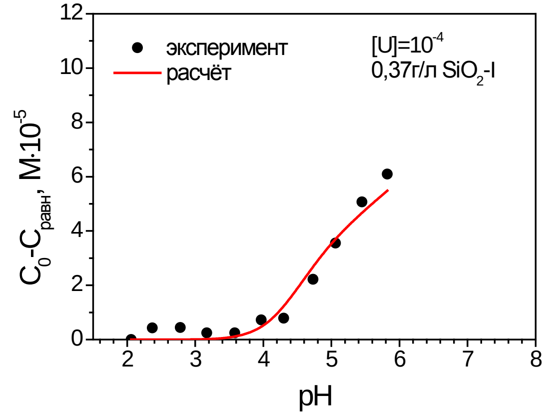

SiO_2-I
[U] 10^{-4}M
lgK_1 = -2,4
lgK_2 = -6,63

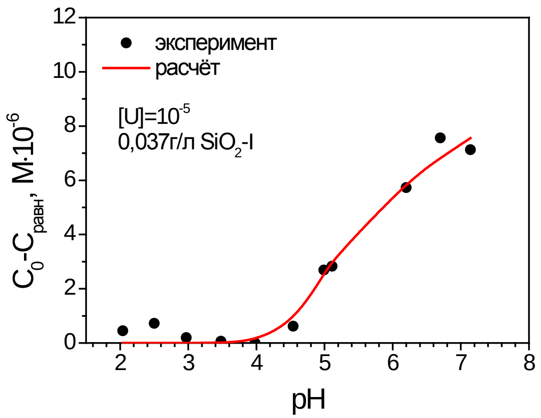

SiO_2-I
[U] 10^{-5}M
lgK_1 = -0,94
lgK_2 = -6,87

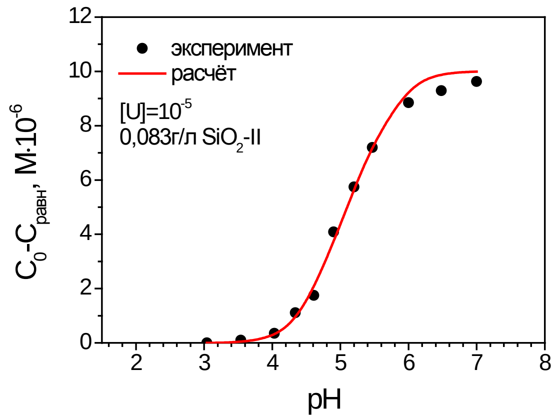

SiO_2-II
[U] 10^{-5}M
lgK_1 = -2,26
lgK_2 = -6,15

Surface complexation modeling

Average values: lgK$_1$ = -1,9; lgK$_2$ = -6,46

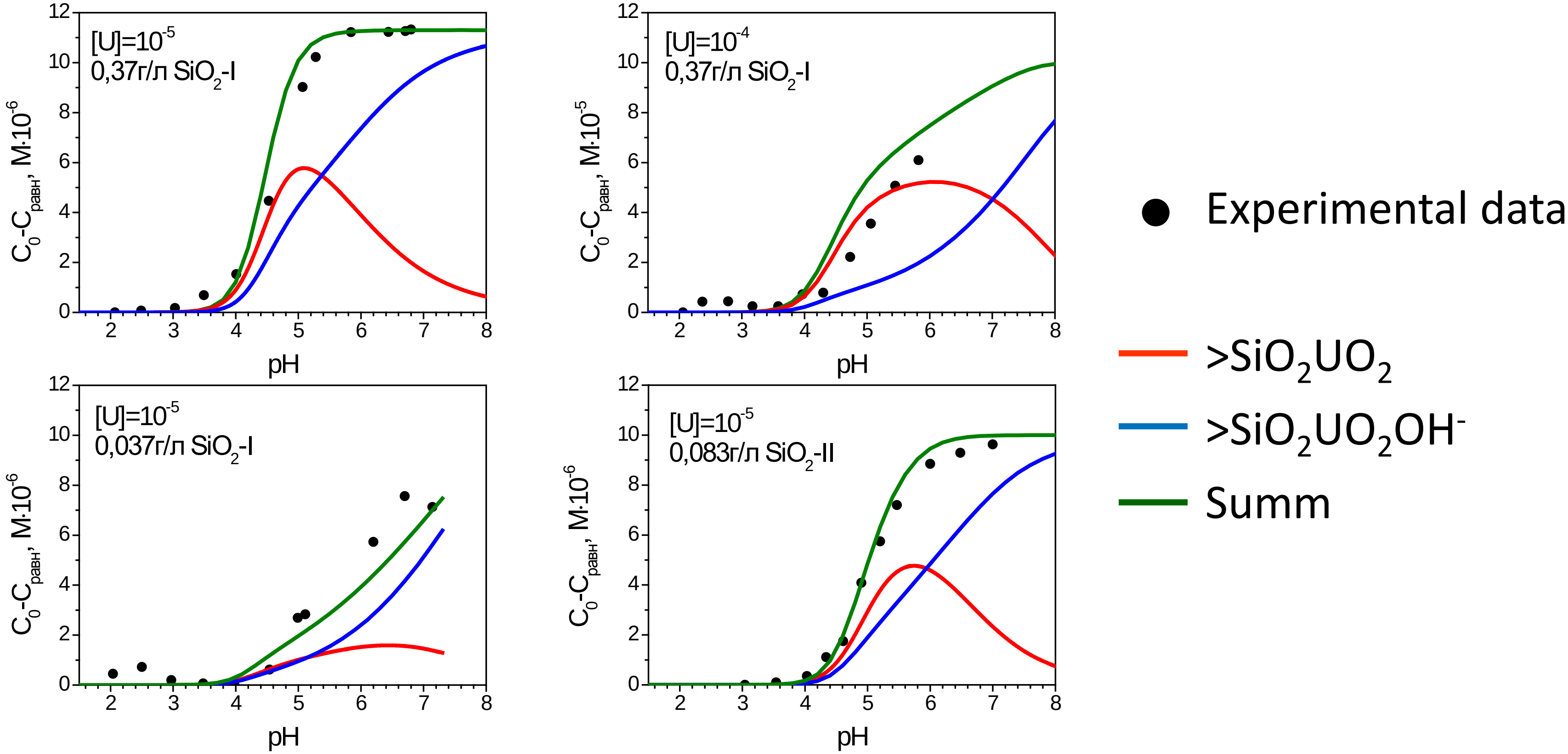

The model that is based on the spectroscopic data adequately describe experimental sorption data!

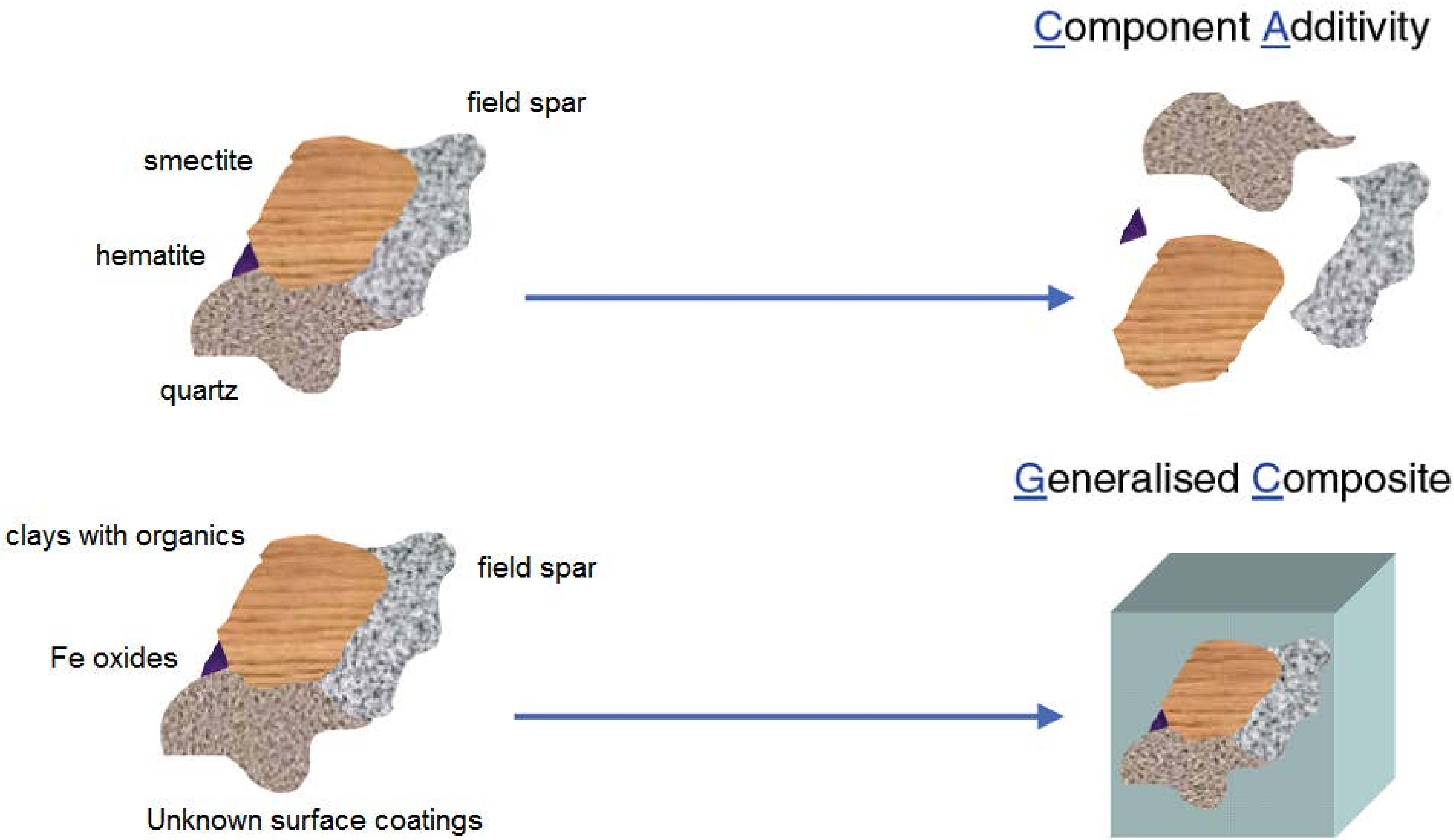
Component Additivity
field spar
smectite
hematite
quartz
Generalised Composite
clays with organics
field spar
Fe oxides
Unknown surface coatings

Actinide sorption onto hematite

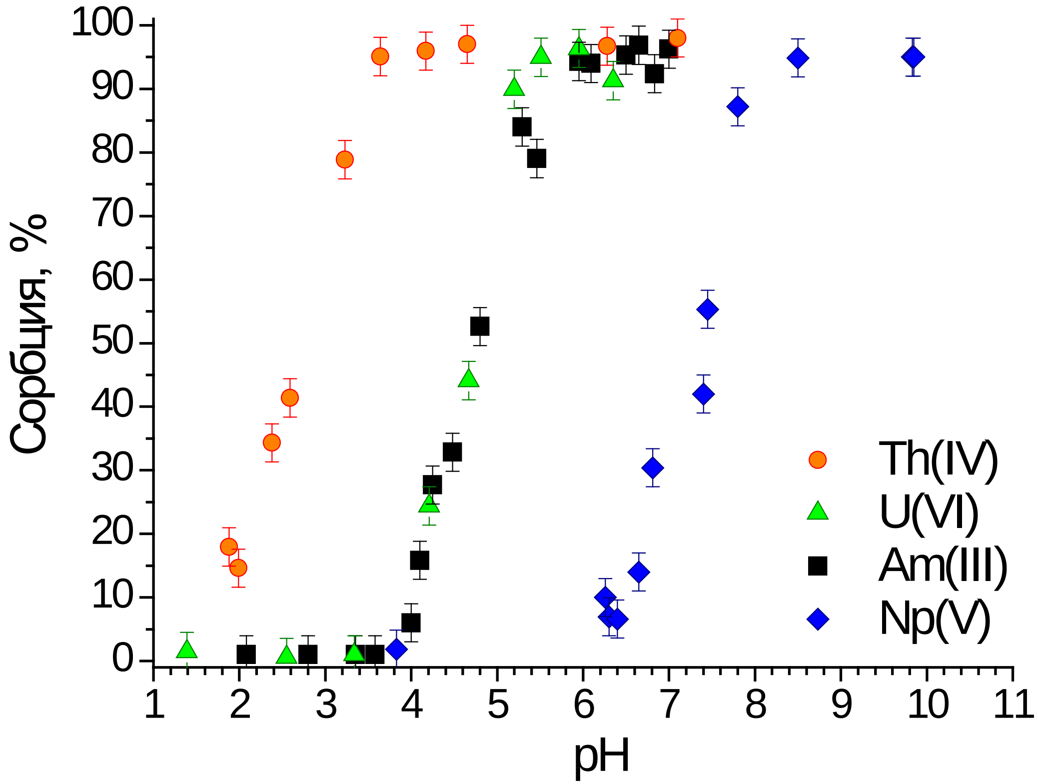

C(Th(IV)) = $3,9\cdot10^{-10}$ M
C(U(VI)) = $7,9\cdot10^{-8}$ M
C(Am(III)) = $1,9\cdot10^{-10}$ M
C(Np(V)) = $7,7\cdot10^{-7}$ M

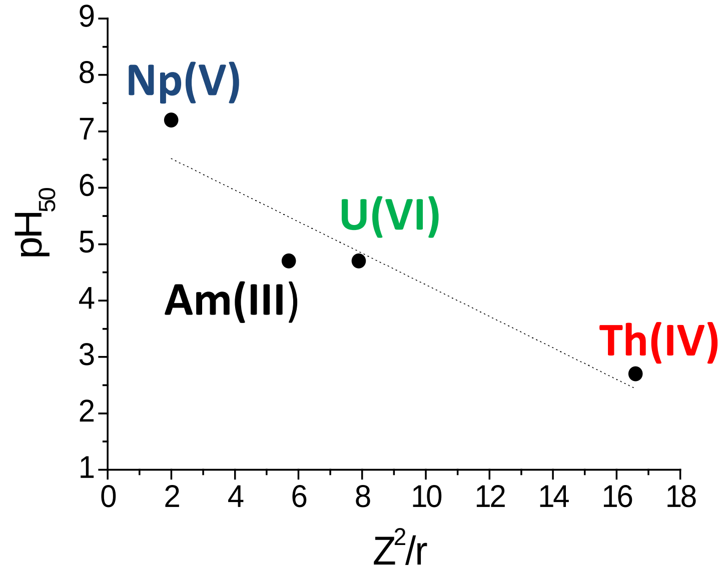

$Th(IV)^{4+} < Am(III) \leq U(VI)O_2^{2+} < Np(V)O_2^{+}$

+4 +3 +3,2 +2,2

A.Yu. Romanchuk, S.N. Kalmykov, Radiochimica Acta

Free energy linear relationship

$$Cat^{n} + \equiv FeOH \leftrightarrows \equiv FeO\text{-}Cat^{n-1} + H^{+}$$

$$Cat^{n} + HOH \leftrightarrows HO\text{-}Cat^{n-1} + H^{+}$$

- $\equiv FeOH + \mathbf{Am^{3+}} \leftrightarrows \equiv FeOAm^{2+} + H^{+}$

  $\lg \boldsymbol{K} = 5{,}91 \pm 0{,}04$
- $\equiv FeOH + \mathbf{NpO_2^{+}} \leftrightarrows \equiv FeONpO_2 + H^{+}$

  $\lg \boldsymbol{K} = -3{,}32 \pm 0{,}02$
- $\equiv FeOH + \mathbf{Th^{4+}} + \leftrightarrows \equiv FeOTh^{3+} + H^{+}$

  $\lg \boldsymbol{K_1} = 12{,}22 \pm 0{,}03$
- $\equiv FeOH + \mathbf{Th^{4+}} + H_2O \leftrightarrows \equiv FeOThOH^{2+} + 2H^{+}$

  $\lg \boldsymbol{K_2} = 4{,}13 \pm 1{,}37$

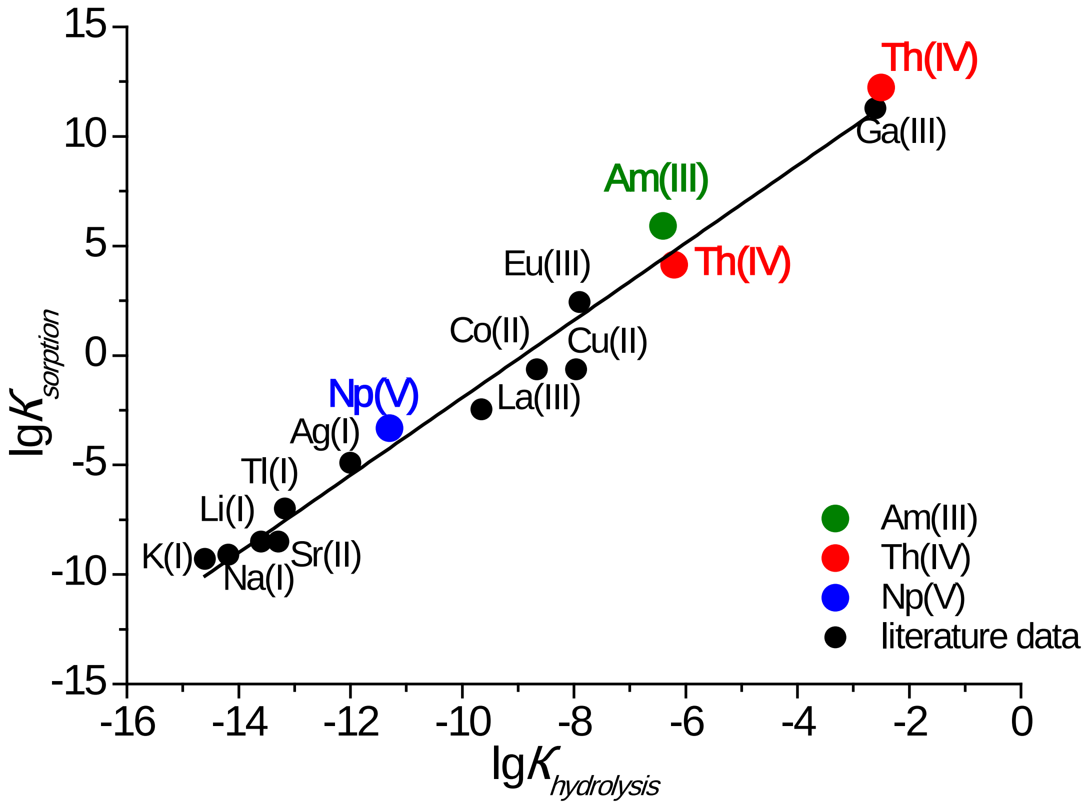

Free energy linear relationship

$$Cat^n + \equiv FeOH \leftrightarrows \equiv FeO\text{-}Cat^{n-1} + H^+$$
$$Cat^n + HOH \leftrightarrows HO\text{-}Cat^{n-1} + H^+$$

- $\equiv FeOH + \mathbf{Am^{3+}} \leftrightarrows \equiv FeOAm^{2+} + H^+$
  $\lg \boldsymbol{K} = 5{,}91 \pm 0{,}04$
- $\equiv FeOH + \mathbf{NpO_2^+} \leftrightarrows \equiv FeONpO_2 + H^+$
  $\lg \boldsymbol{K} = -3{,}32 \pm 0{,}02$
- $\equiv FeOH + \mathbf{Th^{4+}} + \leftrightarrows \equiv FeOTh^{3+} + H^+$
  $\lg \boldsymbol{K_1} = 12{,}22 \pm 0{,}03$
- $\equiv FeOH + \mathbf{Th^{4+}} + H_2O \leftrightarrows \equiv FeOThOH^{2+} + 2H^+$
  $\lg \boldsymbol{K_2} = 4{,}13 \pm 1{,}37$

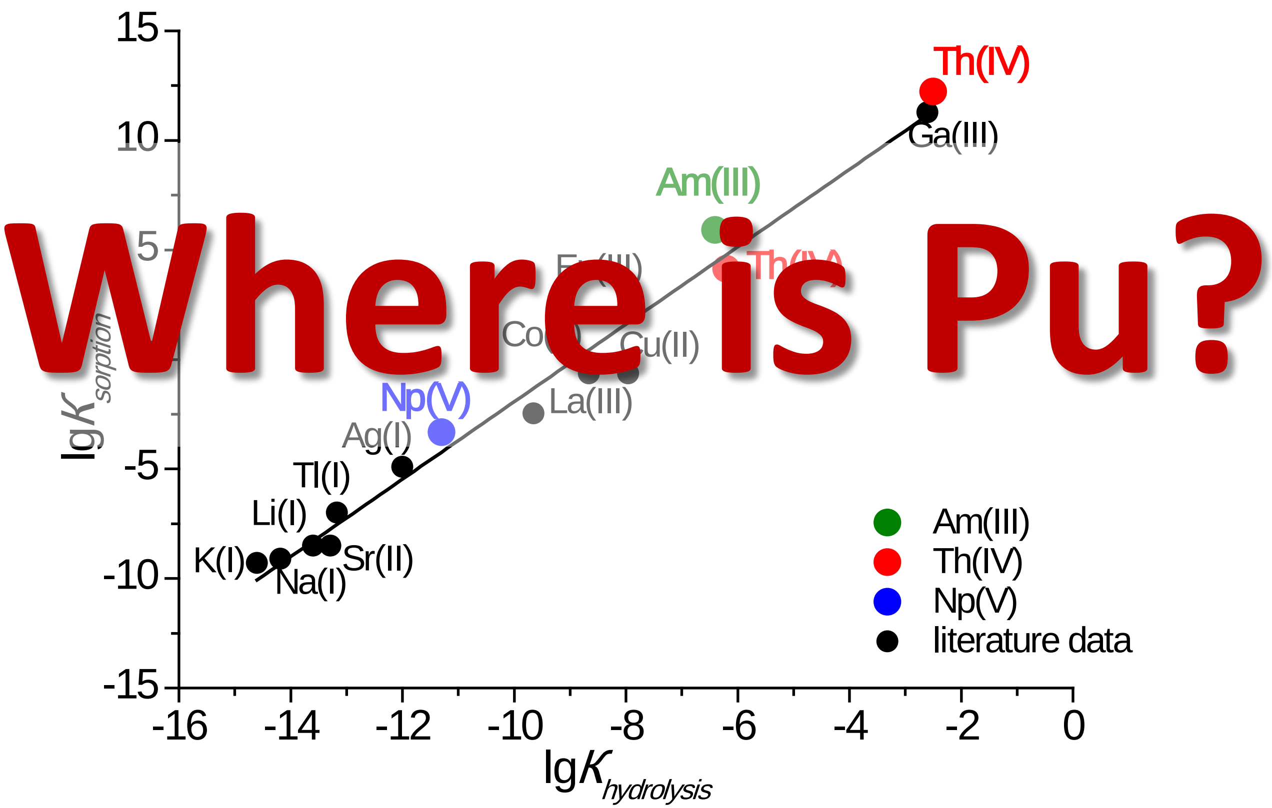

Pu(V) sorption onto hematite

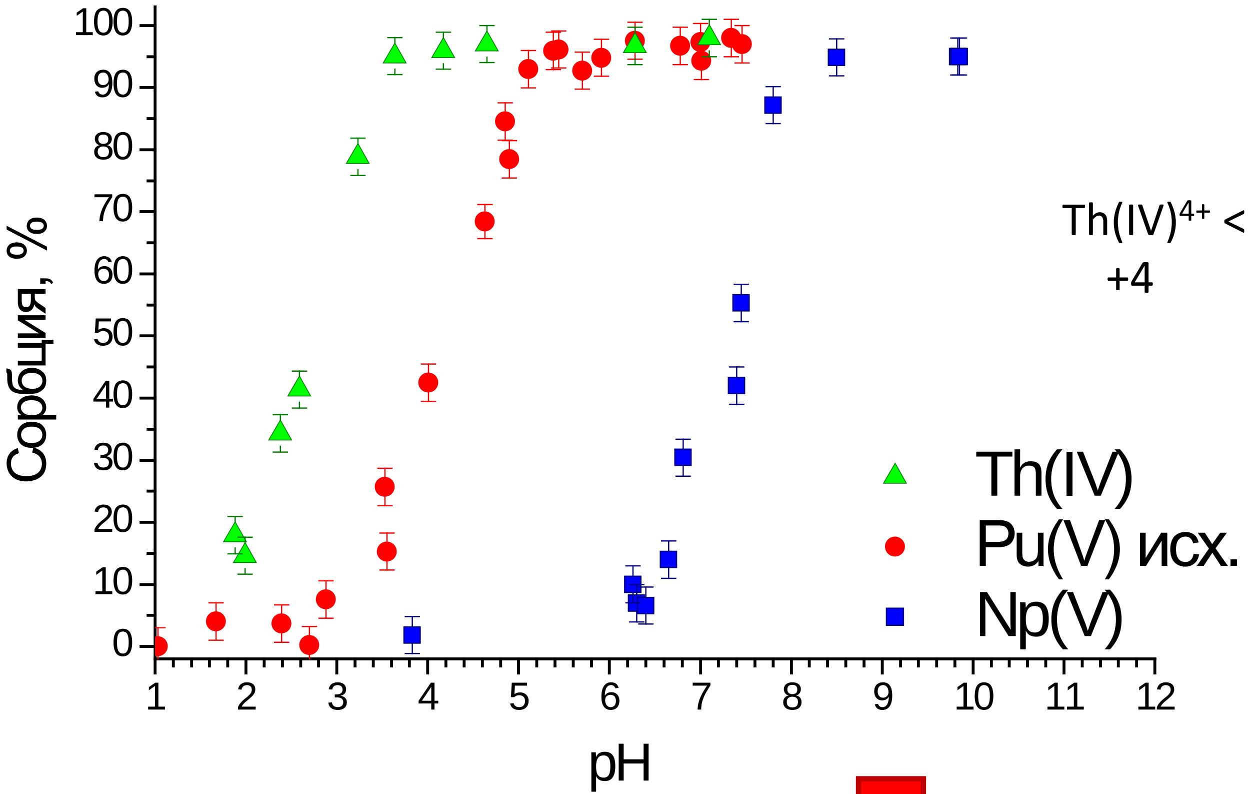

$Th(IV)^{4+}$ < Pu(???) < $Np(V)O_2^+$

+4 +2,2

Redox reactions?

Different total concentrations of Pu

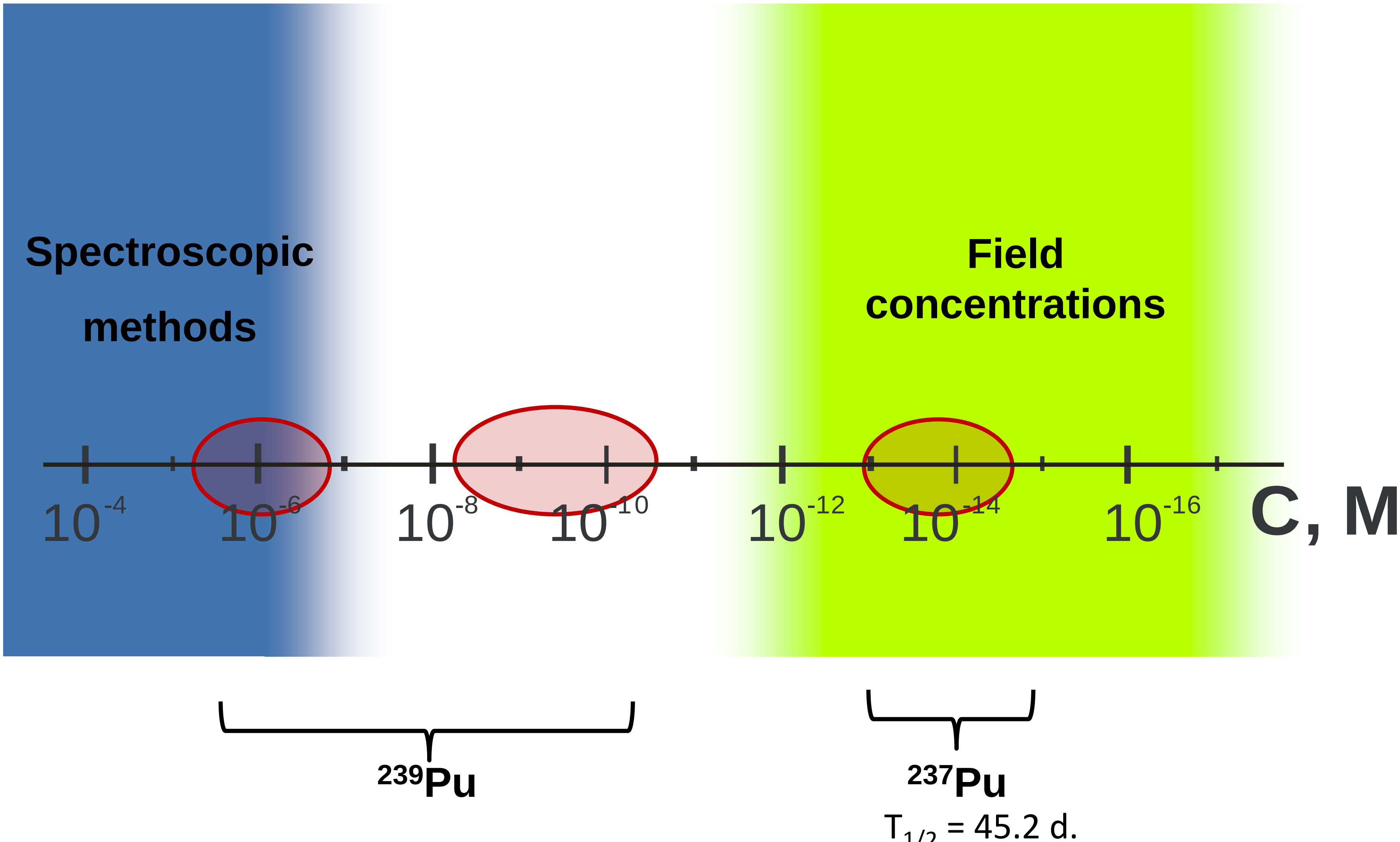

Pu interaction with hematite

Average particle size, nm	20-40
Lattice parameters, Å	a = 5.031(1) c = 13.78(1)
Surface area, m^2/g	35
pH_{pzc}	8.0

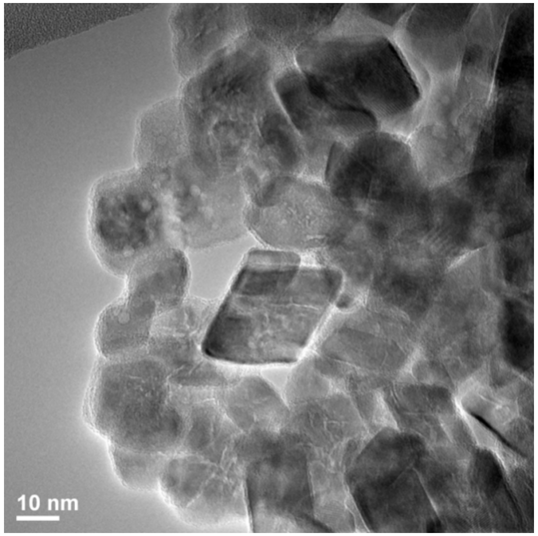

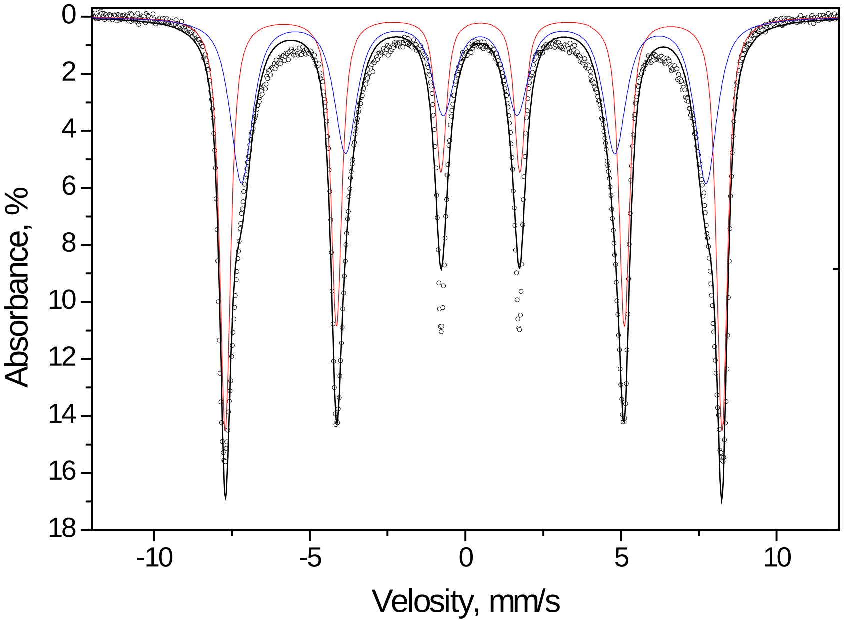

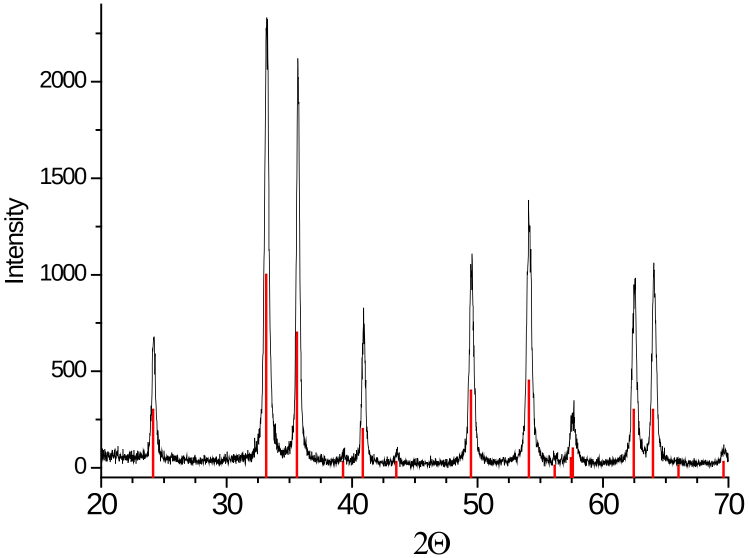

Experiment: Starting from soluble Pu(VI) at $C_{tot}(Pu) > 10^{-9}$ M

Blank experiments at C(Pu) = 10^{-6} M

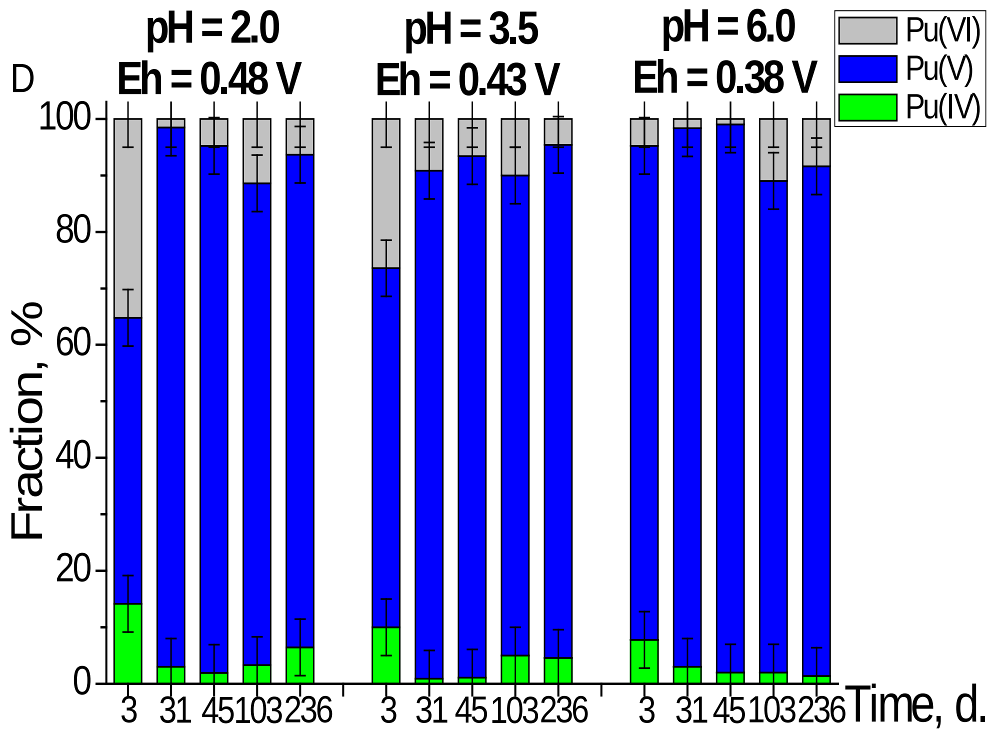

Pu(V) shows high **kinetic** stability **in pure solution** (despite thermodynamics)

Pu L_{III} XANES

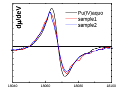

Pu(VI). $2 \cdot 10^{-6}$ M

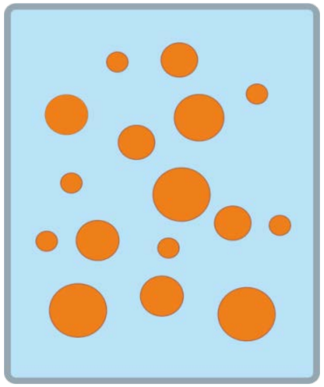

Eh = 400 – 600 мВ

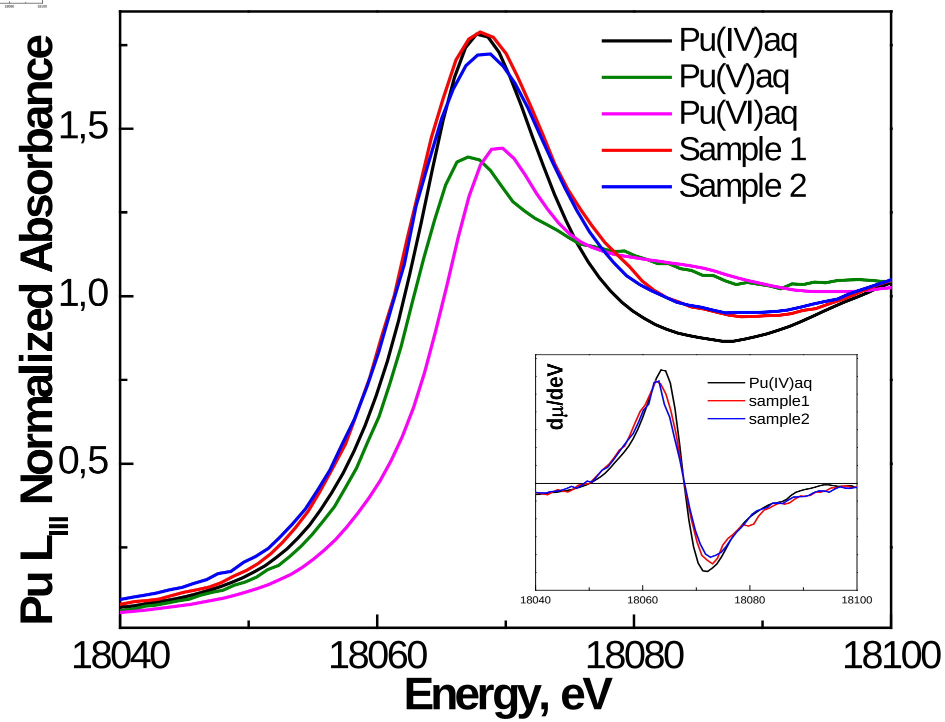

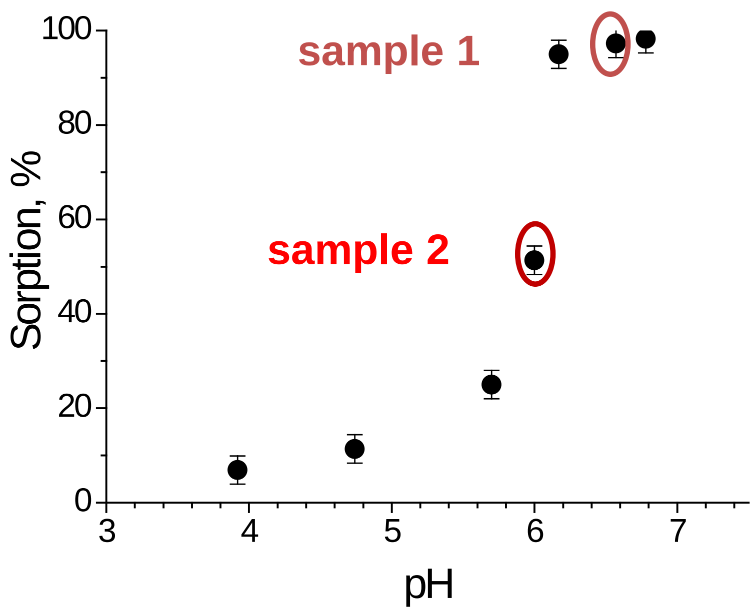

Stabilization of Pu(IV) on hematite surface

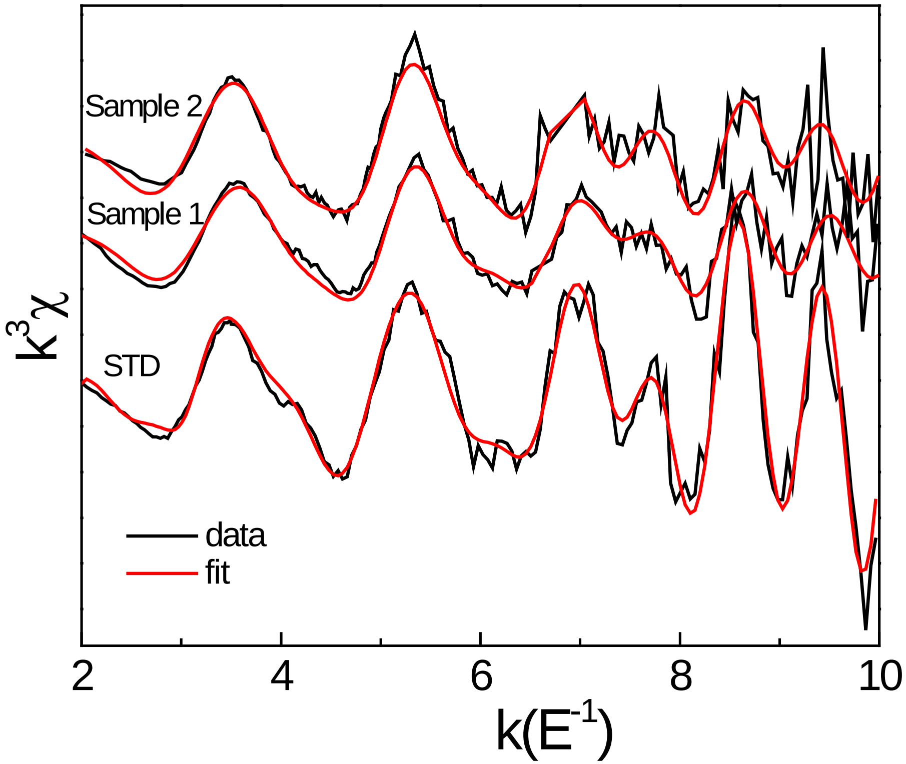

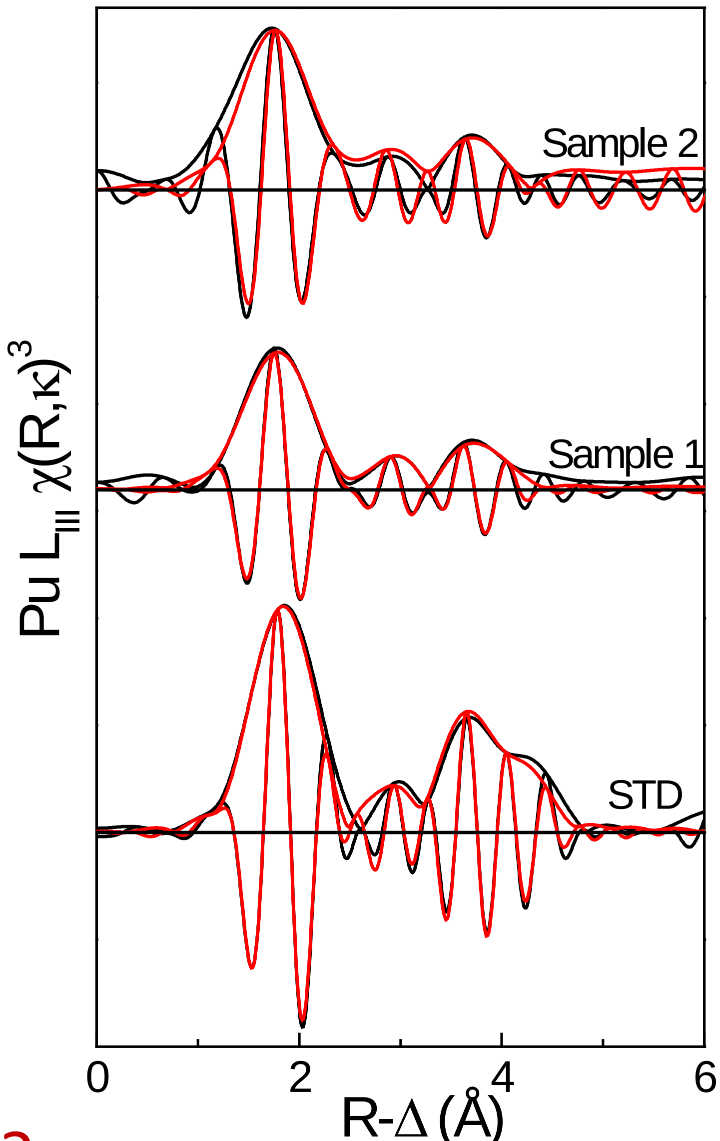

$PuO_{2+x}\cdot nH_2O$ - like species ???

A.Yu. Romanchuk, S.N. Kalmykov, et al. Geochim. et Cosmochim. Acta, (2013), 121, 29-40

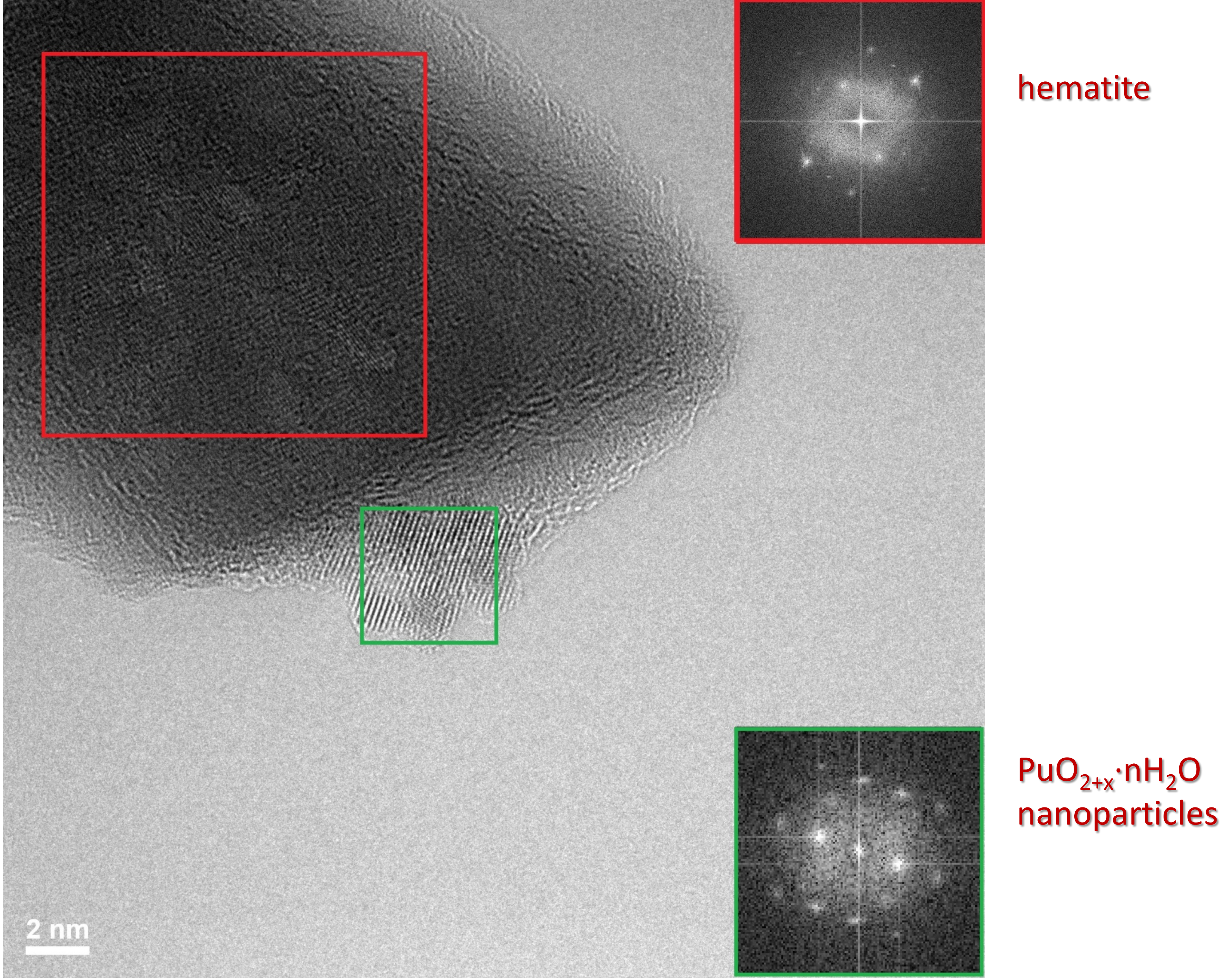

hematite
$PuO_{2+x} \cdot nH_2O$
nanoparticles
2 nm

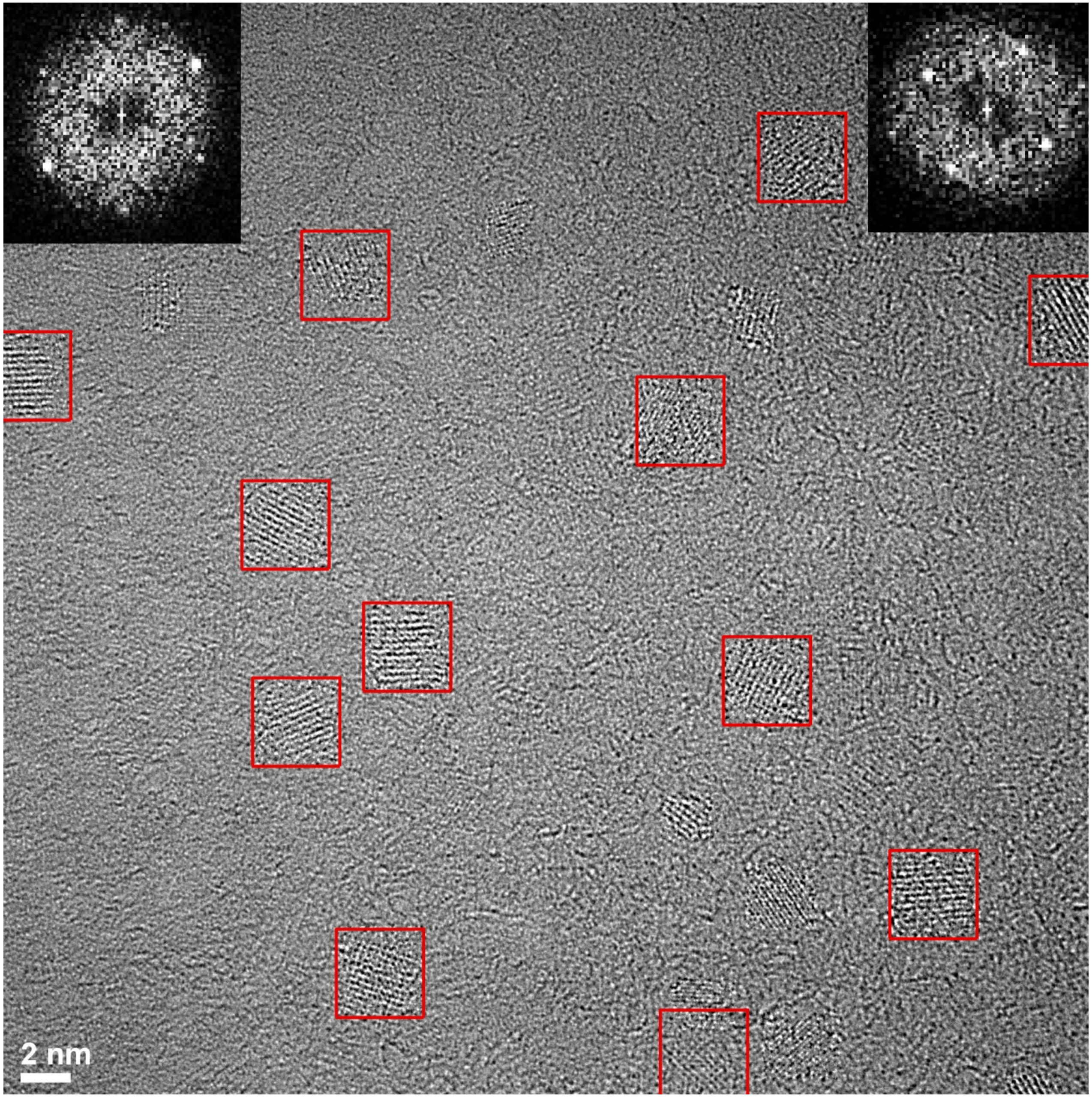

$[Pu]_{tot}=10^{-9}$ M

Kinetics of Pu(IV,VI) sorption on hematite at different $C_{tot}(Pu)$

	$C_{tot}(Pu)$ ~10^{-14} M	$C_{tot}(Pu)$ ~10^{-10} M
Pu(IV)	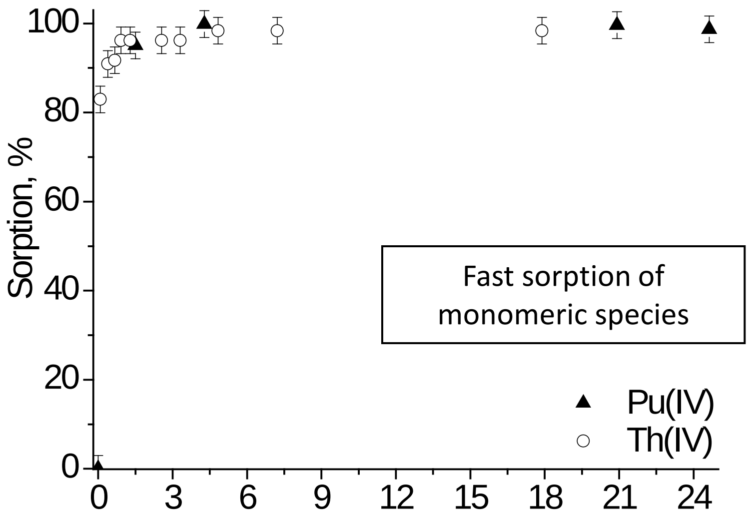	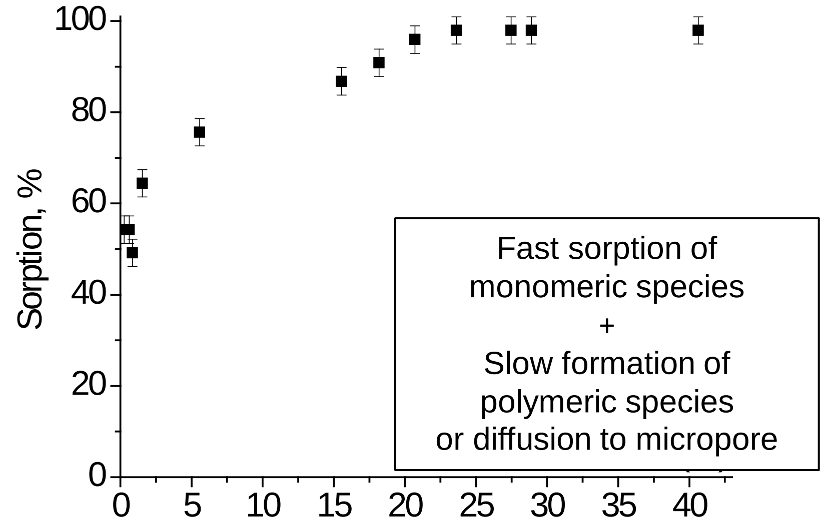
Pu(VI)	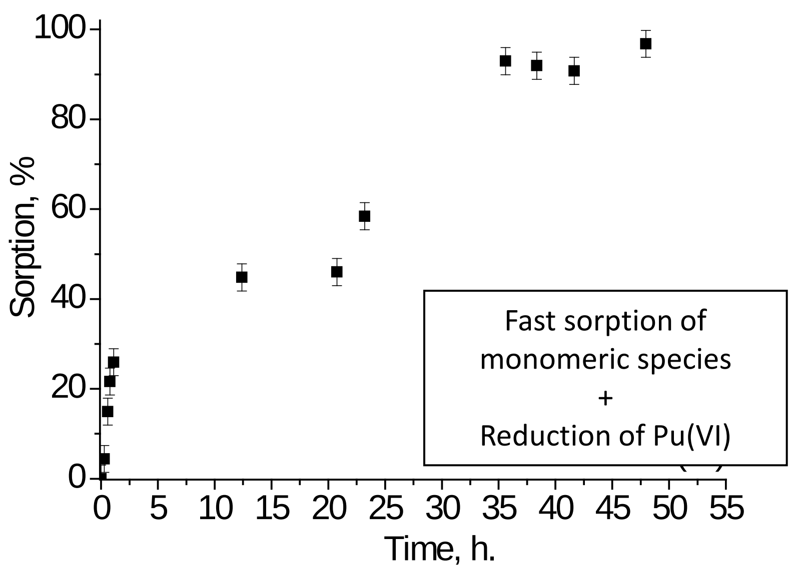	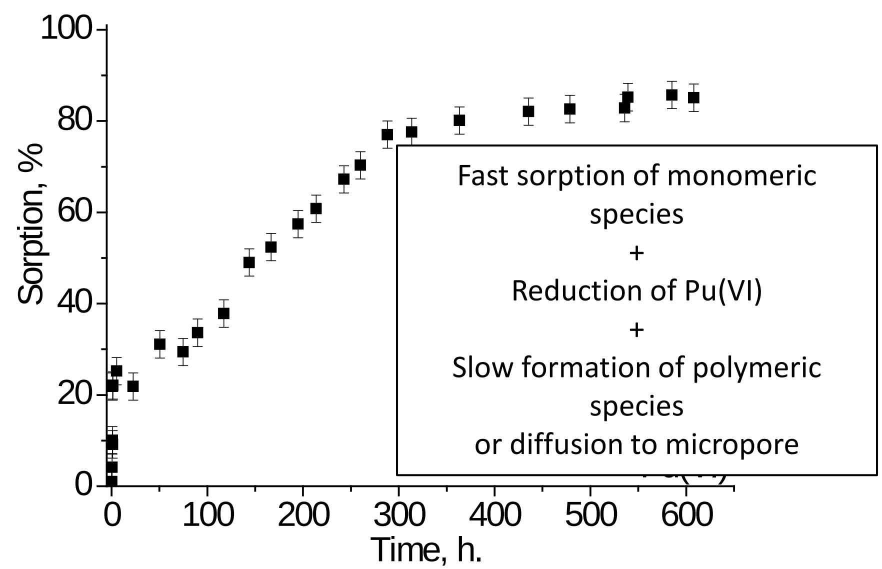

Chart 1 (Pu(IV), $C_{tot}(Pu)$ ~10^{-14} M):

Chart 2 (Pu(IV), $C_{tot}(Pu)$ ~10^{-10} M):

Chart 3 (Pu(VI), $C_{tot}(Pu)$ ~10^{-14} M):

Chart 4 (Pu(VI), $C_{tot}(Pu)$ ~10^{-10} M):

Romanchuk et al., Radiochim. Acta, 2011

Kinetics of Pu(VI) sorption onto α-Fe_2O_3 in the darkness

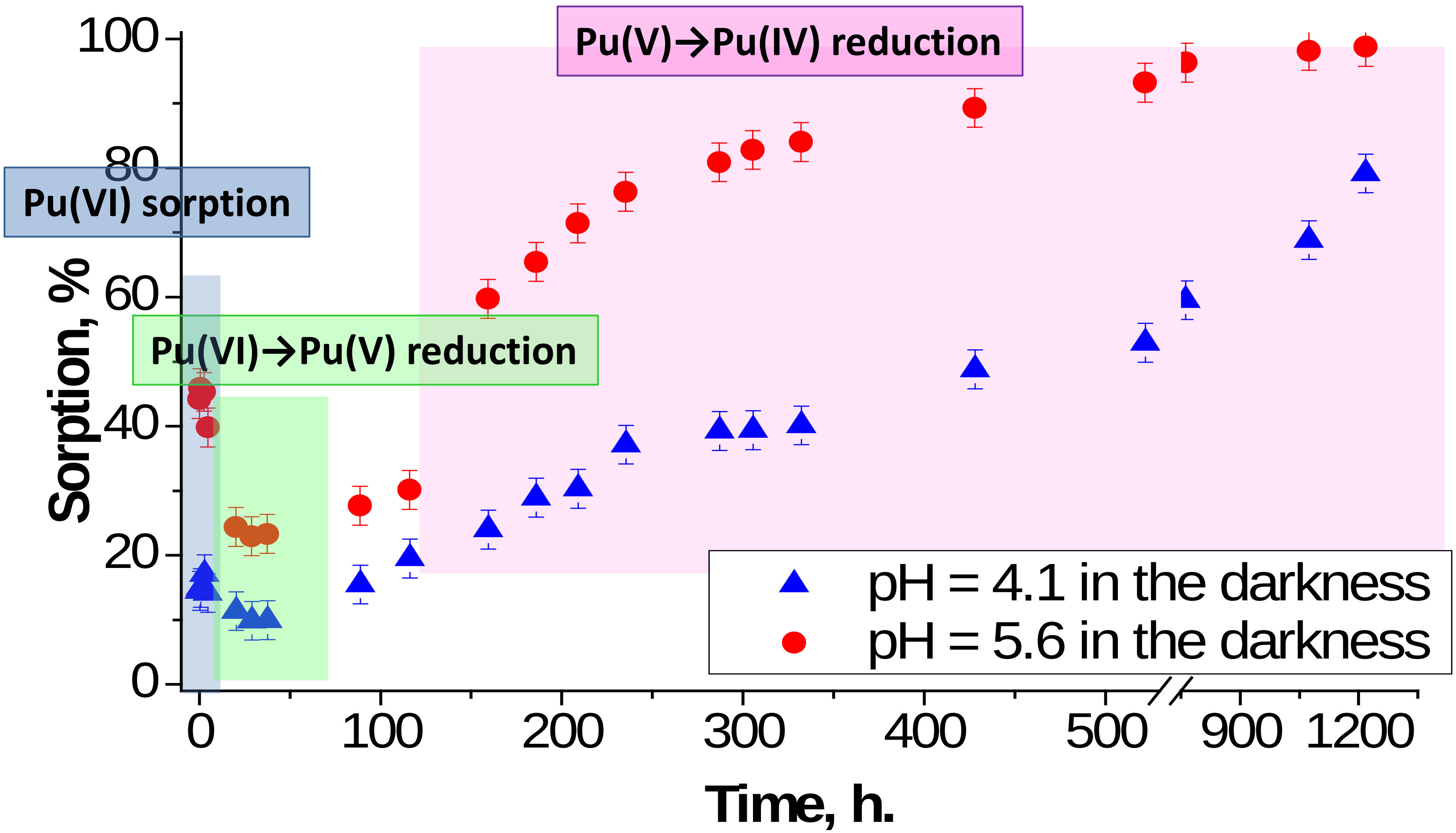

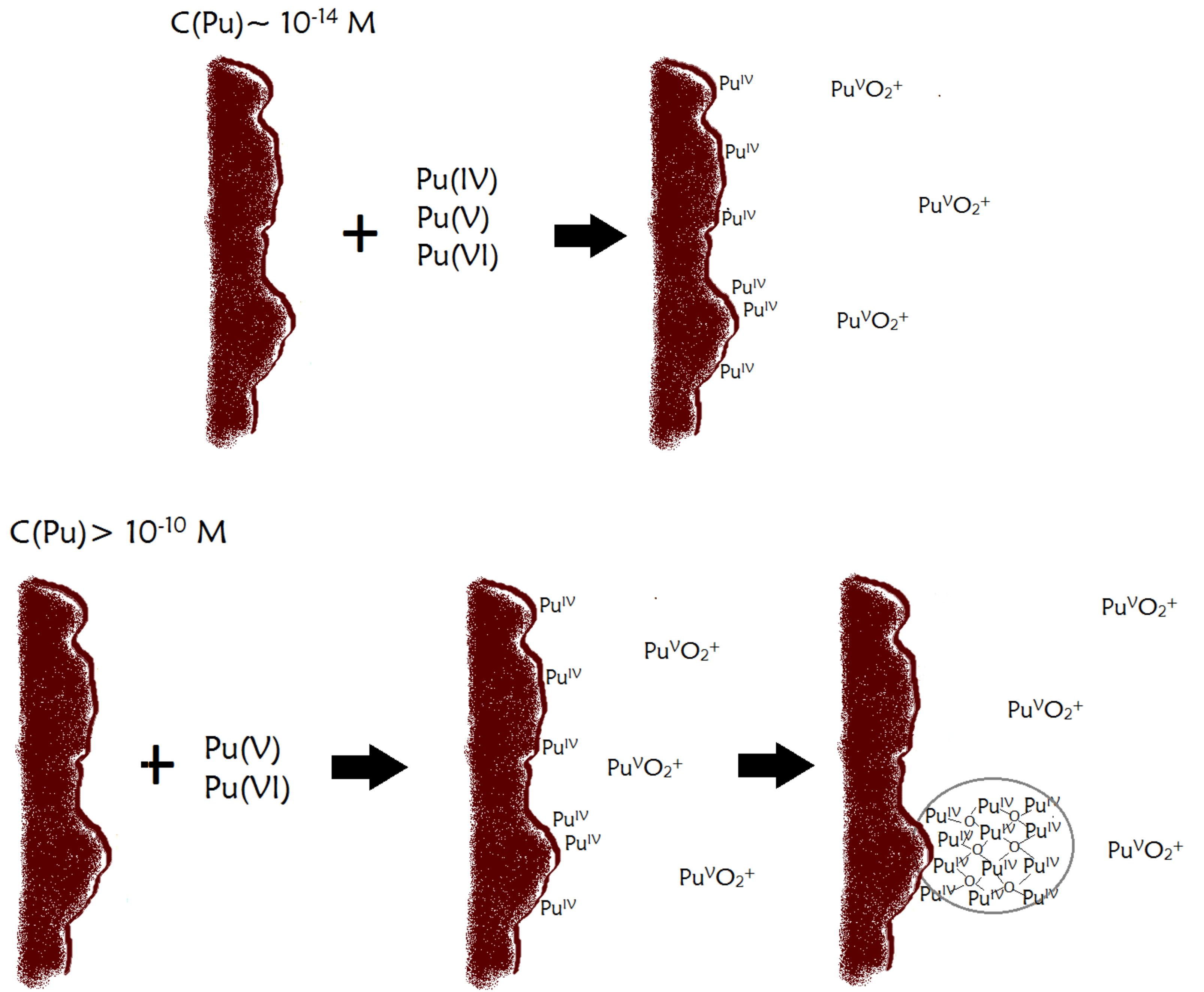

C(Pu)~ 10-14 M
Pu(IV)
Pu(V)
Pu(VI)
PuIV
PuVO2+
C(Pu)> 10-10 M
Pu(V)
Pu(VI)

$\boxed{\text{What is the mechanism of reduction of Pu(VI)?}}$

Possible mechanism of Pu(V,VI) reduction onto hematite:

- ~~Disproportionation~~ in EDL of hematite
- ~~Self-reduction~~
- Trace amount of Fe(II)
- Semiconductors properties of hematite
- ……

Romanchuk et al., RCA, 2011

TiO_2 vs. α-Fe_2O_3

semiconductors with band gap:

3.1 eV → 400 nm

2.2 eV → 560 nm

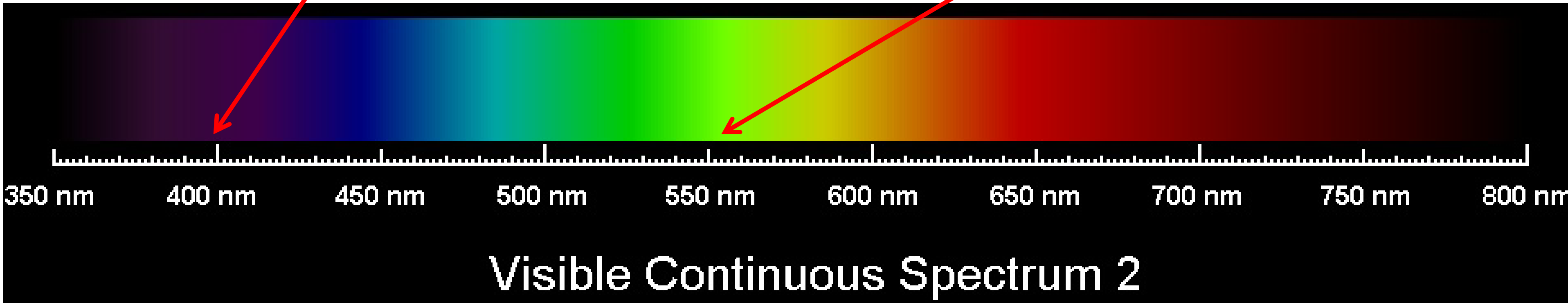

Kinetics of Pu(VI) sorption

$[Pu]=10^{-8}$ M

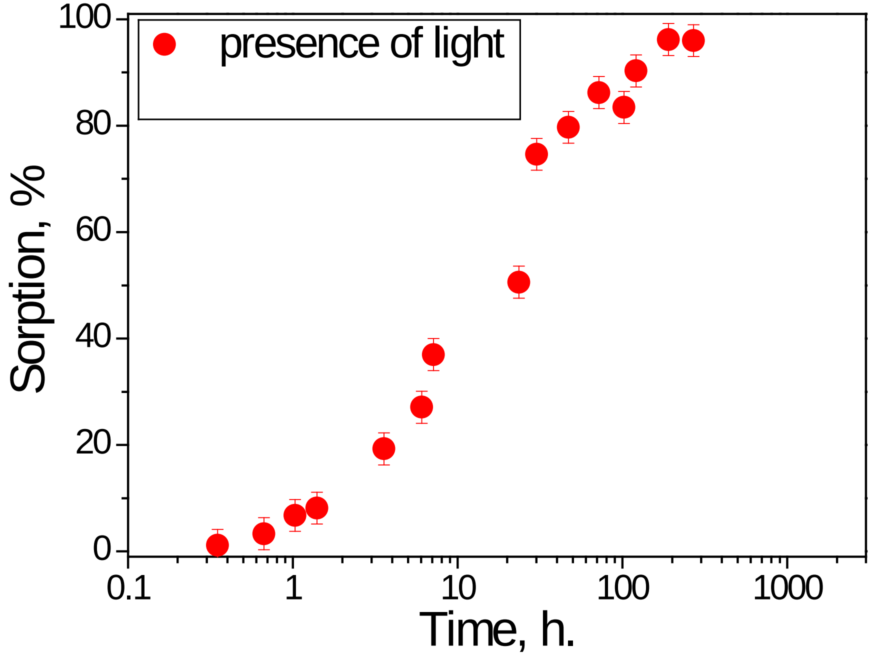

$[Pu]=10^{-6}$ M

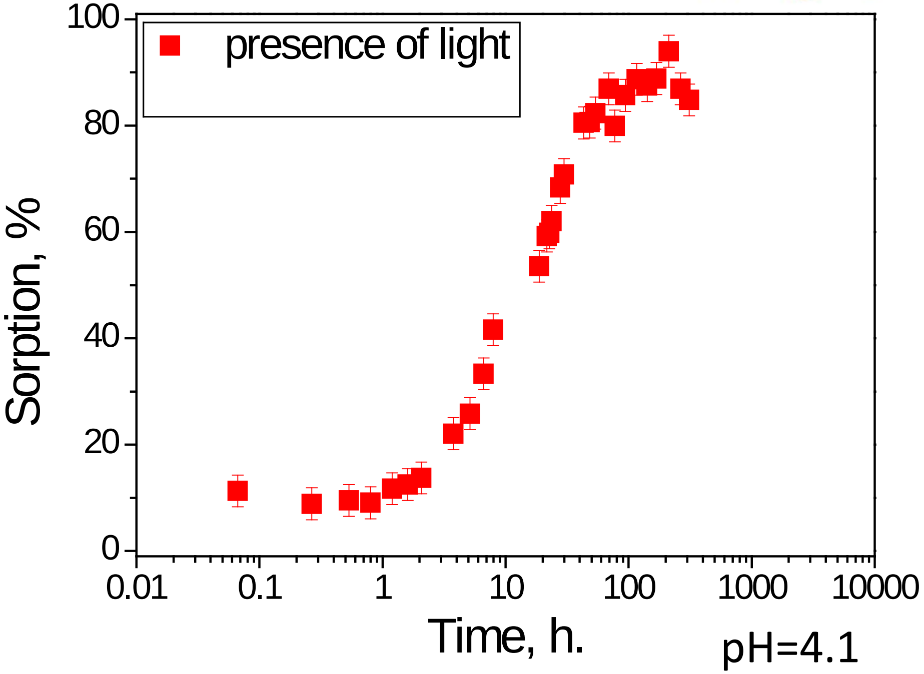

pH=4.1

Relatively slow sorption – redox reaction occurs

Kinetics of Pu(VI) sorption: Effect of light

$[Pu]=10^{-8}$ M

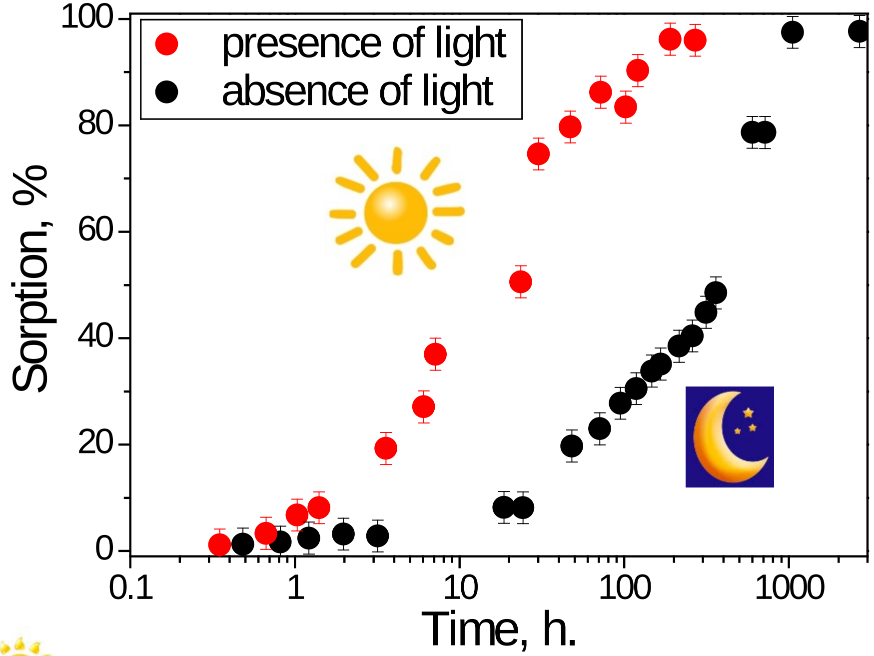

$[Pu]=10^{-6}$ M

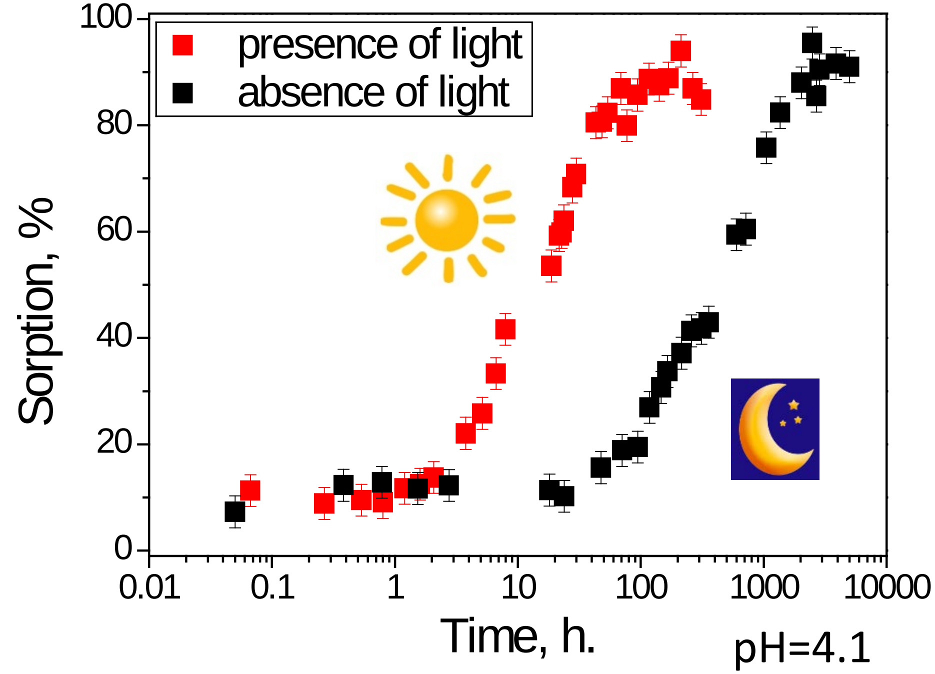

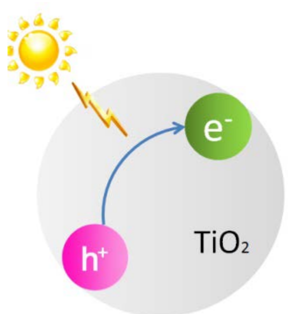

In the absence of light sorption is much slower.
Photocatalysis plays role in reduction of Pu(V,VI).

Speciation of Pu by XANES

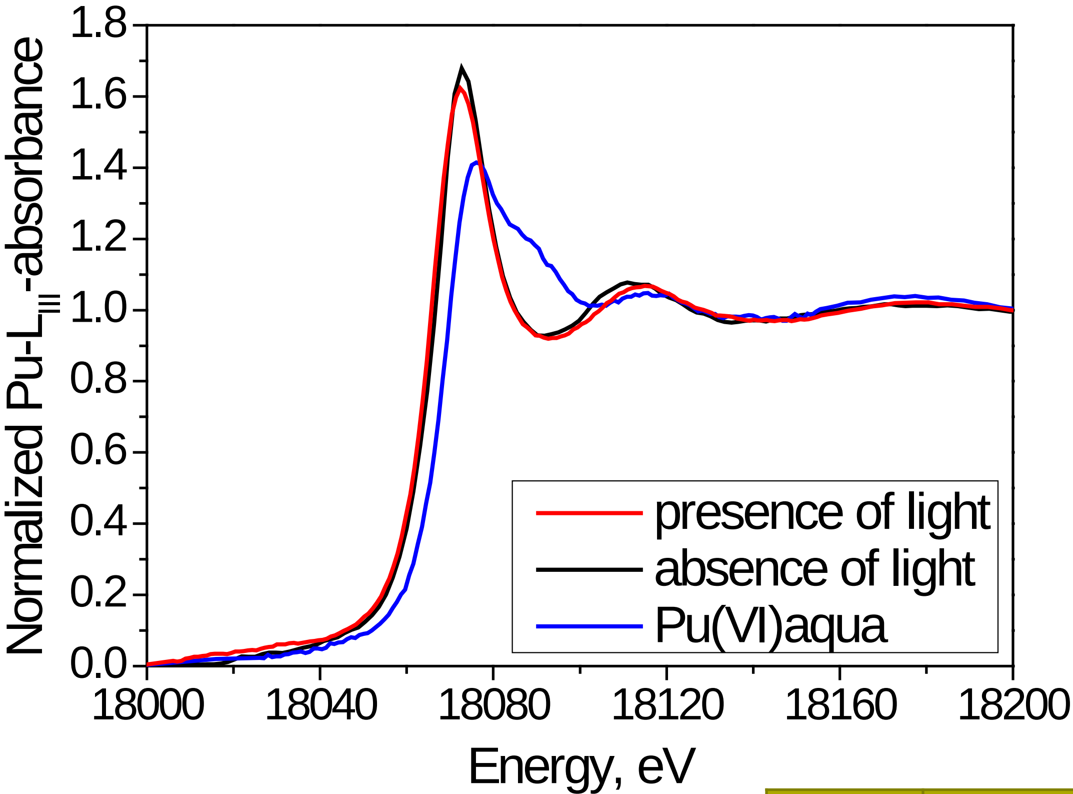

XANES confirms reduction of Pu(VI) to Pu(IV) under different light conditions

[Pu]	[TiO_2]	pH	Equilibration	Light
10^{-6}M	2.4 m^2/L	6.5	11 months	presence
10^{-6}M	2.6 m^2/L	6.3	2 months	absence

Speciation of Pu by EXAFS

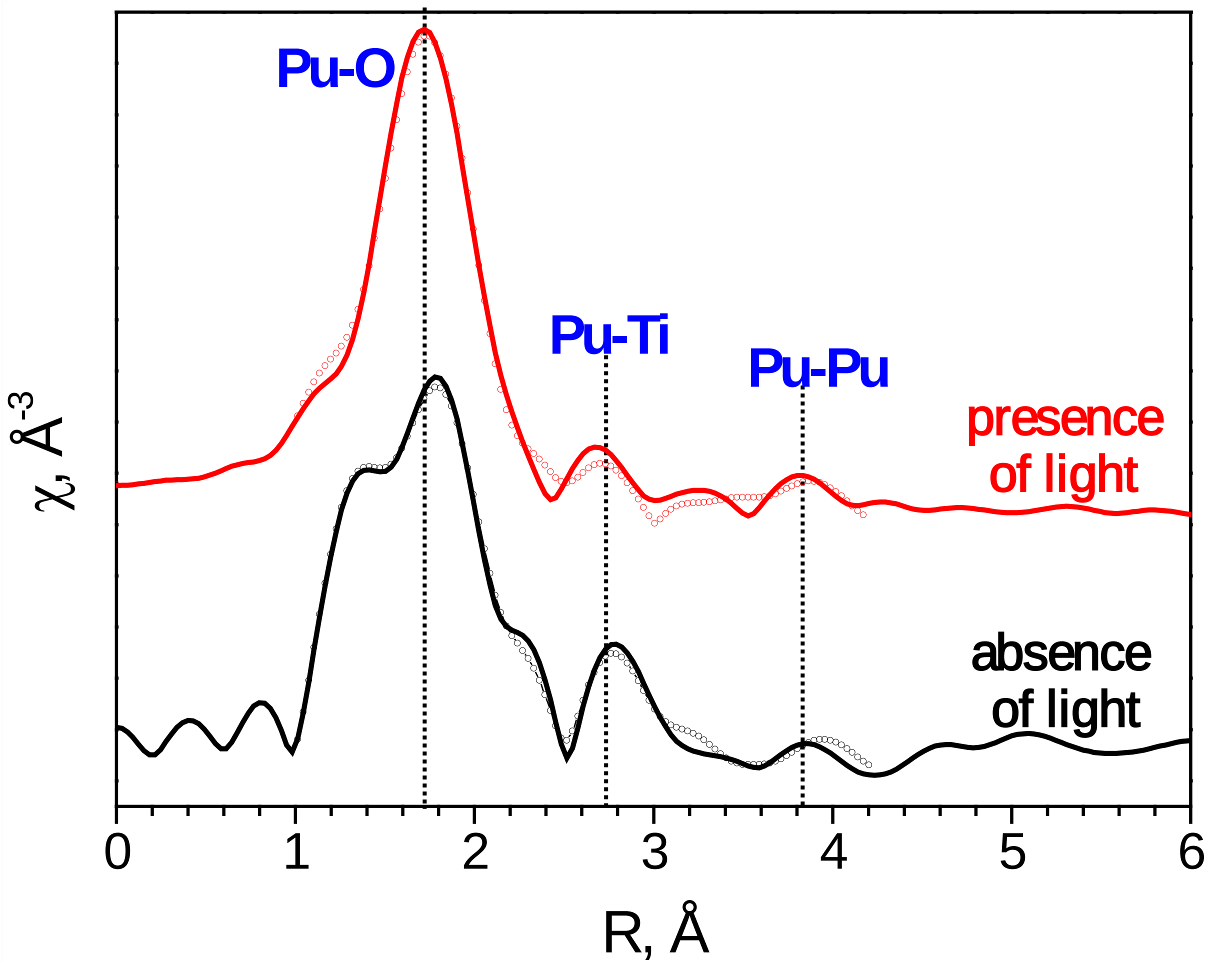

Light conditions does not affect Pu speciation

Along with Pu-Ti interaction, Pu-Pu is present in spectra - PuO_2-like particles formation

Distribution of Pu onto TiO_2 (HRTEM)

Elemental maps

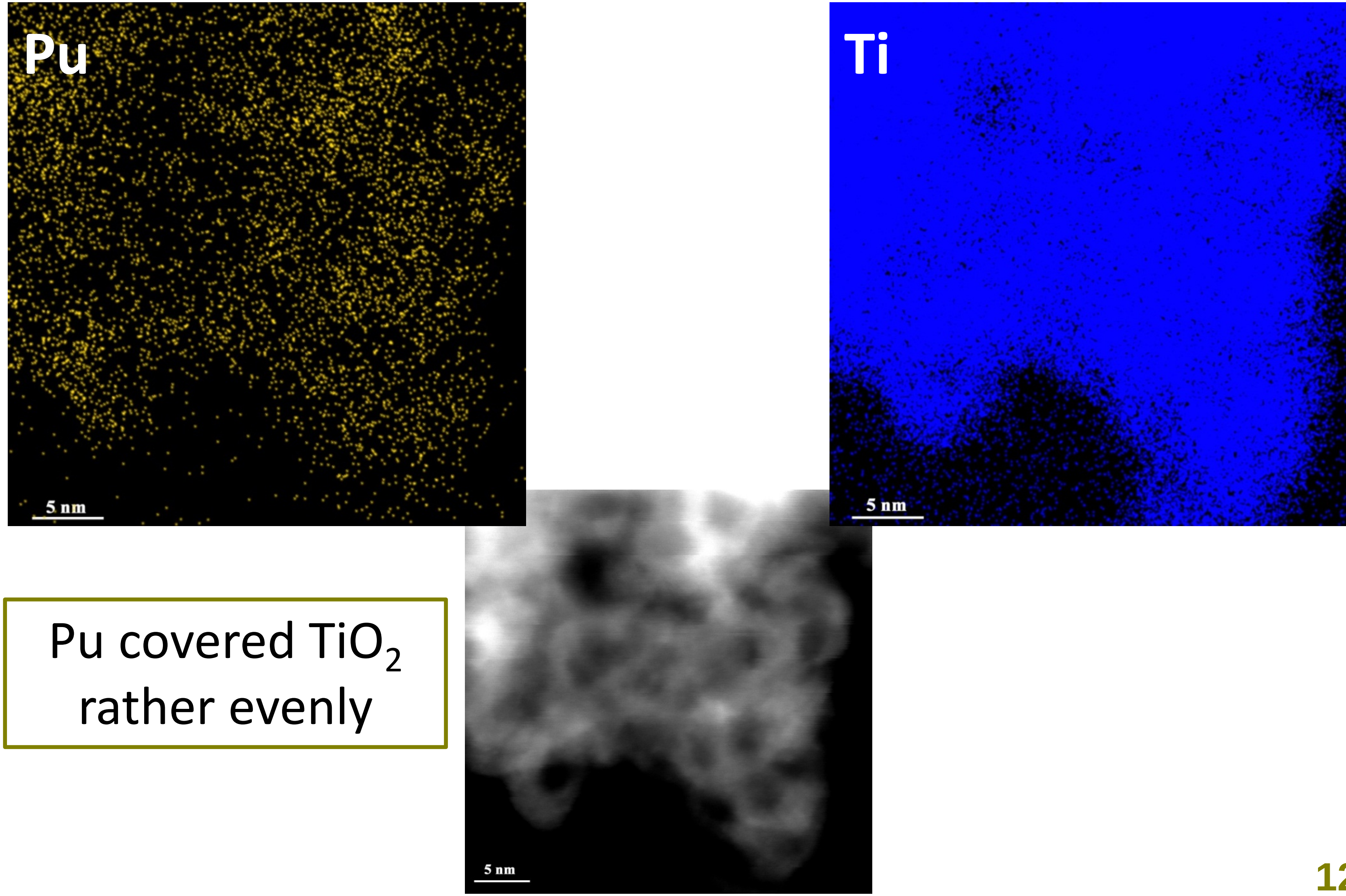

Pu covered TiO_2 rather evenly

Distribution of Pu onto TiO_2 (HRTEM)

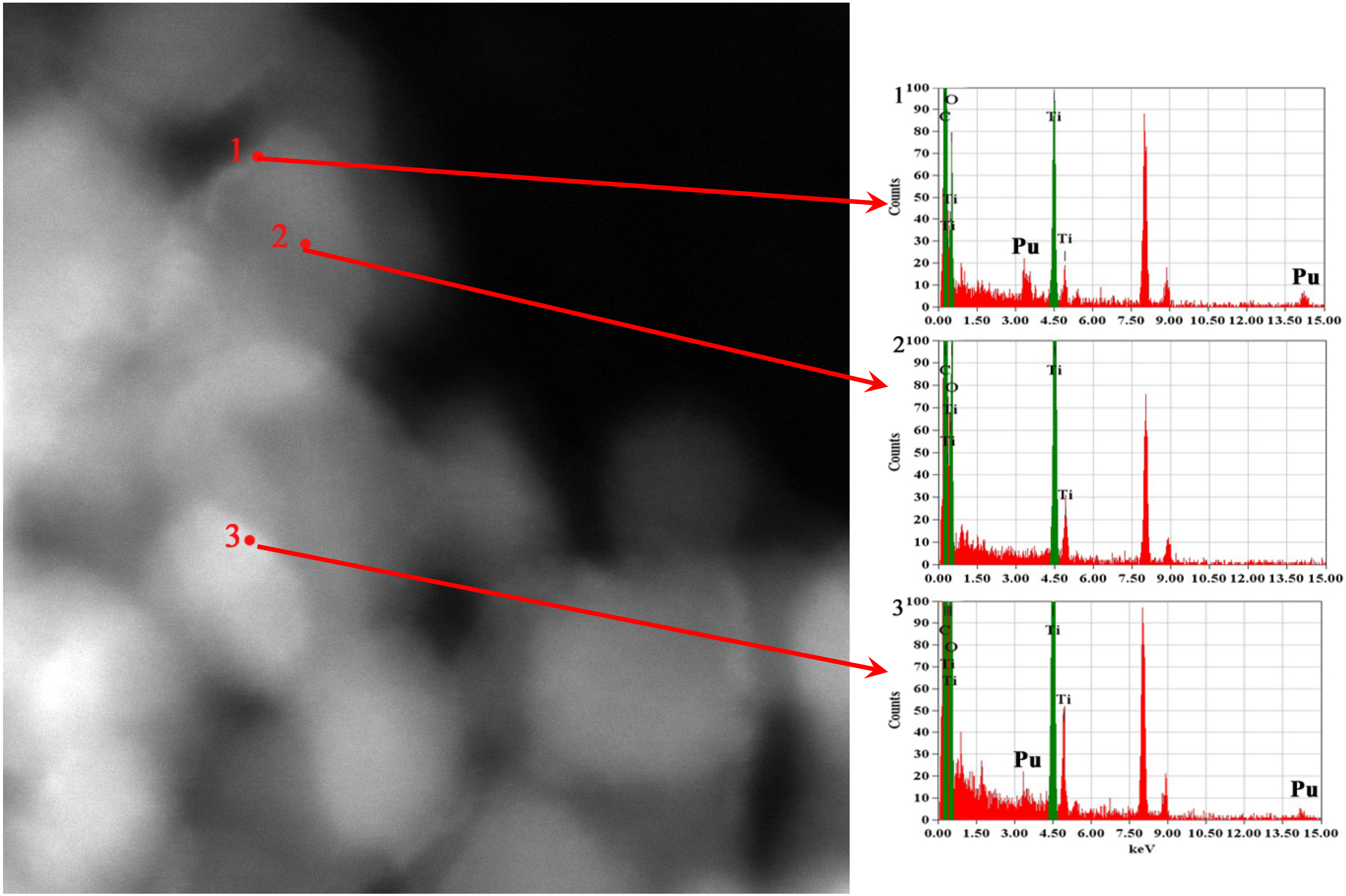

Distribution of Pu onto TiO_2 (HRTEM)

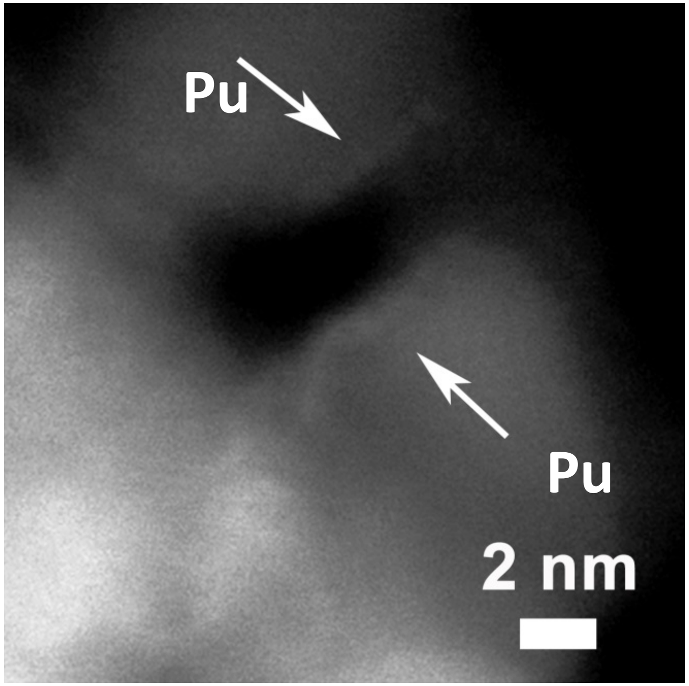

Pu is concentrated at the boundary of some TiO_2 particles. Nanoclusters with the structure of PuO_2 are formed.

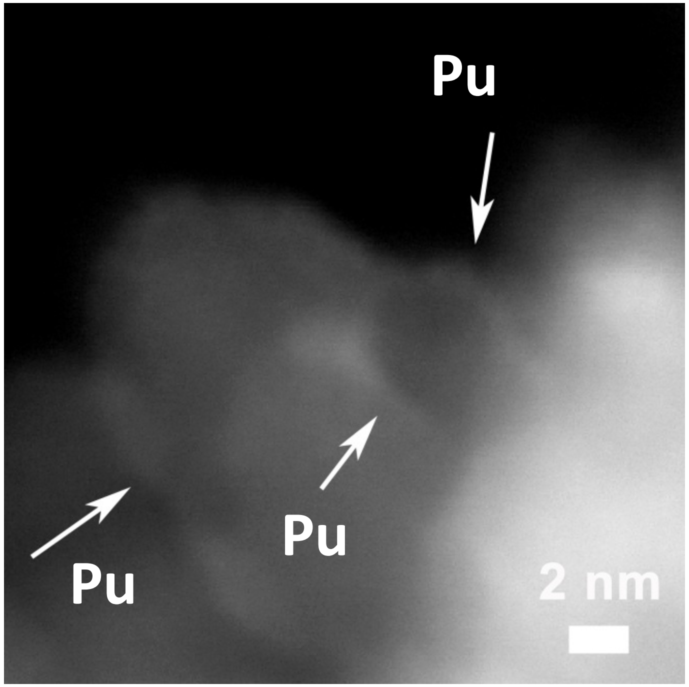

Leaching of Pu from surface

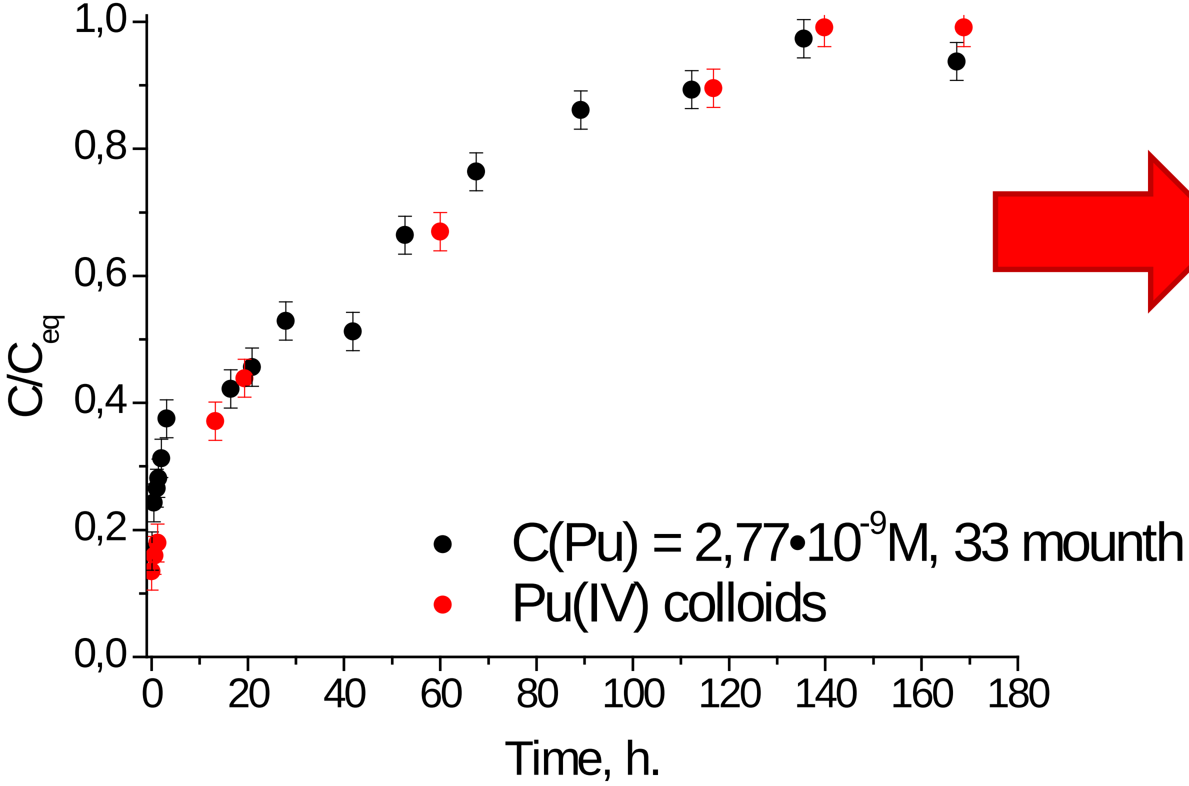

Kinetics of Pu leaching from hematite surface at nano- and micromolar concentration similar to leaching of Pu(IV) intristic colloids

Romanchuk et al., Radiochim. Acta, 2011

Properties of nanoparticles

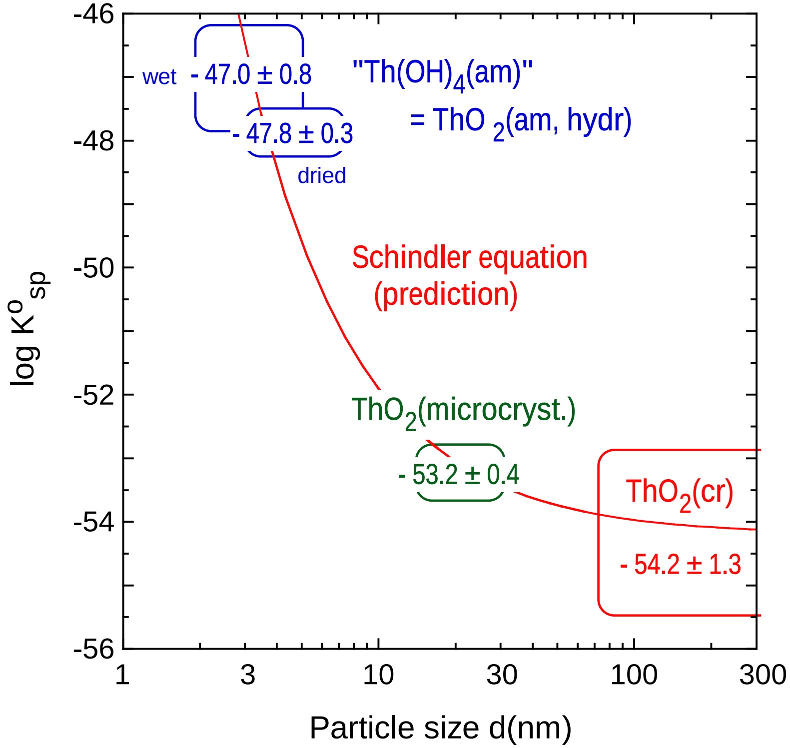

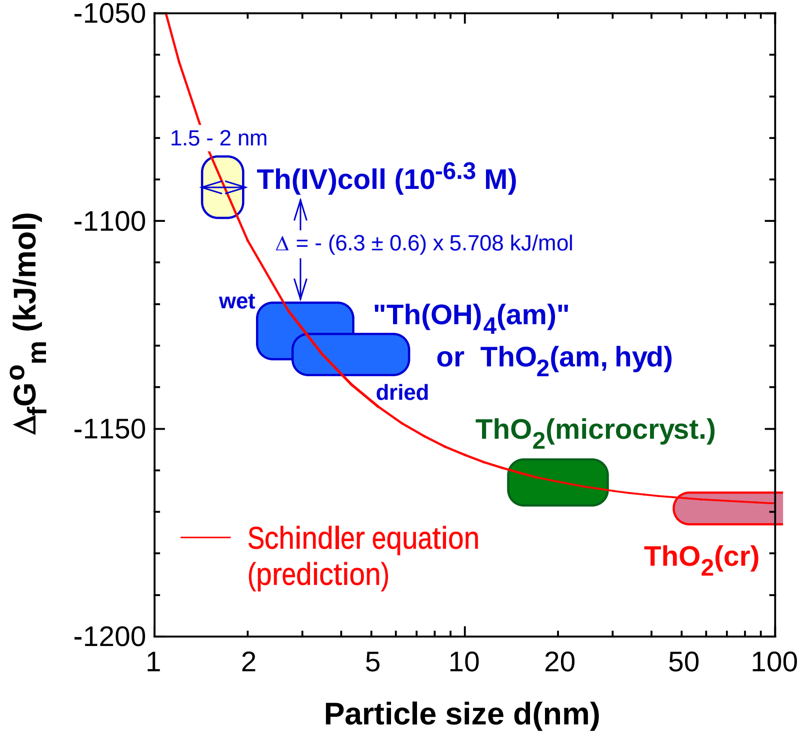

$$\Delta(\Delta_f G^\circ_m) = RT \ln \frac{K^\circ_{sp}(S)}{K^\circ_{sp}(S \rightarrow 0)} = \frac{2}{3}\gamma S$$

Neck et al.

Free energy linear relationship

$$Cat^n + \equiv FeOH \leftrightarrows \equiv FeO\text{-}Cat^{n-1} + H^+$$
$$Cat^n + HOH \leftrightarrows HO\text{-}Cat^{n-1} + H^+$$

- $\equiv FeOH + \mathbf{Am^{3+}} \leftrightarrows \equiv FeOAm^{2+} + H^+$

  $\lg \boldsymbol{K} = 5{,}91 \pm 0{,}04$
- $\equiv FeOH + \mathbf{NpO_2^+} \leftrightarrows \equiv FeONpO_2 + H^+$

  $\lg \boldsymbol{K} = -3{,}32 \pm 0{,}02$
- $\equiv FeOH + \mathbf{Th^{4+}} + \leftrightarrows \equiv FeOTh^{3+} + H^+$

  $\lg \boldsymbol{K_1} = 12{,}22 \pm 0{,}03$
- $\equiv FeOH + \mathbf{Th^{4+}} + H_2O \leftrightarrows \equiv FeOThOH^{2+} + 2H^+$

  $\lg \boldsymbol{K_2} = 4{,}13 \pm 1{,}37$

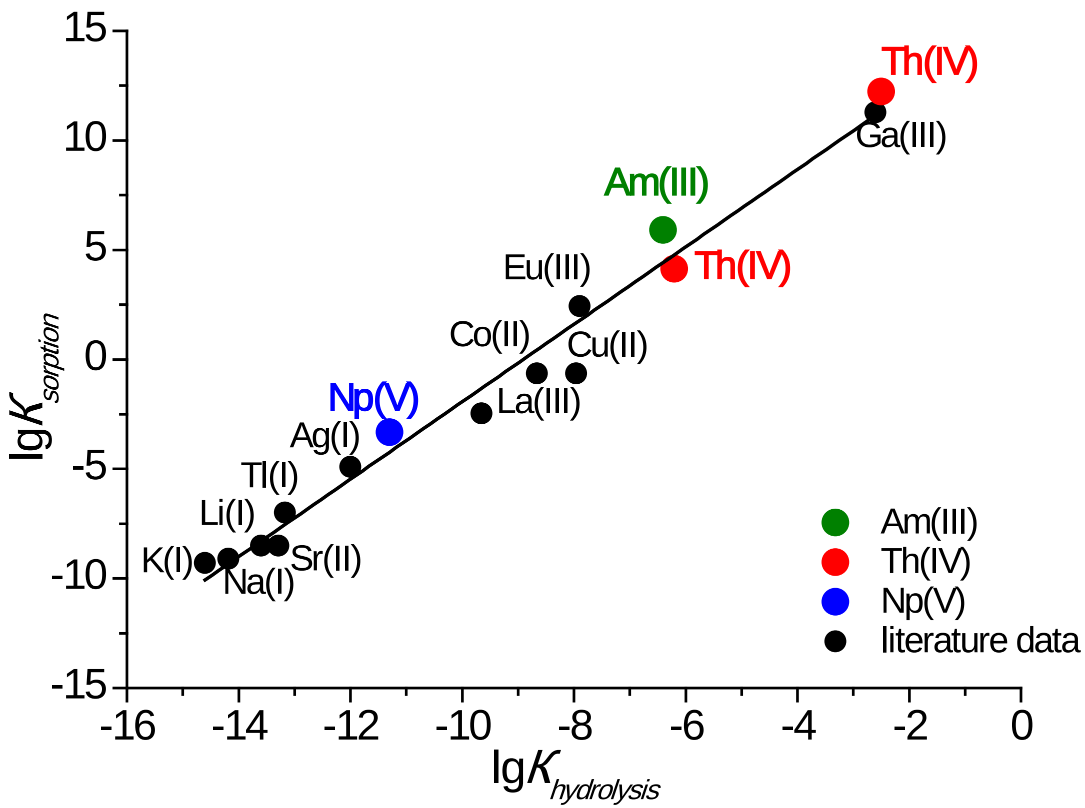

Modeling

α-Fe_2O_3

[Pu]=10^{-14}M

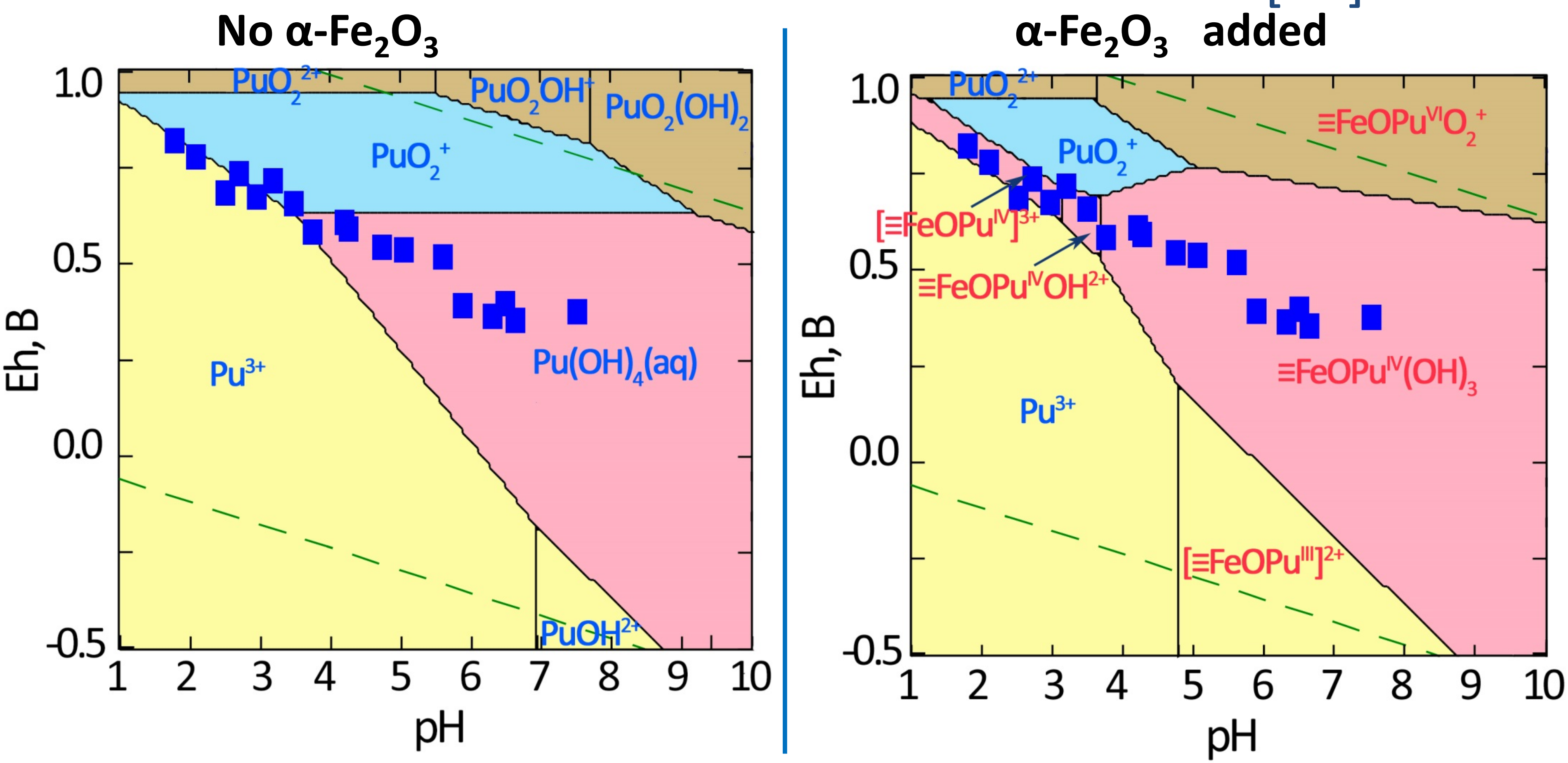

pH dependence of sorption

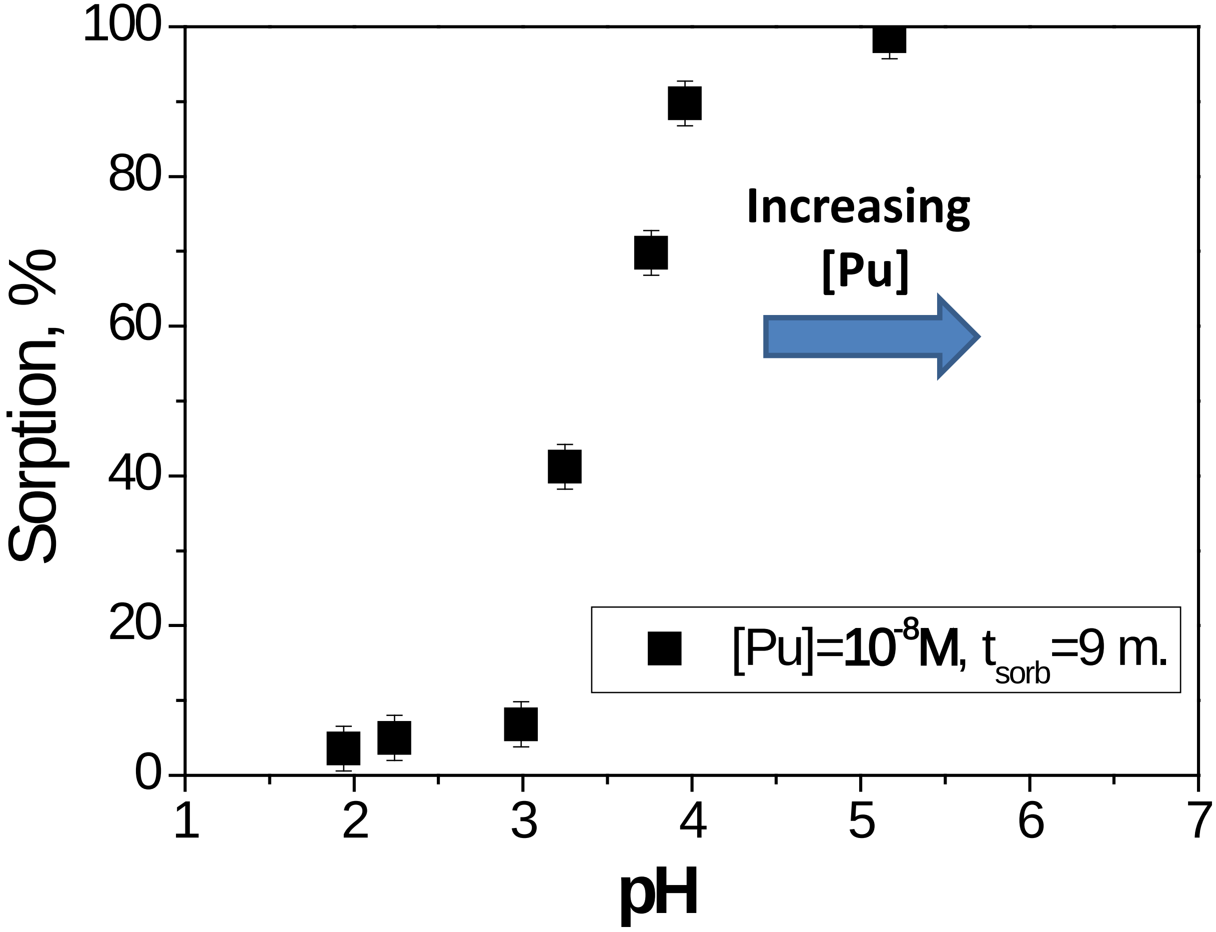

[Pu]=10^{-8} M

TiO_2

pH dependence of sorption: non-typical position

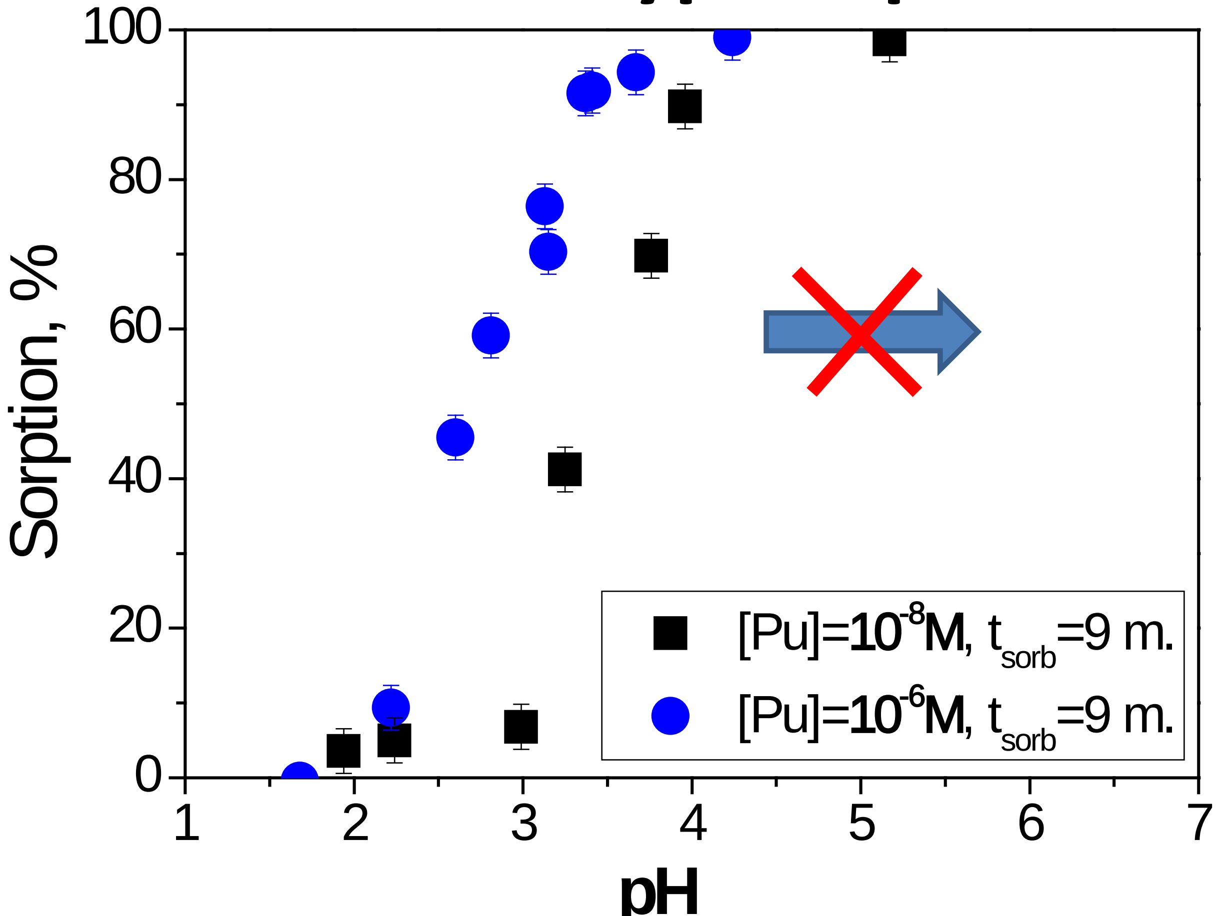

[Pu]=10^{-8}M

[Pu]=10^{-6}M

Is it not chemisorption?

Is reaction controlled by solubility of PuO_{2+x}?

Redox solubility of PuO_{2+x}

$$PuO_2^+ + e^- + 4H^+ \leftrightarrows Pu^{3+} + 2H_2O$$
$$PuO_2 \leftrightarrows PuO_2^+ + e^-$$

+

pH+pe=14,0±0,5

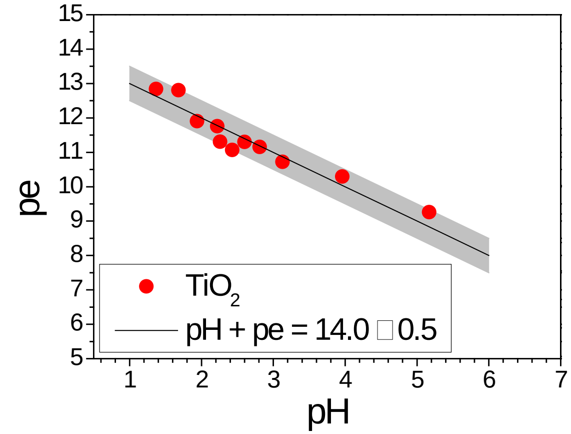

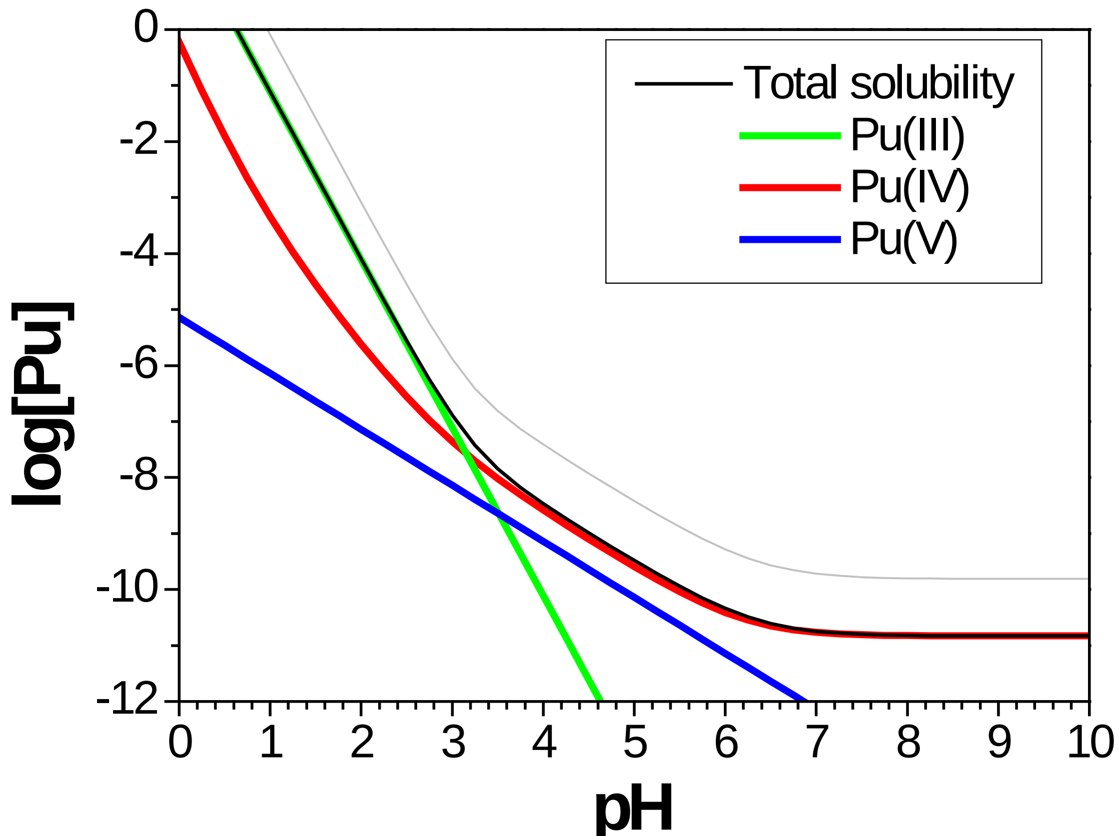

Pu(III) in solution at low pH (<3)

Constants from Neck et al. 2007

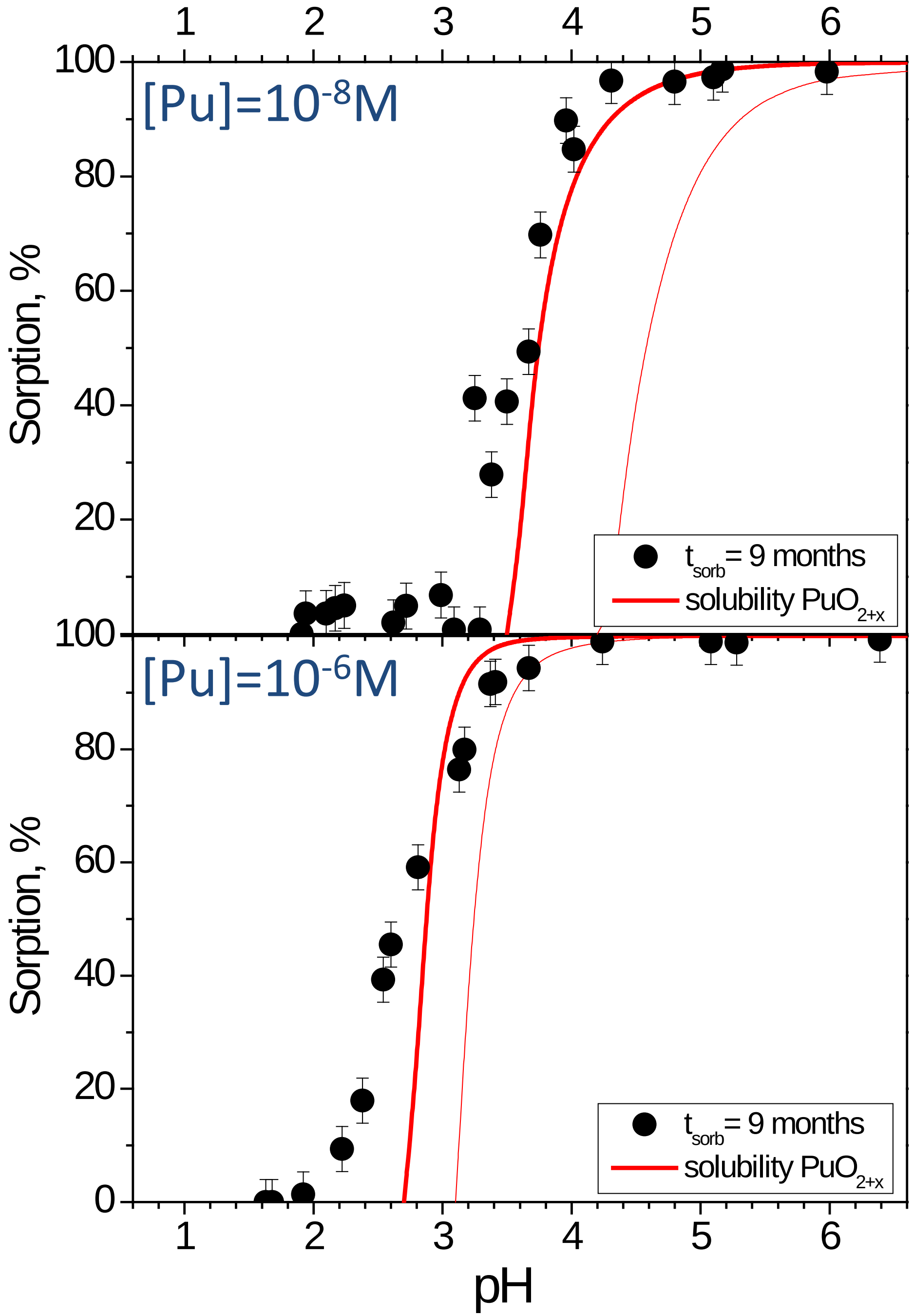

Modeling Pu speciation by solubility of PuO_{2+x}

Distribution of Pu in TiO_2 suspension can be modeled
as solubility of PuO_{2+x}
(even at [Pu] = 10^{-8}M)

Conclusions

The need for molecular-scale radionuclide speciation is needed for performance assessment of geological repositories of SNF or NW,

Generally radionuclide behavior (sorption, precipitation, complexation) could be relatively easily described thermodynamically,

Plutonium – “the element of surprise” could form oxide-like particles even in diluted solutions that show high kinetic stability,

Two processes are competing – chemisorption and solubility